THE RADIO AND ELECTRONIC ENGINEER

The Journal of the Institution of Electronic and Radio Engineers

FOUNDED 1925 INCORPORATED BY ROYAL CHARTER 1961

"To promote the advancement of radio, electronics and kindred subjects by the exchange of information in these branches of engineering."

VOLUME 32 AUGUST 1966 NUMBER 2

ELECTRONIC ENGINEERING IN OCEANOGRAPHY

THE second major Institution Conference to be held this year—at the University of Southampton from 12th to 15th September—presents an opportunity for electronic engineers to meet scientists and engineers active in another discipline to discuss ways in which electronic techniques can be employed to solve a variety of problems: in this case in oceanography, both physical and biological. There have been several conferences and conventions organized by the Institution in recent years having an objective of this kind: few have had a theme of such vital importance to the whole of mankind.

When the Conference was announced, in *The Radio and Electronic Engineer* for November 1965, it was suggested that 'we probably know less about the deep oceans which extend over nearly three-quarters of the Earth's surface than we do about outer space'. Yet these oceans are potentially the greatest source of protein and the enormous rate of increase which is taking place in the world's population makes it imperative that this source should be systematically exploited. The age-old techniques of fishing are inadequate for such a task and it is only recently that scientific thought and effort have been brought to bear on this problem.

Running through many of the papers in the forthcoming Conference is the underlying theme of how the productivity of the seas can be increased. One afternoon will be concerned specifically with direct fishery applications and there will be an opening address to this session by Sir Frederick Brundrett, K.C.B., who is Chairman of the research and development committee of the White Fish Authority. The British fishery and marine laboratories will also present several papers.

Those concerned with the problems of 'fisheries oceanography' will find much of the basic data essential to their investigations in sessions dealing with the physical and chemical properties of the sea. Some of this work has sprung from the needs of military sonar and it is encouraging to find that the naval authorities of several nations have put forward details of the techniques which have been developed.

The third day of the Conference is basically more concerned with techniques, such as wave measurements, for use in that branch of engineering which is coming to be known as 'ocean engineering' and with geophysical requirements. The latter embrace magnetic measurements, as well as the better known work associated with seismic studies, and the investigation of the nature of the sea bed. These investigations are, of course, important to the winning of minerals and the exploration of new oil and gas fields.

On the final day it may be said that the engineer really comes to the fore with sessions on instrument platforms. Avoidance of the severe strain often placed upon the human observer at sea in rough weather points naturally to the use of electronic techniques. (Whatever its other limitations, electronic equipment never gets sea-sick!) The papers in these sessions will describe some of the more ambitious schemes for oceanographic investigation and techniques of telemetry and data handling will receive attention.

Returning to our original theme of the importance of the Conference in the world-wide problem of food production, the Organizing Committee has been greatly encouraged by the wide interest which has been shown from many countries in what is believed to be the first conference of its kind to be held in Europe. Authors from six countries outside Great Britain are contributing 21 out of 48 papers, and the attendance of scientists and engineers from many more countries is expected. A truly international response to an internationally important subject!

P. W. WARDEN

I.E.R.E. Conference on Electronic Engineering in Oceanography

at the University of Southampton, 12th to 15th September, 1966

Synopsis of some of the Papers to be presented at the Conference

Monday, 12th September, 2.0–5.30 p.m.

Opening of Conference by Dr. G. E. R. DEACON, F.R.S.

SESSION I—MEASUREMENTS CONCERNED WITH THE BODY OF THE SEA

(a) Physical and Chemical Properties

Electronic Engineering in Oceanography—An Introductory Survey

M. J. TUCKER. (*National Institute of Oceanography, Wormley, Godalming, Surrey.*)

Future Needs for Electronic Instrumentation in the Field of Hydrography and Oceanography in the Royal Navy

LT.-COMMANDER D. P. D. SCOTT. (*Ministry of Defence (Navy), Hydrographic Department.*)

A Survey of the Application of Electronics to Oceanographic Sensors

A. M. EAST. (*The Plessey Company Ltd., Electronics Division, Ilford, Essex.*)

This paper is an integrating paper which compares some of the classical methods of measuring the various chemical and physical properties of the oceans with some of the modern methods which use electronics. In particular, it discusses devices which measure the following properties:

Current speed and direction; temperature; salinity; depth; speed of sound in sea water.

The paper includes a discussion of the factors which have to be taken into account when designing oceanographic instruments and a general survey of expendable instruments.

Salinity of Sea Water and its Measurement

R. A. COX. (*National Institute of Oceanography, Wormley, Godalming, Surrey.*)

Salinity (salt content) of sea water is a useful measure to the oceanographer, serving to identify a particular water mass, and as the starting point in the calculation of ocean currents, sound velocity and other things. The usual method today of determining salinity is to measure the electrical conductivity.

This paper will deal with certain aspects of the theory and practice of conductivity measurement which are of importance in routine salinity work, and of such problems as temperature and pressure compensation. The precision expected today in routine salinity measurements is about 1 in 10^4, and for special purposes approaches 1 in 10^5. The problem of absolute standards of conductivity is discussed, and the measures which have been taken to provide a reliable absolute conductivity standard are described.

The Development of a Precise Set of Data Relating Conductivity to Salinity and Temperature

NEIL L. BROWN. (*The Bissett-Berman Corporation, San Diego, California, U.S.A.*)

The development of equipment to measure precisely the relationship of conductivity to salinity and temperature and the results of measurements performed are discussed. This data is essential to the further development of precise conductivity type salinometers for laboratory and *in situ* use.

The equipment consisted of a pair of inductively-coupled conductivity sensors made of quartz in an oil bath controlled to within $\pm$ 0·001 deg C in temperature. The ratio of conductivity of the sample to standard sea water was measured for salinities from 1 to 50 parts in 10^3 and temperatures from -2°C to $+$ 40°C. The absolute conductivity is determined from an absolute conductivity determination on standard sea water performed in a parallel programme at the National Institute of Oceanography in England.

In situ Measurements and Automatic Recordings of Conductivity, Temperature and Pressure

G. SIEDLER. (*Institut für Meereskunde der Universität, Kiel, Germany.*)

For measuring electrical conductivity, temperature, and pressure *in situ* an electronic system called 'Bathysonde' has been in use for many years at German oceanographic institutions. A frequency modulation technique is used to achieve a transmission of data which is undisturbed by the cable resistance. A short description of the principles of operation is given. The problems involved with continuous *in situ* measurements at sea are discussed in more detail, and different systems of recording in analogue and digital form which have been in use on board of some research ships are described. Examples are shown of typical results that have been received in the open ocean and in sea straits.

Sensors for *in situ* Measurement of Dissolved Oxygen and Carbon Dioxide

A. EDWARD WHEELER. (*Beckman Instruments Inc., Fullerton, California, U.S.A.*)

The requirements for instruments to measure the physical and chemical properties of sea water have expanded considerably during recent years, and the development of equipment for automatic recording and analysis of data, both aboard ships and in shore-based laboratories, has dictated new operational parameters for these instruments. As *in situ* measurements of these properties assume new and increased importance, the development of corresponding oceanographic monitoring and analysis instruments presents challenging problems. One recently developed system provides *in situ* measurement of the dissolved oxygen content of sea water at depths as great as 1500 metres. This system utilizes an oxygen-permeable membrane, and a non-permeable diaphragm which serves to equalize the internal and external pressures to which the sensor is subjected. Flow sensitivity has been minimized by careful design, and temperature compensation is achieved by means of a precision thermistor and appropriate circuitry.

Another recent development is a dissolved carbon dioxide measuring system suitable for similar depths. This sensor determines carbon dioxide partial pressure by detecting pH changes in an electrolyte, which surrounds a pressure resistant glass electrode and is retained by a membrane permeable to carbon dioxide. Temperature compensation circuitry is incorporated into this unit also. These systems are representative of the manner in which engineering problems can be overcome and known techniques adapted to meet the rigours of *in situ* application.

5.30–6.45 p.m. Conference Reception

Tuesday 13th September, 9.15 a.m.–12.30 p.m.

Session 1(a) cont.

A Towed Thermistor Chain for Temperature Measurement at Various Depths

R. BOWERS AND D. G. BISHOP. (*National Institute of Oceanography, Wormley, Godalming, Surrey.*)

In the ocean there is often a surface layer of warm water floating on the colder, denser water below. The interface between the layers oscillates to form 'Internal Waves' analogous to those on the sea surface. Since these waves are important, particularly to submarine detection, their generation, propagation and decay are being studied by means of the thermistor chain.

This is a device for measuring internal waves from ships under way at speeds up to 12 knots, and depths up to 2000 ft. The temperature sensing units are towed at 50 ft or 100 ft intervals of a single-core double-armoured cable.

An Instrument for Measuring the Velocity of Sound in Water with Improved Accuracy in Turbulence and Under Towed Conditions

MISS E. EADY AND R. WILLIAMSON. (*The Plessey Company Limited, Electronics Group, Ilford, Essex.*)

The paper describes some of the problems encountered in the engineering development of a sound velocity meter using a single crystal transducer for both transmit and receive operation of sound pulses generated.

A baffle plate and spherical reflector surface is used to reduce the secondary echoes received and improve the definition and level of the reflected signal.

Error due to water flow across the sound path is reduced by the use of only one crystal transducer and by the velocity measurement being made in both directions along the same sound path. By the suitable selection of path length and divide circuits, the read-out can be shown as a direct indication in feet per second or metres per second on a standard frequency counter.

The method of mechanically mounting the crystal transducer to provide pressure balance and satisfactory operation for deep water working and the problems of providing a suitable means for testing and calibrating the instrument are discussed.

The Engineering for Production of a Recording Current Meter

G. F. HODGES. (*Marine Systems Engineering Department, Plessey Co. Ltd., Electronics Group, Ilford, Essex.*)

This paper describes a recording current meter which, in its original form was designed and developed at the Christian Michelson Institute, Bergen, Norway. This instrument makes full use of a novel electro-mechanical analogue-to-digital converter to achieve the transfer of information on to standard domestic magnetic tape.

To measure the current flow the original meter was designed to fit a Savonius type rotor but the subsequent user requirement was for a propeller type rotor. This paper describes the further development and engineering carried out to adapt the meter to use a sensitive propeller rotor and also the changes introduced to make the unit more suitable for quantity production.

Reference is also made to the tape translation unit designed to convert the recorded information from the magnetic to punched paper tape for final computer in-feed.

Current-shear Measurements from a Drifting Ship

G. KRAUSE. (*Institut für Meereskunde der Universität, Kiel, Germany.*)

Knowledge of current-shear is as important as the absolute current speed in establishing the theory of friction in ocean currents, and a current-shear meter has been constructed to be used from drifting ships. The meter consists of two Savonius rotors fixed at the ends of a long aluminium tube; the distance is variable from 2 to 10 metres or more. Current speeds at the two ends of the tube, current direction, inclination of the tube, depth, and temperature gradient are measured. Because the influence of the ship's drift on the rotors is cancelled out when only the difference of their revolutions is measured, the result is independent of the ship's speed.

Mechanical and electronic construction of this meter is described and some results are presented from measurements in the Indian Ocean and in the Baltic. Further possibilities for its application are given.

A Low Cost Expendable Bathythermograph

S. A. FRANCIS AND G. C. CAMPBELL. (*The Sippican Corporation, Marion, Massachusetts, U.S.A.*)

An expendable bathythermograph is a new, low cost method for obtaining reliable temperature/depth measurements from vessels underway. A continuous 0 to 1000 ft temperature/depth profile, in the range of $-2°$ to $+30°$C, can be obtained in one minute. Other ocean temperature measurement methods require that the ship be slowed or stopped at each sampling point, and are generally more costly, inefficient and less flexible for data presentation and analysis.

Applications for an expendable bathythermograph range from purely research activities, including physical oceanography, marine biology, fisheries investigation programs and weather bureau data, to a.s.w. and oceanographic data collection activities.

An Artificial Ocean—The Calibration and Evaluation Facilities of the U.S. Naval Oceanographic Instrumentation Center

FRED ALT. (*U.S. Naval Oceanographic Instrumentation Center.*)

This paper calls attention to a U.S. Navy Department function which has recently been made available as a service to the entire oceanographic community: the evaluation and standardization programme of the Naval Oceanographic Instrumentation Center.

A testing laboratory in which the physical environment of the ocean can be simulated—the 'Artificial Ocean' of the title—has been completed to a state where instruments are subjected to controlled environmental testing. Information thus obtained by the Center is now being made available to the scientific community as a whole, beyond the limits of the U.S. Government. This policy not only allows the outflow of information from the Center, but equally facilitates its reverse influx into the Center from oceanographers, instrument users, and manufacturers everywhere. In this way the Center can operate as a focal point for standardization of oceanographic measuring methods and instruments.

The paper will briefly describe the present Center test facilities which simulate the conditions of the ocean; it will give examples of recent tests on an advanced electronic, computerized shipboard survey system and on various electronic instruments. Present research by its standards engineers on measurement methods will be described. The standardization-directed information dissemination and retrieval programme will be discussed in detail, namely the issue of evaluation reports and the questionnaires to users for collection of field data and operational observations.

An Air-Dropped Acoustic Bathythermograph

H. CASTELLIZ. (*E.M.I.-Cossor Electronics Ltd., Dartmouth, Nova Scotia, Canada.*)

An expendable bathythermograph which can be dropped from the air is described in this paper. The device transmits temperature information acoustically either to a sonobuoy or to ship-mounted listening facilities.

The packaged instrument drops in free fall onto the water surface where the air gear is dispensed and the bathythermograph itself—after a suitable time delay for activation of a sea battery—commences to sink. In this instant acoustic transmission is initiated. Temperature information is impressed as f.m. on a 5 kHz carrier. Depth is calculated from elapsed time and known sink rate. Maximum depth range is in excess of 1000 ft. On the receiving side a special discriminator yields a temperature proportional voltage output which is recorded on a Rustrak pen recorder. Details of mechanical and electrical operation are presented.

A Temperature-Depth Recording System

G. P. FOX. (*Fisheries Laboratory, Lowestoft, Suffolk.*)

The probe described utilizes a potentiometer type Bourdon Tube as a pressure sensing element and a thermistor as temperature sensing element. The two sensors form arms of two separate Wien Bridges, the operating frequencies of which are selected so that the deviations from linearity are a second order effect. The temperature measured has a range of 10 deg C with a resolution of 0/01 deg C; the pressure can have any range divided into 1000 parts with a resolution of 1 part. Both frequencies are conveyed via a miniature coaxial cable to the surface, sampled by a control unit and recorded on a printer in sequence. Provision is made for an X-Y chart presentation.

Some Current Measurements on Deep-Sea Bottom in the Pacific

T. SASAKI, S. WATANABLE AND G. OSHIBA. (*Tokyo University of Fisheries, Japan.*)

Tuesday 13th September, 2.15–5.30 p.m.

Session 1(b)—Fishery Applications

Opening Address by SIR FREDERICK BRUNDRETT (*White Fish Authority*)

Some Applications of Electronic Engineering in the Fishing Industry

P. HEARN. (*White Fish Authority, Industrial Development Unit, Hull.*)

The Need for Automation of Observations in Fisheries Oceanography

R. JOHNSTON AND J. H. STEELE. (*Department of Agriculture and Fisheries for Scotland, Marine Laboratory, Aberdeen.*)

Aboard the research vessel, which is a highly inefficient and expensive platform, a few scientists pursue round-the-clock observations of diverse physical, chemical and biological aspects of sea water, marine life including fishes and the bottom. Their problems are numerous and varied but many could be resolved or simplified with the help of electronics. At the root of the matter is successful co-operation between the marine and the electronics expert on all levels of design, preparing reports and other aspects including business matters such as time schedules, materials and development costs.

The story of the evolution of a continuous surface salinity and temperature recorder illustrates some of the problems facing each of the partners.

Other desirable measurements are shown to pose their own characteristic problems for solution.

Undersea Observations for Fishery Problems

R. E. CRAIG AND R. G. LAWRIE. (*Department of Agriculture and Fisheries for Scotland, Marine Laboratory, Aberdeen.*)

The kinds of information needed in fisheries research include population assessment, identification of fish and shellfish species, behaviour patterns of fish and shellfish, operation of fishing gear, and the nature of the sea bed.

Observations are needed on very different scales to satisfy these requirements. The larger picture can only be sought by acoustic means. On a smaller scale, cameras, television, direct visual and again acoustic means have various merits and disadvantages.

The paper discusses various acoustic methods and shows how changes of parameter and display can give the best results for the various purposes.

The applications of photography and television to gather information on fish behaviour, population, and sea bed formation are also described.

A Digital Echo Counting System for Use in Fisheries Research

B. R. CARPENTER. (*Fisheries Laboratory, Lowestoft, Suffolk.*)

The echo counting system to be described was designed for use in conjunction with a high frequency (100 kHz) echo sounder and was primarily intended for use in surveying pelagic stocks.

The counter incorporates a variable gating system, synchronized to the transmission pulse repetition frequency, enabling signals occurring between any two selected depth limits to be processed.

Time swept gain amplifiers are utilized to compensate for fall-off of signal strength with depth, although the counter differs from previously published systems inasmuch as echo *duration* rather than echo *amplitude* is the parameter under consideration.

The processed information is displayed as an in-line digital read-out from a conventional scaler. A permanent record is taken from a printer coupled to the scaler.

Low-frequency Sound Sources for Underwater Use—Statement of Problem and Some Possible Solutions

B. S. MCCARTNEY. (*National Institute of Oceanography, Wormley, Godalming, Surrey.*)

The main stumbling block of a project to measure the back-scattering cross-section (target strength) of commercial fish at frequencies in the band 200 Hz to 2000 Hz has been that of a suitable sound source. The spectrum level requirement of this source is + 90 dB relative to 1μ bar across the band, or about 100 W peak at any frequency. The general problem of radiating into water these power levels at these frequencies are considered. Several sources employing various principles of transduction and including sparkers, boomers, explosives, hydro-acoustic, electro-dynamic, piezoelectric and magnetostrictive sources, are considered in terms of a common parameter—the maximum output spectrum level—and also efficiency, size and cost. In addition to the stated project any solution of this problem could also be applicable to marine geological surveying work.

Wednesday 14th September, 9.15 a.m.–12.30 p.m.; 2.15–5.30 p.m.

SESSION II—MEASUREMENTS CONCERNED WITH THE SEA SURFACE AND SEA BED

The Problems of Sea-Wave Recording

L. DRAPER. (*National Institute of Oceanography, Wormley, Godalming, Surrey.*)

Problems in the recording of sea waves are discussed. Existing techniques are described for measuring waves in the open sea and close to the shore. It is rarely possible to satisfy all the requirements of the user because of technical, operational and fundamental difficulties; all wave recorder installations for engineering purposes are the result of compromise. The measurement of wave direction on a routine basis for coastal engineering purposes is something which is often asked about but so far the instrumentation is in its infancy.

A System for the Measurement of Magnetic Micropulsations at Sea

R. A. HAFER. (*Pacific Naval Laboratory, Esquimalt, Canada.*)

A free drifting buoy system for making measurements of magnetic micropulsations in the deep ocean is described. A spar buoy system is used to provide a stable platform in low to moderate sea states.

The magnetic sensor, suspended 75 to 500 ft below the surface, is an optically pumped rubidium vapour magnetometer with a sensitivity of about 0·02 gamma in the micro-pulsation band. The magnetometer uses a crossed-beam optical system to minimize heading errors in the vertically suspended buoy configuration and to allow operation at high magnetic latitudes.

Measurements of swell and wave activity are made using an accelerometer, a pressure transducer, and a capacitive wave pole.

The signals from the buoy sensors are telemetered to a nearby ship via a standard f.m./f.m. radio system operating in the v.h.f. band.

To obtain the large dynamic range capabilities of the magnetometer direct digital recording is used. The magnetometer signal, a frequency proportional to the magnetic field strength, is filtered, frequency multiplied, and counted while the wave sensor signals are detected and digitized in an eleven bit analogue-to-digital converter. The resulting digital signals are time multiplexed and recorded on an incremental magnetic tape recorder. Analogue magnetic tape recordings are used as a back-up to the digital system. A paper chart recorder provides a visual display of micropulsation and wave activity.

A Free-Floating Wave Meter

R. GAUL AND NEIL L. BROWN. (*The Bissett-Berman Corporation, San Diego, California, U.S.A.*)

This paper describes a simple system used to measure wave amplitudes and frequency in the open ocean. It consists of a small surface buoy containing a radio transmitter and antenna and having suspended below it a very sensitive vibrating wire pressure transducer.

This system takes advantage of the fact that pressure signals at a fixed depth equal to or greater than the wave lengths being considered are greatly attenuated. Consequently, the transducer will sense pressure signals which are directly related to the rise and fall of the surface buoy due to the action of surface waves. The receiving station consists of a simple radio receiver, a frequency discriminator having a 0 to 5 V output, and a suitable recording system.

In the equipment described, the experiment was recorded on a strip chart recorder and also digitized and recorded on magnetic tape for computer analysis. A comparison of the power spectra was made between the data obtained from this device and the data obtained from a 'wave staff' installed on a 'Texas Tower' in the Gulf of Mexico.

Experiments to Measure the Magnetic Fields of Ocean Waves in Shallow Water

D. C. FRASER. (*Admiralty Underwater Weapons Establishment, Portland, Dorset.*)

A free nuclear precession magnetometer was constructed and laid on the sea bed some five miles from land with a cable leading to recording equipment on shore. Magnetic field fluctuations were observed which appeared to be correlated with wave height. A theory was developed to show how such fluctuations could be caused by electric currents induced in ocean waves by their movement through the Earth's magnetic field. Confirmation of the theory was obtained by analysis and comparison of data obtained from the magnetometer and from a wave height recorder.

The theory of the fluctuations, the design and construction of the magnetometer and data handling equipment, and the analysis of the experimental results are described.

Mechano-Acoustical Detection of Sediment Distribution

H. FREYTAG. (*Institut für Fangtechnik, Hamburg, West Germany.*)

In areas of former diluvial glaciation (estuaries, shelf-regions) the composition of sediment grain-size differs widely. The conventional method of exploring the features of the ground in these areas by bottom-grabbing is very expensive in time. A method of short-time inspection was developed by a mechano-acoustical monitoring system. A sledge is towed on the bottom which is equipped with a hydrophone in direct mass-contact. The source voltage of the hydrophone is led by a screened cable to the input of a tape recorder on the lower deck of the vessel, where steady monitoring for a sedimentologist is possible.

After gaining experience with a given equipment for a short time, different types of sediments can be distinguished: clay/mud, sandy bottom of different size, gravels, shells and stones. Sound samples of different sediments are demonstrated and quantified by oscillograms and 1/3rd octave-analysis for rhythm, frequency and source pressure. The emphasis of this method is on the immediate *in situ* distinction of different sediments, ripple structure of the bottom, mussel-banks, etc. Noise of the ship up to 1 kHz does not hamper the detection of different bottom features.

Digital Read-out Echo Sounder

C. H. COOKE. (*Kelvin Hughes, a Division of Smiths Industries Ltd., Hainault, Essex.*)

The present tendency is towards automatic recording and data analysis of echo-sounding information. A system has been designed to produce depth readings in digital form. These readings can then be logged together with other relevant data, such as time and position fixes, in printed form or on punched paper tape. They can also be displayed on illuminated numerical indicators.

A system of signal selection is used which includes an improved automatic time-gate, triggered from the sea-bed echo. In addition, a special form of automatic gain control on the receiving amplifier varies the level at which the sea-bed echo is gated. This feature maintains optimum amplitude discrimination of echo signals throughout varying conditions and largely eliminates spurious results due to aeration and multiple echoes.

The digital system operates in parallel with an echo-sounder recorder, the latter accepting confirmatory signals from the selection system. In this way, the recorder provides a continuous and permanent check on the operation of the digital read-out.

Details are given of the electronic circuits involved.

Some Recent Developments in Sideways-looking Sonars

R. W. G. HASLETT AND D. HONNOR. (*Kelvin Hughes, a Division of Smiths Industries Ltd., Hainault, Essex.*)

In these devices, used in geological and hydrographic surveys, a fan-shaped beam (narrow in the horizontal plane) looks broadside from the ship and an acoustic plan of the sea bed is produced on a recorder as a result of the ship's forward motion along a straight track.

One equipment, having a maximum range of 1600 yd, follows the National Institute of Oceanography design but with the transducer mounted in an inherently stable fibre-glass towed body, the transmitter power increased to 8 kW, the frequency raised to 48 kHz and a wider record used (18 inches). A high degree of precision in range is obtained.

Another type, mounted on the ship, has a wider vertical beam-angle to accommodate the vessel's roll without deterioration of the record. Tilt of the transducer in the vertical plane can be controlled from the deck.

The latest model, the Transit Sonar, has a range of 600 yd and gives an approximately true plan of the sea bed on dry paper 6 inches wide when the ship moves at 5·7 (or 2·85) knots over the ground. This compact equipment operates from a 24 V battery and has a smaller transducer which can be handled by one man. The transmitter, receiver and stabilized power supply use solid-state devices throughout and are mounted in the recorder case. The transducer can be inclined in the fore-aft direction to minimize the Lloyd mirror effect when the benefits of the latter are not required.

Details are given of the design, performance and calibration of these equipments, as well as typical records of sea-bed features, wrecks and coast-lines. The record produced by the Transit Sonar may be readily correlated with the corresponding Admiralty chart.

Simultaneous Use of Sideways-looking Sonar, Strata Recorder and Echo Sounder

R. W. G. HASLETT AND D. HONNOR. (*Kelvin Hughes, a Division of Smiths Industries Ltd., Hainault, Essex.*)

In geological survey, the simultaneous operation of these three equipments can have considerable merit. (The sideways-looking sonar used in the work is described in the associated paper, 'Some Recent Developments in Sideways-looking Sonars'.)

The Strata Recorder operates at 9·6 kHz in order that the acoustic waves penetrate the sea bed. Good resolution is obtained on dry paper due to the use of short pulses and relatively narrow acoustic beams. A special circuit gives time-varied gain, triggered by the sea-bed echo, to employ the dynamic range of the paper in the optimum way.

The precision echo-sounder records on dry paper 10 inches wide. The condenser-discharge transmissions at 32 kHz are switched by a silicon controlled rectifier.

The position of the survey vessel at any instant may be obtained from a radio position-fixing system or by visual fixes.

A number of examples of interesting sea-bed features are portrayed, each a combination of the simultaneous records correlated in time on the same scale, together with their geological and topographical interpretations. Sand waves of wave-length 13 feet and as little as 9 inches high are resolved quite readily.

Shipbourne Instrumentation for Continuous Recording of Acoustic Reflectivity of the Sea Bed and of Ocean Scattering Layers

K. R. HAIGH. (*Admiralty Underwater Weapons Establishment, Portland, Dorset.*)

The study of means of extending the detection range of sonar equipments to great distances has included investigations into a mode using the sea bed as a reflecting surface.

Measurements of the acoustic reflection loss at the sea bed at a few selected sites over the course of many years, indicated the variable nature of the loss, ranging from nearly zero to over 40 dB. In order to investigate the distribution of bottom loss over a wide area, an expedition was mounted to cover the whole of the North Atlantic. Equipment was designed to measure continuously the amplitude of the returning echoes from the sea bed in the form of peak and energy loss. The equipment was fully automated and stored all its data on punched paper tape for reduction and analysis ashore. By means of gating circuits selected sound scatterers also may be investigated, as has been the case with the Deep Scattering Layer.

The results obtained from this equipment can be correlated with the geological and geophysical properties of the sea bed as these are known to be related to the acoustic loss, and it is thus conceivable that the equipment could be further developed for mineral prospecting.

The paper concludes with comments on the trend of oceanographic data collection.

Acoustic Sub-bottom Profiling in the North-Eastern Atlantic

E. J. W. JONES. (*Department of Geodesy and Geophysics, University of Cambridge, England.*)

Continuous seismic reflection profiling is one of the most powerful techniques developed during the past decade for obtaining information about the soft sediments and the rocks below the sea bed. Seismic profiling is now a routine operation on many research vessels and data have been obtained over many thousands of kilometres of ships' track.

A seismic profiler which utilizes a pneumatic sound source is described. The source produces pulses of high intensity sound at a rate which can be controlled from the ship. A portion of the energy which travels downwards penetrates the sea bottom and is reflected back to the surface by the layers of sediment beneath. The echoes are received on a 10-element towed hydrophone array 50 feet in length and the output is fed to a modified Mufax weather chart recorder which displays the echoes in such a way that a continuous picture of the sub-bottom layers is built up as the ship steams along. The present limitations of the system are discussed and results obtained on a recent cruise of R.R.S. *Discovery* from several physiographic regions in the Eastern Atlantic are presented.

A Buoyant Seismic Recording Apparatus for Use on the Ocean Bed

R. B. WHITMARSH. (*Department of Geodesy and Geophysics, University of Cambridge, England.*)

A knowledge of the vertical variation of the speeds of compressional and shear waves through a deep-sea sediment strata can indicate some of the physical properties of the sediment. These properties are influenced by the processes which turn soft mud into hard rock. This knowledge can only satisfactorily be gained by the seismic refraction method when explosives and receivers are placed on the sea-bed. In a previous experiment an array of receivers was lowered to the bottom by a ship. Due to ship motion the array was noisy except in calm weather.

This paper describes a new apparatus using a buoyant borosilicate glass sphere which houses an 8-channel tape-recorder. A second sphere contains a flashing light and a radar-radio transponder to aid recovery of the apparatus. The tape-recorder directly records signals in the bandwidth 4 to 500 Hz from two transducers, a geophone and a hydrophone, at $\frac{1}{4}$ in/s. Playback is done at $3\frac{3}{4}$ in/s. In an experiment, explosives and pre-set firing clocks, both in pressure containers, are laid in a line on the sea-bed. Each recording apparatus is ballasted so that it falls to the bottom. When recording has finished one of the two devices releases the ballast and the spheres rise to the surface where they are recovered.

The Development and Use of Acoustic Energy Sources for Marine Seismic Profiling

P. A. MARKE. (*E.G. & G. International Inc., New Malden, Surrey.*)

A general description of continuous seismic profiling techniques, instruments, applications and uses is given. The development from the original spark discharge system to techniques depending on boomers, gas guns, air guns, magnetostrictive transducers, and explosives is briefly described.

Harbour developments, pipeline laying, drilling rig foundation studies, and many marine engineering projects require geological detail within the first few feet of the sea bed material and recent developments have enabled this section to be studied. A description of this high resolution technique and records obtained with the system is made.

For surveys requiring a greater amount of penetration it becomes more expedient to use a spark discharge system. A certain amount of resolution of the shallower layers is lost but penetration to one mile can be obtained. A description of some of the experiments involving high energy spark discharges in sea water, the spark discharge technique, and instrumentation is made. Example records obtained in the North Sea and the English Channel are given.

Future lines along which the continuous seismic profiling technique and instrumentation will probably develop are discussed.

7 for 7.30 p.m. Conference Dinner at Polygon Hotel, Southampton

Thursday 15th September, 9.15 a.m.–12.30 p.m.; 2.15–5.30 p.m.

SESSION III—INSTRUMENT PLATFORMS

(Ships, Buoys and Submerged Vehicles, Telemetry, Data Handling and Navigation)

Communications Aspects of Underwater Telemetry

H. O. BERKTAY AND B. K. GAZEY. (*Department of Electronic and Electrical Engineering, University of Birmingham.*)

Problems associated with reliable underwater telemetry are studied in three general categories dictated by the degree to which multi-path propagation effects are experienced. The maximum range obtainable under ideal conditions of a typical telemetry system is investigated as a function of the required information bandwidth.

The relevant acoustic properties of the sea are summarized and systems, originally used in electromagnetic communication to combat 'flat' and 'frequency selective' fading are reviewed and their adaptability to the present application discussed. Inter-symbol distortion arising from large differential delays during multi-path propagation is discussed and some proposals are made for the realization of a practical system particularly suitable for underwater telemetry where large path differentials are encountered.

A Sonar-Buoy for Telemetering Underwater Sound Signals

H. URBAN. (*Fried. Krupp Atlas-Elektronik, Bremen, Germany.*)

A telemetry system for underwater sound signals is described. It consists of a buoy and a measuring set. Underwater sound signals are received by a hydrophone at the buoy, modulated on to a radio carrier wave and transmitted to the measuring set. The buoy is battery-powered and can operate, either anchored or freely floating, up to distances of several kilometres from the receiving set. By means of a special modulation technique, in which the Droitwich radio transmitter is used as an external control source, the transmission link is phase-locked and thus 'cable-like' in its behaviour. The range and bearing of the buoy can be determined either optically or by the ship's radar. The bearing can also be determined by radio direction-finding methods.

Data Collection in Fishing Gear Research

J. J. FOSTER. (*Department of Agriculture and Fisheries for Scotland, Marine Laboratory, Aberdeen.*)

This paper briefly describes the various parameters that need to be measured in fishing gear test experiments. The inter-relationship of these parameters are generally complex in themselves, and are further confused by various irregularities in test conditions, e.g. type and contour of sea bed, and variation in water speed in the column.

The type of instrumentation which has been exploited up to the present is noted and the shortcoming found in both recording and subsequent analysis of records from these instruments is explained.

The urgent need for rapid, on the spot, analysis of data necessitates the use of a ship-borne computer which can act as a data logger and also enable the more lengthy computations to be done during the ship's programme.

Special emphasis is placed on the unsuitability of continuous trace pen-recording for analysis in this kind of work, but their use as a 'quick-look' facility in computation with more sophisticated data logging equipment is considered.

Typical examples and plates are included throughout.

A Digital Acoustic Telemeter for Fishing Gear Research

M. J. D. MOWAT. (*Department of Agriculture and Fisheries for Scotland, Marine Laboratory, Aberdeen.*)

This paper describes a method of using an acoustic link to telemeter engineering measurement from a trawl to the towing ship. As a carrier of information a beam of sound waves in the sea is far from ideal. The medium is noisy and because of the short wavelengths involved Doppler and interference effects are often troublesome. The acoustic link, however, is often the best method available and an attempt is being made at the Marine Laboratory to overcome some of the problems by using a narrow bandwidth digital system with a 'morse code' type of signal.

The subject is dealt with in two parts. The first deals with the performance of an acoustic link of this type under trial conditions and the second with the conversion of the information signals into a suitable form for transmission using electronic logic units for sequence control, for analogue-to-digital conversion and modulation of the transmitter.

A Data Logging System for Ministry Research Vessels

P. G. GRIFFITHS. (*Fisheries Laboratory, Lowestoft, Suffolk.*)

A system of automatic data logging is being developed for use on fishery research vessels. The data to be logged are rather unusual in that they consist of navigational data on ship's position, course, etc., and experimental data which may come from any type of experiment being conducted on a given voyage. 'Industrial' type parameters (engine performance, etc.) are not logged.

The approach to this problem will be to use a comparatively simple data logging system, which will accept analogue and digital information on up to twenty channels, and record this on punched tape.

A series of units will then be developed to accept navigational or experimental data and convert it into a suitable form for feeding into the data logging system. The design of these units will be discussed, together with ideas for future development.

A Low Cost Compact Buoy System for Ship Use to Measure Ocean Structures Over a Month Period

R. FRASSETTO. (*Saclant ASW Research Center, La Spezia, Italy.*)

The oceanographic buoy described is for ship use, and allows a single ship to make synoptic studies of a limited body of water using a number of buoys. The purpose was to develop an economic, simple, dependable sea unit, which allows for accidental losses, matched to a more elaborate data-processing, system, which represents a durable investment.

The unit is of small size, light weight in air and water, and easy to launch and retrieve. The low drag of buoys and cable permits its use in areas of strong currents. The sensing capabilities of the first generation system are temperature, current speed and direction, and depth. The data storage capacity is of 16 000 cycles or 370 000 individual data. Recording is intermittent with maximum sampling rate of 30 seconds. The system is engineered for one month operation, which is considered a reasonable cruising time limit for a ship in a limited area of the ocean.

A sub-surface system can also be used, if needed, with small surface r.f. data transmitter which is composed of an upper array of closely spaced sensors simultaneously recording on a single magnetic tape recorder, and a deep array of widely-spaced, continuously self-recording instruments. The upper array is kept taut between two faired floats. The system permits a simple link between field observations and a digital computer. Corrections for calibrations and motions of the mooring line are made automatically in the data processing phase.

The system has been used since 1963 in the Straits of Sicily and in the Straits of Gibraltar, where unusual oceanographic conditions are found and where the buoys were exposed to strong dynamic forces.

The first generations of the system allowed for substantial improvements as a result of field experience, particularly oriented to reach the utmost simplicity, dependability and sea-worthiness. These qualities will improve along with the progress of technology and the availability of miniaturized components on the market at low cost and better quality.

U.S. Coast and Geodetic Survey Hydrographic and Oceanographic Data Acquisition Systems

T. J. HICKLEY. (*U.S. Coast and Geodetic Survey, Washington Science Center, Rockville, Maryland, U.S.A.*)

The Coast and Geodetic Survey is now in its fifth year of a continuing programme to automate its hydrographic and oceanographic survey vessels. To date, four hydrographic vessels and two oceanographic vessels have been so automated. The hydrographic vessels have been equipped with various types of experimental logger systems some of which work directly on-line with the sensors and others requiring manual entry before recording their data on punched-paper tape. Raw data tapes, accompanied by corrector tapes, are sent to a plotting center at Seattle, Washington. At this center, the tapes are combined through a computer to produce cards used to drive a 48 by 60 inch precision plotter. The plotter then rapidly produces the smooth copy of the hydrographic survey. Methods have been developed for rapidly determining the echo sound velocity corrector by means of a synoptic survey using a velocimeter. Also, telemetering tide gauges have been employed to speed up the data collection further. One ship has been supplied with a logger system which includes a small high speed computer/plotter system. With this system, data leave the ship in a smooth form requiring no further corrections; thus reducing steps to a final navigation chart.

The oceanographic survey vessels carry large computers on-line with many of the oceanographic and geophysical sensors and capable of computing and recording its data in various forms on magnetic tape, punched-paper tape, hard copy, and analogue form. This system will handle such data as meteorological soundings (ocean), navigation, gravity, terrestrial magnetism, and sea surface temperature, and on-station *in situ* measurements of temperature, salinity, and sound velocity. The computer is also used for engine monitor and limited control.

A Free-falling Deep Sea Instrument Capsule

FRANK E. SNODGRASS. (*Institute of Geophysics and Planetary Physics, University of California, La Jolla, U.S.A.*)

The deep sea instrument capsule is currently being used to record on digital magnetic tape the tides and temperatures in the deep sea. The unit is designed to fall freely from a surface ship in water depths up to 6000 metres, remain on bottom for several days to several months, then return to the surface upon command from the ship. Two 60 cm diameter aluminium spheres with 2·5 cm walls house the instruments and provide buoyancy. With a 60 kg payload, 20 kg of buoyancy remains to return the capsule to the surface at 1 m/s.

Automobile batteries provide ballast and the necessary power for the recording system. Recall of the capsule is accomplished by transmitting coded acoustical signals from the ship to activate an explosive release mechanism connected to the battery ballast. When the battery ballast is released, a small frame on the top of the batteries lifts free and returns to the surface with the capsule. A lead-acid battery mounted on the frame provides power for a radio beacon and a flashing light. The frame also supports the pressure and temperature transducers. A pinger attached to the top sphere provides a homing signal for the ship. The pinger pulse rate is controlled by the recorders in the capsule to indicate whether or not the transducers are recording properly, or whether trouble has developed.

Shipboard equipment, mounted in a portable instrument laboratory, consists of a standard Loran receiver, a radio direction finder, an acoustical command transmitter, and a directional acoustical receiver. The ship is navigated by the Loran to within five miles of the capsule on bottom. At this range the acoustical signals can be received by directional hydrophones to guide the ship to a position directly above the capsule. Release of the capsule is then commanded by coded acoustical signals. Upon return to the surface, the capsule is located by the directional radio beacon and a flashing light.

The tide measurement will be made by sensing the bottom pressure with a vibrating wire transducer called the Vibrotron which has a sensitivity of 1·3 Hz/m of water pressure. By measuring the transducer frequency to one part in 10^6, water pressure changes of a few millimetres can be resolved. The recordings are best defined as the ratio of the instrumental noise energy at various frequencies to the energy of the signals to be recorded at these frequencies.

To correct the pressure recordings for temperature effects, the temperature must be measured with a resolution of 10^{-3} deg C. Recordings with this sensitivity can be obtained using either vibrating wire transducers or quartz crystals with intentionally high temperature coefficients. Temperature recordings of 10^{-5} deg C resolutions have been obtained.

An Unattended Oceanographic Data Collection System

G. K. TAJIMA AND P. C. STAHL. (*The Bissett-Berman Corporation, Santa Monica, California, U.S.A.*)

A great deal of interest resides today in the use of instrumented buoys for oceanographic environmental monitoring because of the economies which they offer in making continuous synoptic measurements. In this paper, work is described which is directed towards advancing the state-of-the-art in sensors adapted to long term *in situ* use. Specifically, the sensors must be stable, consume minimum power, be immune to the effect of fouling and corrosion, and be adapted to ease of handling, installation and service. Also described is a complete system involving a network of buoys which measures current speed and direction, temperatures, waves and meteorological variables. This data is transmitted to shore and recorded in a machine-readable format.

Ocean Data Measuring Device

J. GONELLA AND J. MARTIN. (*Laboratoire d'Oceanographic Physique, Museum National d'Histoire Naturelle, Paris.*)

A detailed description of an ocean data measuring device which can record, in uncoded printed form and all corrections made, at a rate of one series every 15 minutes, 18 temperature measurements, 2 relative humidity measurements and 3 other various measurements, one of which may be the global solar radiation integrated over 15 minutes.

The accuracy of the temperature measurements is better than $\pm$ 0·01 deg C and the accuracy of the two relative humidity measurements is about $\pm$ 3% in absolute value and better then 1% in comparative value.

The measuring points are located, on the one hand, on a large manned buoy ('Laboratory-buoy') and, on the other hand, on a small buoy linked to the first by a 330 m long floating multi-core cable. Anemometers are situated near the air-temperature and humidity sensors.

Diagrams, photographs and obtained data sheets are presented.

ODESSA System (Ocean Data Environmental Science Services Acquisition System)

A. J. GOODHEART. (*U.S. Coast and Geodetic Survey, Washington Science Center, Rockville, Maryland, U.S.A.*)

The ODESSA System is the initial attempt in development of a prototype buoy system for collecting depth profile data of the major oceanographic parameters simultaneously from several buoy stations. Each buoy station records the data on a self-contained buoy magnetic tape recorder and also contains an f.m. radio which provides a command telemetering link to a central recording site. The data are recorded, at both sites, in a digital format which assists in using automatic processing techniques in reducing the data. Temperature, conductivity, depth, plus current speed and direction, are the parameters originally selected but provision is made for additional sensors to be added as the requirements dictate. Special solid state electronics are employed in a simple bridge-scanner combination to digitize the sensor outputs.

The intent of this programme is to develop a system for esturine and near shore studies having the capability of also being useful for deep ocean survey programmes. The prototype is now undergoing laboratory evaluation prior to the procurement of additional units. Field testing and project assignments will begin as soon as the weather permits.

Development of an Ocean Data Station

R. F. DEVEREUX, H. Q. DRISCOLL, K. N. JONES, R. F. KOSIC AND S. T. UYEDA. (*General Dynamics Convair Division, San Diego, California, U.S.A.*)

A discus-shaped, general-purpose buoy capable of gathering and transmitting oceanographic and meteorological data to remote shore stations has been developed for the U.S. Navy Office of Naval Research. Two prototypes of the buoy have been built and are undergoing sea tests. One of the prototype buoys has successfully withstood the forces of a hurricane in the Florida Current in 1965.

The buoy is intended for anchorage in deep water for long periods, with proficiency in gathering large quantities of scientific data and relaying it to shore upon demand. Its capabilities include the sensing of as many as 10 meteorological sensors and 100 sub-surface sensors, digitizing and storing the data, and telemetering the data to shore stations up to 2500 miles away. Propane-powered engine/generators aboard the buoy provide electrical power for all buoy systems for at least one year without maintenance.

A network of buoys such as these, stationed in strategic locations, can gather synoptic oceanographic and meteorological data of value to the scientific community.

V.L.F. Relative Navigation

J. H. STANBROUGH, JNR. (*Woods Hole Oceanographic Institution, Woods Hole, Massachusetts, U.S.A.*)

An experimental long-range relative navigation system has been employed on the Research Vessel *Atlantis II* of the Woods Hole Oceanographic Institution during Cruise 8 to the Indian Ocean in 1963 and Cruise 15 which circumnavigated the globe in 1965.

The very low frequencies (v.l.f.) transmitted by stations having stabilized carriers (a few parts in 10^{11}) are attenuated to a much less degree than higher frequencies and can be received throughout the world. The v.l.f. transmissions provide navigational information from the comparison of the received signals of two or more stations with a precision oscillator which serves as a reference. Geographical changes result in phase changes which may be computed to longitude and latitude. Since a known starting point is required, the system is relative.

The *Atlantis II* was able to obtain the loan of a satellite navigation set from the U.S. Navy for Cruise 15. Reference points were supplied several times each day to the v.l.f. system, if needed. Best positioning agreed to within 1–3 nautical miles from best ship's position under favourable conditions. The system also was able to provide (1) a measure of ship's drift on station, (2) precise time and frequencies for the digital computer, data acquisition system, clocks and recorders, and (3) a calibration of the e.m. log while at sea.

A Position-Fixing Aid to Oceanography

J. K. V. LEE. (*The Decca Navigator Company Ltd., Survey Department, New Malden, Surrey.*)

The system known as 'Sea Fix' is employed both for local and for extensive oceanographic projects, and is virtually independent of weather conditions. It utilizes phase-comparison and time-sharing principles which enable it to operate on a single frequency in the hyperbolic or ranging mode. The transmitters are housed in small buoys, and the range is about 30 nautical miles when operating at 2 MHz. Accuracy in optimum coverage and still waters is better than 2 m.

A chain locks-in automatically and the relevant circuits are briefly described. Electronic components are

all solid-state and supplied from 24 V d.c. On account of the drawbacks of using conventional batteries in the buoyed stations, thermo-electric generators and fuel cells are being investigated.

A Chain was used to survey the sea-mount at Lat. 45°N and Long. 8°W on Cruise No. 11 of R.R.S. *Discovery* in April–May this year. The laying of the buoys, checking their positions and plotting the course of the vessel are described. As a result of depth soundings, contours of the sea-mount were drawn; magnetic, gravity and shallow seismic profiles were carried out concurrently.

Data Collection and Position Fixing from a Satellite

G. D. HOGAN AND M. R. TOWNSEND. (*National Aeronautics and Space Administration, Goddard Space Flight Center, Greenbelt, Maryland, U.S.A.*)

The use of a satellite for simultaneous position fixing and data collection is a tool of great potential benefit to the oceanographer. One such system, known as the Interrogation, Recording and Location System (I.R.L.S.), is being developed by the Goddard Space Flight Center of the National Aeronautics and Space Administration with its first launch scheduled early in 1968. Among the applications for this system are *in situ* measurements from buoys, both moored and drifting, and other unattended oceanographic stations; automatic data transmission from ships; and tracking of large marine animals.

Each platform is assigned an address and interrogated at a pre-determined time from the satellite when it is passing overhead. Position fixing, with an accuracy of $\pm$ 2 km, is accomplished by triangulation techniques based on knowing the position of the satellite and two sequential range measurements between it and the platform. After each range measurement, up to 1176 binary bits of data are transmitted by the platform and stored on the satellite, together with the ranging data and the time of interrogation. All these stored data are unloaded as the satellite passes over the ground acquisition and command station, where the data are processed and then disseminated to each user.

The paper describes the present system in detail along with current plans for testing, continues with a discussion of the second phase system scheduled to fly in 1969–1970, and discusses how interested experimenters may participate.

U.D.C. 621.397.62

The 1964 B.R.E.M.A. Colour Television Home Viewing Tests

By

R. N. JACKSON,†

K. E. JOHNSON, B.A. (*Graduate*)†

AND

B. J. ROGERS‡

Summary: During the summer and autumn of 1964 the British Radio Equipment Manufacturers Association (B.R.E.M.A.) carried out extensive tests of N.T.S.C. colour television receivers, to assess their performance under typical domestic operating conditions. This paper describes the organization of these tests and records the results obtained. It was found, somewhat unexpectedly, that the viewers found the (u.h.f.) tuning controls easy to use and this may be regarded as very satisfactory since the quality of the picture obtained was good.

1. Introduction

At a meeting of Study Group XI of the C.C.I.R. in London during February 1964 doubts were raised concerning the reliability and stability of colour receivers for the N.T.S.C. system in the hands of ordinary viewers. Although there have been numerous tests and demonstrations of colour television for a number of years, these have almost invariably omitted this most important aspect: the ordinary viewer and his reactions.

Information was required to fill this gap in the industry's experience. Although there were many N.T.S.C. receivers in use in the U.S.A., the information available from that source was not considered to be adequate to meet this requirement. It was therefore decided that tests should be carried out co-operatively by the members of the British Radio Equipment Manufacturers' Association (B.R.E.M.A.) and the results made available to the C.C.I.R.

The tests were designed to establish, in the hands of non-technical viewers and as far as possible under normal domestic viewing conditions, the following aspects of N.T.S.C. colour television reception and receivers:—

(i) Controllability
(ii) Picture quality
(iii) Reliability

B.R.E.M.A. placed the organization of these tests in the hands of its colour television sub-committee. Since this sub-committee was rather large to handle day-to-day details a small working party, consisting of the authors of this paper, was given the task of designing and managing the tests. The work was divided into three parts.

(i) The experimental design: This was agreed by the sub-committee, following a suggested plan formed by the authors.

(ii) The operation of the tests: This was carried out by the individual member companies of B.R.E.M.A. However, overall responsibility for the organization, monitoring of signals and liaison with the B.B.C. was the task of Rank-Bush-Murphy Ltd.

(iii) The computation and analysis of results: This was carried out by the Mullard Research Laboratories.

The scale of the tests, in terms of how many receivers, viewing sites, questionnaires, etc., should be used was the subject of much discussion in the early stages of planning. A compromise solution had to be found which would produce significant results without imposing impossibly difficult problems of receiver installation and of analysis. The decision to employ a digital computer for analysis of the data simplified this. However, it was still necessary to arrange for some preliminary tabulation of the results by the participating companies in order to reduce the amount of data to be punched for input to the computer and to ensure a fast return of results at the end of each six-week period. This last requirement was further aided by arranging for the computer to print out the results in a standardized and readily assimilable manner. Each manufacturer then received copies of the actual 'print-up' of results.

Details of the numbers of receivers, sites and questionnaires are given in the appropriate sections below, but some preliminary idea of the scale of the exercise may be gained from the fact that in all some 1660 returned questionnaires (containing 34 000 separate pieces of data) were processed during the total period of the tests.

† Mullard Research Laboratories, Redhill, Surrey.
‡ Rank-Bush-Murphy Ltd, Chiswick, London, W.4.

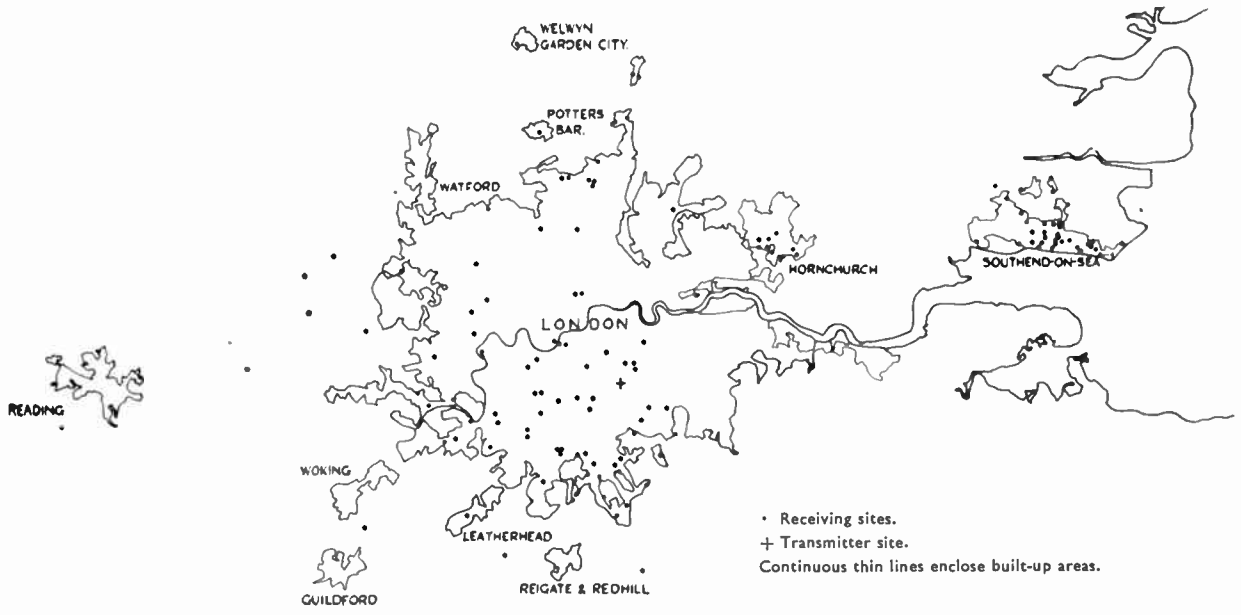

Fig. 1. Map showing location of receiving sites.

2. The Organization of the Tests

The tests started on the 6th July 1964 and ended on the 13th November 1964. They were divided into three consecutive six-week periods. The same receivers but different locations were used for each period; thus each receiver was used at three locations.

2.1. *Choice of Receiving Locations and Viewers*

Each of the manufacturers contributing colour receivers to the tests was responsible for selecting suitable locations. One method used was to approach retailers for suitable addresses. An alternative method was to use 'friends of friends' of employees of the contributing manufacturers. However, the following groups of persons were not accepted to take part in the tests:

(i) Persons employed technically in the field of television.

(ii) Persons employed by any of the companies manufacturing television receivers or equipment, even in a non-technical capacity.

(iii) Persons employed by either the B.B.C., the I.T.A. or any of the I.T.A. programme contracting companies.

Since the primary purpose of the tests was to assess controllability, no address was used where the received colour picture or monochrome picture was worse than grade three on the E.B.U. standard six-point quality scale (see Table 5, scale (ii)); only one such site was found. This precaution avoided confusion between controllability and other factors resulting from the receiving conditions.

A total of 42 receivers was used at 127 sites. Six manufacturers took part and provided, on average, the following numbers of receivers: 12 receivers each were provided by three of the manufacturers, one manufacturer provided four, and the remaining two manufacturers one each. Details of these receivers are given in Appendix 1.

Figure 1 is a map showing the receiving locations.

2.2. *Programme Timing and Content*

The colour transmissions were made at the close of the B.B.C.-2 programme on three evenings per week and, to give daylight viewing experience, on Sunday afternoon.

The programme timing was as follows:

0– 5	minutes	Colour bars
5– 6	,,	Announcement caption
6– 7	,,	'Ski Girl' slide (Slide U.S.A. 2)
7–13	,,	Announcer live from studio
13–33	,,	Documentary film
33–34	,,	Announcer live from studio
34–54	,,	Feature film (serialized)
54–55	,,	Announcer live from studio
55–56	,,	Closing caption
56–60	,,	Colour bars

This schedule was chosen to simulate so far as possible a typical programme. The reasons for the above choice of content were as follows:

Colour bars: Transmitted for transmitter adjustment and monitoring use *only*. (Viewers were instructed not to make adjustments on this signal.)

'Ski Girl' slide: A colour picture of repeatable high quality, whose accuracy could be verified by measurement.

Live studio: Provided naturalness and very high quality pictures with areas of high saturation.

Documentary film: Chosen for highest quality colour on film.

Feature film: Included for programme interest since it was not possible under existing conditions to combine programmes of general interest with the best colour quality in one film.

The complete series of films was repeated twice in each period, that is, every three weeks.

All transmissions were radiated from the B.B.C. Crystal Palace transmitter on Channel 33. The modified N.T.S.C. colour standard was used throughout the tests as specified in the B.B.C. document—'Specification of monochrome and colour television standards for experimental 625-line transmissions, March 1963'.

The programmes were originated from the B.B.C. Lime Grove studios.

2.3. *Monitoring*

An independent monitoring station was set up in Forest Hill (South-East London) approximately 3·5 km air-line from the transmitter, to provide a complete record of all transmissions, and for correlation purposes.

The following equipment was used: Two 10+10 element stacked Yagi arrays were mounted well above roof level and some 40 feet apart. They were carefully installed to give a clean signal of approximately 15 mV. A further 8+8 element stacked Yagi array was mounted on a portable mast and could be located anywhere in a garden of approximately 120 ft × 40 ft. This provided a double check for any effects that might be attributable to propagation.

Two professional quality receiving units provided composite encoded video signals. These could be switched to drive a vectorscope, an oscilloscope or two decoding monitors. A locally-generated encoded colour signal was available.

The vectorscope and oscilloscope were fitted with a recording camera, and photographic records of instrument indications were made at the start, during and at the end of all transmissions. The results obtained at the independent monitoring station were compared with those obtained by the B.B.C.'s monitoring of the transmission, and were shown to be within the tolerances of the instruments in use.

2.4. *Method of Assessment*

2.4.1. The controls

The use of three controls was assessed, namely:

(i) Tuning
(ii) Colour intensity (saturation)
(iii) Hue

These names for the controls were standardized for use throughout the tests and the controls on the receivers were labelled accordingly.

2.4.2. The questionnaires

The viewers' reactions were assessed by means of two types of questionnaires. Only the person operating the receiver can assess 'Controllability', so a simple questionnaire was produced for the operator's use. This questionnaire also asked whether the viewing room was illuminated and if light fell on the viewing screen. The questionnaire is reproduced in Appendix 2 (Form 1).

As other viewers would be present a second short questionnaire was designed for picture quality assessments. This was to be filled in by both the operator and any other viewers present. This questionnaire also asked for an assessment of the monochrome picture produced by the colour receiver. This was to ensure that the assessment of the colour picture was not influenced by a poor grey scale or by misconvergence. The distances from the screen at which the pictures were viewed were also recorded on this questionnaire, which is reproduced in Appendix 3 (Form 2).

The installing engineer also filled in a questionnaire giving an assessment of picture quality, more details of the viewing conditions and any additional information worth recording. This questionnaire is reproduced in Appendix 4 (Form 3).

2.5. *The Test Procedure*

The user was instructed by the installing engineer as to the operation of the receiver and the use of the questionnaire. A document was left at each address containing operating instructions and describing the use of the questionnaires. In order to avoid the initial period after installation when viewers tend to be insufficiently critical, and to allow them to become familiar with the operation of the receiver, questionnaires were not to be filled in during the first week after installation. Thereafter it was requested that one operator's questionnaire and three viewers' questionnaires be filled in for each of the remaining five weeks.

After the initial warm-up period the user was instructed to tune the receiver correctly to Channel 33, to detune to a specific channel, then to retune to Channel 33. This was to simulate the tuning operations required when more than one transmitter radiates

a programme. The user was instructed not to make any adjustments during the radiation of the colour bar signal or the announcement caption. Viewers were instructed to make the 'initial adjustments', if necessary, *after* the announcement caption. These adjustments, and the number of others coincidental with programme changes or for other reasons, were to be recorded on the questionnaire. Finally, the 'ease of adjustment' assessment and the answer to the question on room illumination were to be recorded.

3. The Test Results

The results are presented here under the three main headings of Controllability, Picture Quality and Reliability. The Controllability results are based on replies from a total of 499 questionnaires (Form 1, Appendix 2) The results for Picture Quality are based on replies from 1161 questionnaires (Form 2, Appendix 3). The Reliability data are based on records kept by the engineers-in-charge of the receiver installation and maintenance.

The viewing times recorded on the questionnaires show that these results are based on a total of approximately 1600 man-hours of viewing. However, there is evidence that, apart from these recorded occasions when viewers were filling in questionnaires, the receivers were used extensively for viewing B.B.C. programmes in monochrome and on other occasions for colour transmissions.

Before proceeding to the main results, however, the data are presented first concerning the viewing distances and lighting conditions, obtained from the questionnaires. These are presented first since they are essential to the proper interpretation of the other results.

3.1. *Viewing Conditions*

3.1.1. Viewing distance

A histogram giving the percentage of viewers sitting at a given distance from the receiver screen is shown in Fig. 2. The mean viewing distance was 9·58 ft (2·92 metres) with a standard deviation of 2·48 ft (0·76 metres). The average height of a picture displayed on the (21 in) screens of the receivers used was found to be 15 in.

The distribution of viewing distances shows some interesting features. It appears to be bi-modal with a main mode at 10 ft (24·0%) and a much smaller mode at 15 ft (2·2%). The unexpectedly large number of viewers sitting at 18 ft (1·7%) arose almost completely from one site. Viewing distances recorded at a given site were in general much more widely scattered than at this site. The viewers showed a very marked reluctance to record a viewing distance of 13 ft (0·3%) and the distribution is almost divided into two distinct parts at this value. Lesser minima also occur at 9 ft and 11 ft.

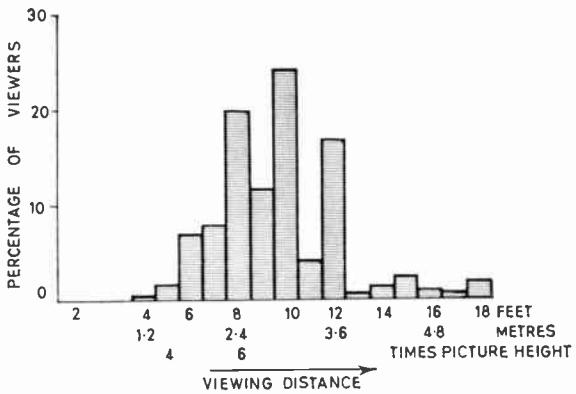

Fig. 2. Distribution of viewing distances showing the percentages of viewers sitting at given distances from the receiver screen.

The major part of the distribution (below 13 ft, representing 93·7% of viewers) resembles in its overall shape a normal distribution with values of mean and standard deviation close to those quoted above for the whole distribution, but truncated at 13 ft. This truncated shape is almost certainly due to the limitation placed on maximum viewing distance by the size of the average living room.

In connection with these results there is no reason to suppose that this distribution was unduly influenced by large numbers of viewers viewing simultaneously at one site. Such conditions, as judged by the number of viewers filling in 'ordinary viewer' (Form 2, Appendix 3) forms at a given site on a given date, occurred on only one or two occasions out of the total of 499 viewing sessions. (This figure for the number of viewing sessions assumes that one Questionnaire Form 1 and one Questionnaire Form 2 were filled in by every controlling viewer for each viewing session, as was requested in the instructions to the viewers.) In general a typical figure for the number of viewers at a given session was two.

These results for viewing distance are believed to agree fairly closely in all their major features with the results of recent tests carried out by both the B.B.C. and the Swiss P.T.T. (unpublished at the time of writing).

3.1.2. Ambient illumination

The controlling viewer was asked two questions concerning ambient illumination (Questions 5 and 6, Form 1, Appendix 2):

'Were there any room lights on?'

'Did any light—including daylight—fall directly upon the screen?'

For 66·3% of viewing sessions the room lights were on (answer 'Yes' to question 5). Examination of the

engineers' report forms (Question 4, Form 3, Appendix 4) showed that the majority of these lights were tungsten; only seven sites out of the total of 127 sites had fluorescent lighting.

An analysis of the answers to Question 6 for those occasions when no room lights were on (answer 'No' to Question 5) showed that 28·9% of the viewing sessions took place under dark viewing conditions (answer 'No' to Question 6), while 4·2% of the viewing sessions took place in daylight with some light falling directly on the screen (answer 'Yes' to Question 6).

Further analysis of the ambient illumination data with reference to the picture quality obtained is given in Section 3.3 of this paper.

3.2. *Controllability*

Controllability was assessed by determining the number of control adjustments made and the ease or difficulty experienced in making them.

3.2.1. Number of adjustments

The viewers in control of the receivers were asked to state how many times they made adjustments to the tuning, colour intensity and hue controls, and to say whether they were 'initial adjustments' made at the start of the colour programme or if they were 'occasioned by a programme change' or for some 'other reason'.

(a) Tuning: Table 1(a) gives a summary of the total adjustments made to the tuning control for all reasons.

The distribution shown in Table 1(a) indicates that there was a strong tendency, on the part of the controlling viewers, to make either no adjustments or very few adjustments to the tuning control. In 73% of all sessions no adjustments were made for any reason. This distribution has been found to be in good agreement with the theoretical distribution known as Poisson's distribution.

Poisson's distribution has the general form:

$$1 = e^{-z}.e^{z} = e^{-z}\left(1 + z + \frac{z^2}{2!} + \frac{z^3}{3!} + \ldots\right)$$

where z is the average number of occurrences of an event (e.g. adjustment of the tuning control). The probability of this event occurring 0, 1, 2, 3,..., etc., times is then given by the successive terms of expansion:

$$e^{-z}, \quad ze^{-z}, \quad \frac{z^2}{2!}.e^{-z}, \quad \frac{z^3}{3!}.e^{-z}\ldots\text{etc.}$$

The average number of adjustments per viewing session of the tuning control was (from Table 1(a)) 0·35. Using this value for z Table 1(b) was derived.

The Poisson distribution has been found to describe quite closely the occurrence of isolated events in a continuum. Its appropriateness in this instance is interesting and suggests that the expected percentages of adjustments (one, two, three times, etc) are constant from session to session. This in turn implies that there is little variation in the *motivation* for making tuning adjustments from session to session; such factors as programme quality, reception conditions, etc., contributing only slightly to the reasons for adjustment. This is borne out by the break-down of adjustments according to reasons which is given in Table 1(c). Further discussion on this point is given in Section 3.2.3.

Table 1(a)

Adjustments to the TUNING control

Number of adjustments	0	1	2	3	4	5	6
Percentage of viewing sessions in which the above number of adjustments was made	73%	21%	4%	2%	0	0	0

Table 1(b)

Number of adjustments	0	1	2	3	4	5
Probability	0·70	0·245	0·04	0·01	0	0
Expected per cent of viewing sessions	70	24·5	4	1	0	0
Actual per cent of viewing sessions	73	21	4	2	0	0

Table 1(c)

	Percentage of viewing sessions in which the given number of adjustments was made		
	(i)	(ii)	(iii)
Number of adjustments	At the start of the colour programme	Due to a programme change	For any other reason
0	76%	95%	95%
1	24%	4%	4%
2	—	1%	1%
3	—	0	0

(b) Colour intensity: A summary of the total adjustments to the colour intensity control for all reasons is given in Table 2(a).

The distribution for the colour intensity control indicates the same general tendency of the viewers to make few or no adjustments, as in the case of the tuning control. On 44% of viewing sessions no adjustments were made at all to this control and on 73% of sessions one or no adjustments were made. However, in this case the agreement with Poisson's distribution is not so good. This suggests that there are more disturbing

Table 2(a)

Adjustments to the COLOUR INTENSITY control

Number of adjustments	0	1	2	3	4	5	6
Percentage of viewing sessions in which the above number of adjustments was made	44%	29%	14%	6%	3%	3%	1%

Table 2(b)

Number of adjustments	Percentage of viewing sessions in which the given number of adjustments was made		
	(i) At the start of the colour programme	(ii) Due to a programme change	(iii) For any other reason
0	51%	77%	83%
1	49%	16%	8%
2	—	6%	8%
3	—	1%	1%
4	—	0	0

factors, which result in the expected percentages of adjustments not being constant from session to session. Table 2(b), which gives a break-down of the replies concerning adjustments to the colour intensity control, according to reasons for adjustment, tends to confirm this point (see Sect. 3.2.3).

(c) Hue: The results for the hue control are very similar to those for the colour intensity control and the same remarks concerning the distribution of adjustments apply. The summary of total adjustments for all reasons is given in Table 3.

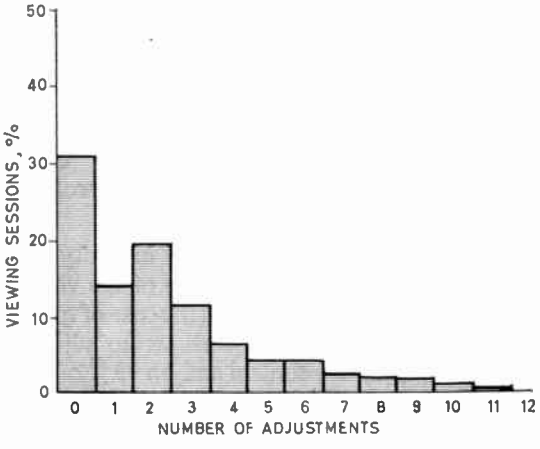

Fig. 3. Adjustments to all three controls.

Table 3(a)

Adjustments to the HUE control

Number of adjustments	0	1	2	3	4	5	6
Percentage of viewing sessions in which the above number of adjustments was made	45%	30%	13%	5%	3%	3%	1%

On 45% of sessions no adjustments to the hue control were made for any reason; on 75% of sessions one or no adjustments were made. Details of the hue control adjustments are given in Table 3(b).

Table 3(b)

Number of adjustments	Percentage of viewing sessions in which the given number of adjustments was made		
	(i) At the start of the colour programme	(ii) Due to a programme change	(iii) For any other reason
0	49%	79%	83%
1	51%	14%	7%
2	—	5%	8%
3	—	2%	2%
4	—	0	0

3.2.2. Adjustments to all controls

Some further figures have been derived relating to the total number of adjustments made to any of the three controls for any reason, during the test sessions. These figures are shown in histogram form in Fig. 3. Here the vertical columns represent the percentage of viewing sessions in which the number of control adjustments indicated on the horizontal axis took place. This distribution is more extended than those for the individual controls, more sessions in which multiple control adjustments were made being recorded. This is expected since more than one control could be adjusted in any given session. However, the distribution again shows the same general tendency for there to be many sessions in which there were few adjustments. On 31% of the viewing sessions there were no adjustments at all made to any control and on 45% of sessions one or no adjustments were made.

It is interesting to note that there is a slight subsidiary mode for two adjustments per viewing session. This may possibly be explained by a tendency of viewers to adjust the hue and colour intensity controls in association with one another.

3.2.3. Reasons for adjustments

Another point of interest concerns the reasons why the viewers made control adjustments. A breakdown

of the total number of adjustments made, according to the reasons for adjustment is given in Table 4.

Table 4

Reasons for adjustments

	Tuning	Intensity	Hue	Total
Initial adjustment	9·3%	18·8%	19·5%	47·6%
Programme	2·7%	12·8%	12·4%	27·9%
Other	2·7%	10·5%	11·3%	24·5%
Total	14·7%	42·1%	43·2%	100·0%

Percentage adjustments to three controls
100% = 1300 adjustments

A word of caution must be given here about the interpretation of these figures. So far the figures given (Tables 1(a), 2(a) and 3(a)) have been in terms of the *percentage of viewing sessions* in which a given number of control adjustments were made. The figures in Table 4, however, are in terms of the *percentage of (all) adjustments* made for a given reason.

As can be seen from the table, 48% of all the control adjustments were made at the start of the colour programmes ('initial adjustments'); 28% were 'occasioned by programme changes' and 24% were for 'other reasons'. However, only 15% of all adjustments were tuning control adjustments.

3.2.4. Ease of adjustment

It was considered to be a most important objective of these tests to obtain some data as to the ease or difficulty experienced by the viewers in making control adjustments. With this in mind a search was made for a suitable opinion rating scale which could be used for this assessment. However, no suitable scale could be found. In the absence of a scale specifically designed for assessing ease of operation, the use of the standard E.B.U. quality rating scale (Scale (ii), Table 5) was considered. However, this was rejected as not being well-suited for this particular task. Finally a new six-point scale was devised to meet the need (Scale (iii), Table 5).

Initially the relative merits of this six-point scale and similar five-point and seven-point versions were considered. Difficulty was experienced in choosing a suitable phrase for the mid-point of these odd numbered scales and the six-point version, which had the advantage of being similar in form to the standard quality scale (also used in these tests) was decided upon.

3.2.5. Laboratory tests of ease and difficulty scale

Before the new scale was finally agreed and questionnaire forms were printed, a laboratory experiment was carried out to test the use both of this scale and the form of question used in the questionnaire.

Table 5

Subjective comment scales used for the tests

(i) *Impairment*
1. Imperceptible
2. Just Perceptible
3. Definitely Perceptible, but not Disturbing
4. Somewhat Objectionable
5. Definitely Objectionable
6. Unusable

(ii) *Quality*
1. Excellent
2. Good
3. Fairly Good
4. Rather Poor
5. Poor
6. Very Poor

(iii) *Ease or Difficulty*
1. Very Easy
2. Easy
3. Fairly Easy
4. Rather Difficult
5. Difficult
6. Very Difficult

In this laboratory test, three non-technical observers each made six trials in which they adjusted the hue and colour intensity controls of a laboratory N.T.S.C. decoder. Before each trial the controls were deliberately maladjusted to simulate a possible field condition. Nine conditions of maladjustment were used, each condition being encountered twice over the whole series of trials (all observers). The sequence of conditions was decided by a random selection from a set of numbered counters. Two still pictures were used, one showing a close-up portrait and the other a bowl of fruit.

The results of this test are given in Fig. 4 which shows histograms of the percentage of comments occurring in each of the given scale grades (1 to 6) for each control. The mean rating found for the hue control in this experiment was 2·43 and for the colour intensity control 2·33. Thus both controls were rated as between 'fairly easy' and 'easy' to adjust.

As is shown below these laboratory test results turned out to be pessimistic when compared with the actual field test results. The 'average viewer' in the field trials found the controls rather easier to adjust than did the test observers. However, it was established that the scale was satisfactory for use by non-technical viewers and the test therefore fulfilled its main purpose.

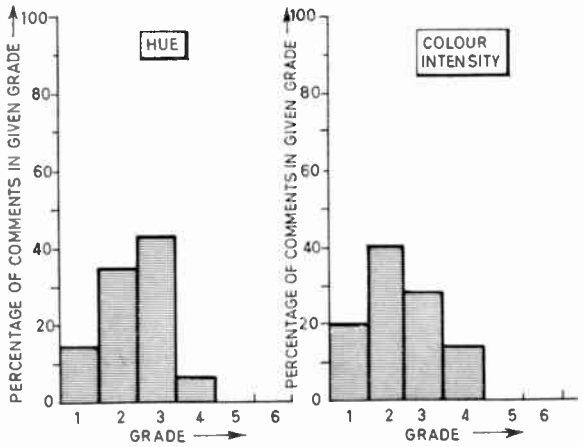

Fig. 4. Results of laboratory experiment to test scale of ease/difficulty.

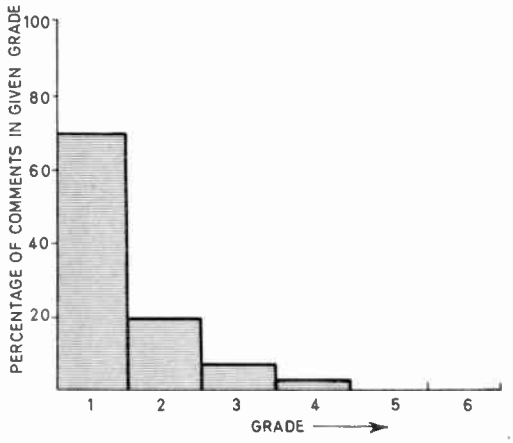

Fig. 5. Distribution of comments for 'Ease of Adjustment' of the tuning control.

For comparison each of the observers also assessed the ease of adjustment of the tuning control of a v.h.f. radio receiver using the same scale.

The mean rating achieved was 1·67 in this case, but this result should be treated as very approximate since it is the result of only six trials in all (two per observer).

3.2.6. Field test results

In the actual field tests the question asked on the controlling viewers' questionnaires (Question 4, Form 1, Appendix 2) was as follows:

> 'Please describe the EASE or DIFFICULTY of adjustments of any controls used, in accordance with Scale (iii) below.'

There were 410 replies to this question for the tuning control, 434 for the colour intensity control, and 436 for the hue control. Histograms for the results obtained for all three controls are shown in Figs. 5, 6 and 7(a).

(a) Tuning (Fig. 5): The mean rating for the ease of adjustment of the tuning control was 1·43 with a standard deviation of 0·78 grade. The percentage of comments in the adverse grades 4, 5 and 6 was 2·7%. The distribution shows a pronounced mode (peak) at grade 1 and the mean rating corresponds to mid-way between 'Very Easy' or 'Easy' on the scale. Ninety per cent of the sample rated the operation of the tuning control as 'Very Easy' or 'Easy'.

(b) Colour intensity (Fig. 6): The mean rating for the ease of adjustment of the colour intensity control was 1·82 with a standard deviation of 0·95 grade. The percentage of comments in grades 4, 5 and 6 was 5·1%. The mean rating corresponds to rather better than 'Easy' on the scale and 76% of the sample rated the operation 'Easy' or 'Very Easy'.

(c) Hue (Fig. 7(a)): The mean rating for the ease of adjustment of the hue control was 1·86 with a standard deviation of 0·98 grade. The percentage of comments in grades 4, 5 and 6 was 5·5%. The mean rating again corresponds to rather better than 'Easy' on the scale and 75% of the sample rated the operation 'Very Easy' or 'Easy'.

In Fig. 7(b) the corresponding histogram for the laboratory test referred to above is also shown for comparison. The difference between the laboratory results and the field test results can be clearly seen.

3.3. *Picture Quality and Consistency*

3.3.1. Colour picture quality

The viewers were asked the following question concerning the quality of the colour picture (Question 2(a), Form 2, Appendix 3):

> 'If you have been viewing a colour programme will you please say, using Scale (ii) [the standard E.B.U. six-point quality scale, Table 5], what in your

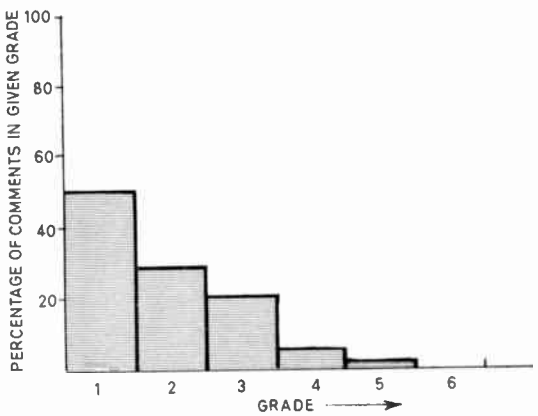

Fig. 6. Distribution of comments for 'Ease of Adjustment' of the colour intensity control.

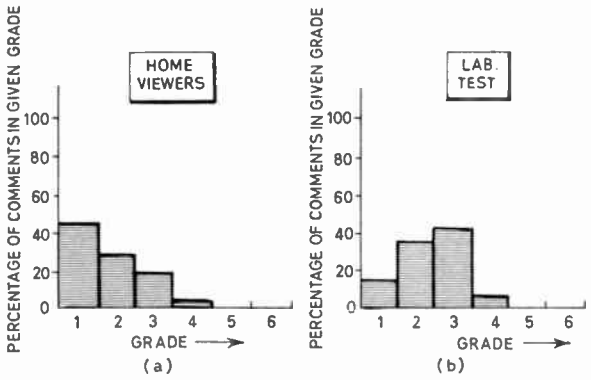

Fig. 7. Distribution of comments for 'Ease of adjustment' of the hue control.

opinion was the overall quality of the colour picture.'

The total number of replies to this question was 1149. A histogram of the percentage of viewers' replies in a given grade plotted as a function of the grade is shown in Fig. 8. The mean quality rating was 1·75 with a standard deviation of 0·75 grade. The number of replies in grades 4, 5 and 6 was 1·5%. This mean rating corresponds to a picture quality rather better than 'Good'.

The installing engineers were also asked to assess the colour picture quality (Question 2(b), Form 3, Appendix 4). The distribution of their replies is shown in Fig. 9. The mean rating was 1·74 with a standard deviation of 0·61 grade. There were no replies in grades 4, 5 and 6, by design (see Sect. 1 on choice of receiving locations). The mean rating given by the engineers agrees very closely with that given by the ordinary viewers.

3.3.2. Comparison with previous tests

It is interesting to compare these results with the results of previous N.T.S.C. field tests such as those

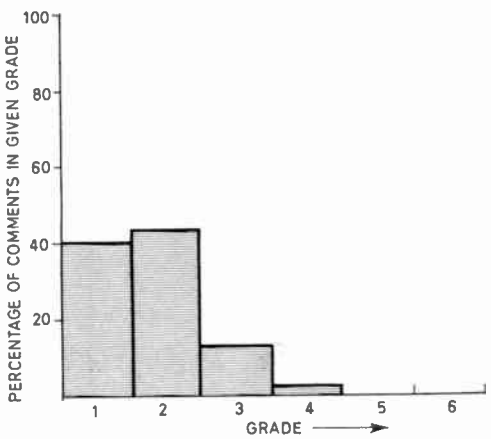

Fig. 8. Distribution of comments for colour picture quality.

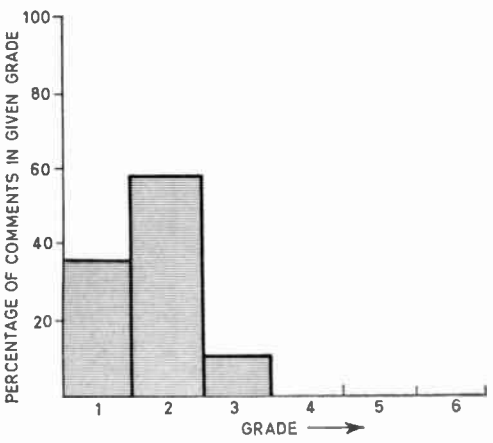

Fig. 9. Distribution of engineers' comments for colour picture quality.

conducted by the B.B.C. in 1956–57 (using technical and non-technical observers) and in 1962–63 (using selected observers including engineers). Figures 10(a), (b) and (c) show histograms for the overall colour picture quality assessments obtained in these two series of tests,[1, 2] compared with the corresponding data for the present test. The means for these distributions are 1·82 for the 1956–57 tests and 1·96 for the 1962–63 tests, with standard deviations of 0·67 and 0·92 grade, respectively. This compares with a mean of 1·75 and standard deviation of 0·75 for the B.R.E.M.A. test. Applications of 'Student's t-test' to these means shows that there is a chance of just less than one in four of the difference between the 1956–57 series of tests and the B.R.E.M.A. tests being due to random causes. This is not sufficiently unlikely for the difference to be regarded as significant.

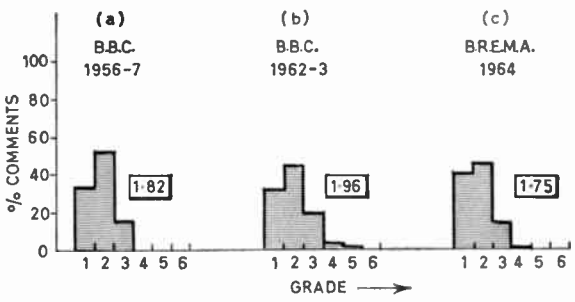

Fig. 10. Comparison of assessments of colour picture quality in various tests.

The 1962–63 tests, however, produced a mean rating significantly higher than the present series; that is, the picture quality was judged to be worse. The chance of this difference being due to random causes is less than one in a thousand.

3.3.3. Variation of quality with ambient illumination

An analysis was also made of viewers' ratings of colour picture quality during the full duration of the B.R.E.M.A. test for the following conditions of ambient illumination:

(a) dark viewing conditions;

(b) daylight viewing with some light falling directly on the screen;

(c) all other viewing conditions (which in practice may be taken to be tungsten lighting).

The mean ratings and standard deviations found were, respectively, for

(a) 1·62 and 0·70 grade, based on 227 replies; for

(b) 1·79 and 0·91 grade, based on 34 replies; and for

(c) 1·78 and 0·75 grade, based on 888 replies.

None of these means is statistically significantly different from any of the others or from the overall mean of all the conditions taken together. (The probability level for means to be considered significantly different was arbitrarily chosen to be 10% (or 1 chance in 10).) However, there was some tendency for dark viewing conditions to give a rather better mean rating of colour quality than any of the other conditions, and for daylight viewing conditions, with light falling directly on the screen, to yield a slightly poorer mean rating than average, as would be expected.

3.3.4. Consistency

In connection with the question on colour picture quality the viewers were asked the following question (Question 2(b), Form 2, Appendix 3):

'Was it [i.e. the colour picture quality] consistent throughout the programme?'

Seventy-eight per cent of the 1131 replies to this question stated that the quality was consistent throughout the programme.

3.3.5. Relations between consistency and picture quality

An analysis of a small sample of 108 of these replies was made to investigate if there was any relation between viewers' ratings of colour quality and their opinions about its consistency. For the 87 favourable replies to the consistency question there was a corresponding mean quality rating of 1·52 with a standard deviation of 0·55 grade. For the remaining 21 unfavourable replies the mean rating was 1·86 with a standard deviation of 0·48. There is a chance of only one in a hundred that the difference between these means was due to random causes. It therefore seems very likely that viewers' ratings of colour quality were related to their opinions about its consistency. It is worth noting that even on those occasions when the quality was judged to be inconsistent, the mean rating it achieved was still rather better than 'good'.

A further analysis of the replies to this question was made to investigate some possible factors which could have affected the consistency. The factors considered were:

(i) variations between receiver types;

(ii) variations of transmission quality;

(iii) variations of the colour quality of the programme material (e.g. of some of the films);

(iv) omission of the recommended setting-up slide (slide U.S.A. 2, 'Ski Girl').

This analysis was carried out on the results of the first 12 weeks of the tests only except for condition (i) which was also checked at 18 weeks.

3.3.6. Variations between receiver types

The procedure adopted for this factor was as follows. The figures for the consistency of colour quality from each receiving location were used to calculate a mean consistency for each receiver type. These means were compared for statistically significant differences between each of them in turn, and between each of them and the overall consistency for all receiver types. No statistically significant difference was found (assuming a 10% significance level as above). It was therefore judged unlikely, on this assessment, that differences between receiver types were a major influence on the overall consistency of the colour picture quality.

Further analysis of the consistency of picture quality of different receiver types after the completion of the third test period revealed a significant difference between the types achieving the highest and lowest average performances. This, however, could be attributed to two particular receivers which performed badly in the third period only. The conclusions reached after 12 weeks and reported above remain valid after 18 weeks if these two receivers are excluded.

3.3.7. Transmission quality, programme quality and setting-up

For the remaining three factors investigated the following procedure was adopted. The records of the independent monitoring station (see Sect. 2) were scanned to find days on which entries which could be attributed to any of these factors had been made. A fourth group of days was also noted on which both transmitter performance and programme quality were completely satisfactory. The viewers' results were then used to find a figure for the mean consistency for each of the four groups of days. These means were compared for statistically significant differences.

It was found that there was no significant difference (again assuming a 10% significance level) between the mean consistency for the completely satisfactory days

(based on 148 replies) and those for the days on which transmission quality had been variable (136 replies). However, for the days on which certain films were transmitted the mean consistency (based on 154 replies) showed a sufficient difference from that for the completely satisfactory days for there to be a chance of less than one in ten of this difference arising from random causes. In particular further analysis showed that one film contributed very largely to this difference; the mean consistency for days on which this film was transmitted (based on 84 replies) was sufficiently different from that for the completely satisfactory days for there to be a chance of less than one in twenty of the difference arising from random causes.

When the mean consistency for the days on which the recommended setting-up slide was omitted (based on 87 replies) was compared with that for the satisfactory days a further significant difference was found. The likelihood of this difference being due to random causes was less than one chance in forty.

To summarize this analysis of the first 12 weeks' results: differences between receiver types and variations of transmission quality do not appear to have contributed largely to viewers' judgments of the consistency of the colour quality. The quality of the programme material, however (in particular that of one film), and omission of the recommended setting-up slide appear to have had a significant effect on judgments of consistency.

3.3.8. Monochrome picture

This series of home-viewing tests was not designed to investigate the question of compatibility. Nevertheless it was important in these tests to know how well the colour receivers performed on black and white pictures, since good monochrome performance is a pre-requisite of good colour performance. This was measured in two ways.

In the first method the installing engineer was asked to assess the overall monochrome picture quality according to the six-point quality scale used by the ordinary viewers (see Question 2(a), Form 3, Appendix 4). The distribution of the engineers' replies is shown in Fig. 11. The mean quality rating was 1·66 with a standard deviation of 0·60 grade. The number of replies in grades 4, 5 and 6 was zero, by design (see Sect. 1). The engineers' rating of monochrome picture quality thus showed a slight improvement on their rating of colour picture quality, but the difference was not statistically significant at the 10% level.

The second method was used to test whether good adjustment of the Shadowmask tube was maintained throughout the test period. The ordinary viewers were asked two questions (Questions 1(a) and (b), Form 2, Appendix 3):

'If you have been viewing a black and white programme, will you please say:

(a) Using Scale (i) [six-point E.B.U. impairment scale] did the picture have a colour cast?

(b) If so, did this cover the whole screen area?'

The object of these questions was to assess what colour error, if any, was noticed by the viewers. The results are therefore of interest mainly from the point of view of the performance of a particular set at a particular site. No receiver behaved so badly during any test period that the results from it had to be rejected.

The complete distribution of viewers' comments is, however, of some additional interest in providing, together with the engineers' comments, a measure of the overall standard of adjustment of the display tubes throughout the tests. This distribution is shown in Fig. 12, and represents replies from 920 viewers. The mean impairment rating was 1·94 with a standard deviation of 0·73 grade. The percentage of replies in

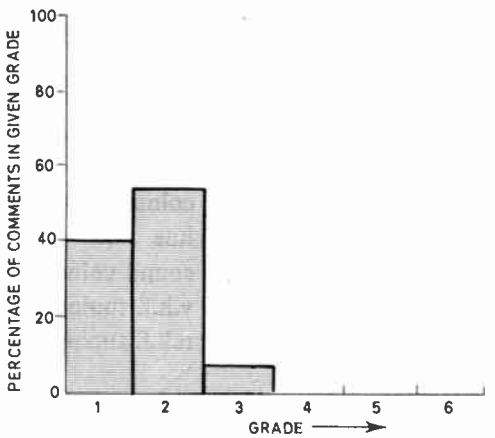

Fig. 11. Distribution of engineers' comments for monochrome picture quality.

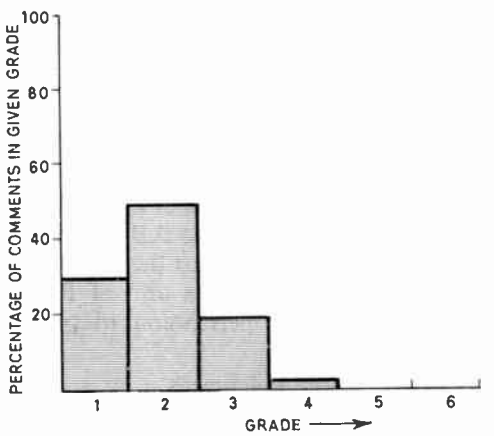

Fig. 12. Distribution of comments for impairment of the monochrome picture due to 'colour cast'.

grades 4, 5 and 6 was 0·7%. This mean rating corresponds to a 'just perceptible' picture impairment.

3.4. *Reliability*

Reliability could not be measured in the same way as controllability and picture quality. For this reason the conclusion is based on the experience of the installing engineers. This was that the receivers required very few adjustments or repairs. In all, only nine service calls were made, and the faults found were of a trivial nature, such as a broken thermistor and an open-circuit boost capacitor. Details of these faults are given in Appendix 5.

4. Conclusions

So far as the authors are aware the test described here was the first major controlled test of colour television carried out entirely with unskilled viewers in their own homes. Although a large scale audience reaction test using unskilled viewers was carried out by the Radio Corporation of America in 1952,[3] the viewers were then seated in viewing booths in a theatre lounge, a condition which the authors considered to be somewhat artificial. No great difficulty was experienced in conducting the B.R.E.M.A. test with normal domestic viewing conditions.

The results presented in the preceding section are the conclusions of the experiment and need little further comment; however, we feel that one feature should be highlighted. The results show that the viewers found the (u.h.f.) tuning controls easy to use. While it is true that the majority of the receivers used had some form of aid to tuning, a separate analysis has shown that even for those receivers without any tuning aid 71% of comments were that the tuning was 'Very Easy' or 'Easy' and there were only 6·5% of adverse comments. This result was somewhat unexpected and may be regarded as very satisfactory since the colour picture quality obtained was good.

These results were presented to Study Group XI of the C.C.I.R. at its meeting in Vienna in March 1965.

5. Acknowledgments

The authors wish to express their thanks first of all to their colleagues in the member companies of the B.R.E.M.A. and in particular to the members of the colour television sub-committee and the secretariat, for the valuable part they played in the conduct of the tests. Thanks are also due to the B.B.C. who supplied all the test transmissions and to the directors of the Mullard Research Laboratories and of Rank-Bush-Murphy Ltd., for their permission to publish this paper.

6. References

1. W. N. Sproson, S. N. Watson and M. Campbell, 'The B.B.C. colour television tests: An appraisal of results', *B.B.C. Engineering Monograph* No. 13, May 1958. (See Appendix VII, Test 3, Part 2, 35 mm film only.)
2. W. N. Sproson, '1962–63 U.H.F. Home-viewing Tests: The Reception of Colour Pictures for Three Colour Television Systems". B.B.C. Research Department, Technical Memorandum No. T1061/1 (see p. 14, Table 2).
3. Federal Communications Commission, 'Petition of R.C.A. and N.B.C. Inc. for approval of color standards for the R.C.A. color television system', June 1953. Appendix E, p. 610, A Survey of Audience Reaction.

7. Appendix 1

7.1. *Brief Description of Receivers Used*

1. Provision of receivers

The number of receivers contributed by the various manufacturers was:

Manufacturers A, B and C	12 sets each
Manufacturer D	4 sets
Manufacturers E and F	1 set each

(The receivers provided by Manufacturers A and F were similar in detail.)

2. Front panel controls for viewer's use

A/F	B	C
brightness	brightness	brightness
contrast	contrast	
colour intensity	colour intensity	colour intensity; colour killer
hue	hue	hue
sound volume; tone	sound volume	sound volume; on/off mains
speech/music	a.f.c. switch	a.f.c. switch
colour killer		
on/off mains		
v.h.f. tuning	v.h.f. tuning	
u.h.f. tuning	u.h.f. tuning	u.h.f. tuning (push button)

D	E
brightness	brightness; on/off mains
	contrast
colour intensity	colour intensity
hue	hue
sound volume	sound volume
v.h.f. tuning	v.h.f. tuning
u.h.f. tuning	u.h.f. tuning

3. Range of the hue control

Manufacturer	A/F	B	C	D	E
Range in degrees	32°	70°	60°	90°	60°

4. Aids to tuning

A/F	B	C	D	E
magic eye	a.f.c.	push button tuner and a.f.c.	none	none

5. Types of i.f. detection and sound reception

(Inter-carrier sound reception is used unless otherwise stated.)

A/F (1) luminance
(2) chrominance and inter-carrier
(3) tuning indicator

B (1) common luminance/chrominance/ inter-carrier

C (1) common luminance/chrominance
(2) sound and a.f.c.
(Inter-carrier sound reception is *not* used)

D (1) common luminance/chrominance
(2) sound inter-carrier

E (1) common luminance/chrominance
(2) sound inter-carrier

6. Percentage of d.c. component of luminance signal at display tube

Manufacturer	A/F	B	C	D	E
Percentage	nearly 100	90	100	30	100

7. Percentage of d.c. component of colour difference signals at display tube

Manufacturer	A/F	B	C	D	E
Percentage	50	80	100	100	90

8. Amplitude/frequency response of luminance channel in decibels relative to 100 kHz

Manufacturer	A/F	B	C	D	E
2·5 MHz	−2	−1·5	0	0	0
3·0 MHz	−3·5	−2	+3	−3	0
4·0 MHz	−10	−6	+6	−4·5	−1
4·5 MHz	−17	−10	−12	−6	−6
5·0 MHz		−17	−18	−10	−9

9. Bandwidth of colour difference signals at various response levels, relative to response at 50 kHz

Manufacturer	A/F	B	C	D	E	
−1 dB		400	600	650	600	kHz
−3 dB		500	800	800	800	kHz
−6 dB	650					kHz

10. Number of colour difference signal detectors and angles of demodulation

Manufacturer	Number	Angles
A/F	2	X and Z ($R-Y+206$ and 239 degrees)
B	2	X and Z (separated by 63 degrees)
C	3	$R-Y$, $B-Y$ and $G-Y$
D	2	X and Z
E	2	X and Z

All receivers used quartz crystal sub-carrier regenerators.

8. Appendix 2

(Form 1)

Make of Receiver.....

Site .....

Type No..... Set No.....

Questionnaire to be filled in by person in charge of receiver for the viewing session.

Name .....

Date .....

Time of Viewing. From..... to.....
Immediately after the warming-up period de-tune to Channel 26 and then re-tune to Channel 33.

Do not make any adjustments to the receiver between the end of B.B.C.-2 and the start of the colour programme (i.e. not during vertical colour bars).

1. When the colour programmes started were adjustments necessary to control:

(a) Tuning.....Yes/No

(b) Colour Intensity .....Yes/No

(c) Hue .....Yes/No

2. Were any further adjustments of these controls occasioned by a programme change? If so, state how many:

(a) Tuning .....

(b) Colour Intensity .....

(c) Hue.....

3. On how many other occasions were adjustments made during the programme to control:

(a) Tuning .....

(b) Colour Intensity .....

(c) Hue.....

4. Please describe the EASE or DIFFICULTY of adjustments of any controls used, in accordance with Scale (iii) below:

   (a) Tuning.....
   (b) Colour Intensity.....
   (c) Hue .....

   Please answer by scale number

5. Were there any room lights on?.....Yes/No

6. Did any light—including daylight—fall directly upon the screen? ..... Yes/No

ALSO, PLEASE FILL IN FORM 2

Scale (iii)

1. Very Easy
2. Easy
3. Fairly Easy
4. Rather Difficult
5. Difficult
6. Very Difficult

Should you wish to make any further comments, please use the back of this form

9. Appendix 3

(Form 2)

Make of Receiver.....

Site .....

Type No. ..... Set No. .....

Questionnaire to be filled in by

(a) The person in charge of the receiver for the viewing session (additional to Form 1).

(b) Other viewers present.

Name .....

Date .....

Time of Viewing. From..... to.....

Viewing Distance from Screen (approx.).....

1. Black and White Programme

   If you have been viewing a black and white programme, will you please say:

   (a) Using Scale (i), did the picture have a colour cast?
   .....(*Please answer by scale number*)

   (b) If so, did this cover the whole screen area?
   .....Yes/No

2. Colour Programme

   If you have been viewing a colour programme, will you please say:

   (a) Using Scale (ii), what in your opinion was the overall quality of the colour picture?
   .....(*Please answer by scale number*)

   (b) Was it consistent throughout the programme?
   .....Yes/No

Scale (i)

1. Imperceptible
2. Just Perceptible
3. Definitely Perceptible, but not Disturbing
4. Somewhat Objectionable
5. Definitely Objectionable
6. Unusable

Scale (ii)

1. Excellent
2. Good
3. Fairly Good
4. Rather Poor
5. Poor
6. Very Poor

Should you wish to make any further comments, please use the back of this form

10. Appendix 4

(Form 3)

Make of Receiver.....

Site .....

Type No..... Set No.....

Engineer's Questionnaire

1. Were there any defects in performance or freak reception conditions? (give details).

2. Using Scale (ii) on the viewer's questionnaire (Form 2), what is:

   (a) The overall monochrome picture grading?.....

   (b) The overall colour picture grading?.....

3. Please sketch the room plan in the space below, showing:

   (a) Position of windows

   (b) Position of receiver

   (c) Position of room lights

4. Are the room lights tungsten or fluorescent?

11. Appendix 5

Details of Service Calls

Broken thermistor;

Colour sync. error (2);

Open circuit resistance in blue gun circuit;

Corona due to faulty capacitor;

Boost capacitor open circuit;

Re-adjustment of grey scale tracking and convergence (3).

Manuscript received by the Institution on 3rd November 1965. (Paper No. 1058/T35.)

U.D.C. 621.396.677

The Detection Performance for Some Cases of Multiplicative Radar Signal Processing

By

V. GREGERS HANSEN,
M.Sc.†

Summary: The detection performance for four typical cases of multiplicative radar signal processing is determined and a comparison is made with similar cases using linear addition.

Both i.f. multiplication as it might be used in multiplicative arrays and video multiplication as used in radar diversity combiners are considered for non-fading and Rayleigh-fading signal amplitudes.

In most of the cases considered the losses introduced by the use of multiplicative processing are quite small. Exceptions are when signals of significantly different signal/noise ratios, or equal-frequency i.f. signals of random relative phase are multiplied together.

1. Introduction

Multiplicative methods of signal processing have in the past frequently been proposed and occasionally used in radar systems. Typical examples are multiplicative arrays,[1–4] radar diversity combiners,[5] twin-frequency m.t.i.,[6] and pulse-to-pulse correlators for interference reduction.

The purpose of this paper is to determine the detection performance for some typical cases of multiplicative processing and compare them with the similar cases using linear addition. No other performance criterion than that of detectability is considered. Only single multiplication without post-detection integration is treated.

Similar investigations have been carried out by Herscovici and Detape[5] and Tucker.[7]‡ However, the somewhat ambiguous criterion of video signal/noise ratio has been used by Tucker and fading has not been considered.[7] Herscovici *et al.*[5] present results for some cases of video multiplication but use a rather specialized detection criterion. However, the losses given are very similar to those found in the present paper for Cases III and IV, that is for two video signals of equal amplitude with no fading, and for two video signals with independent Rayleigh-fading amplitudes of the same mean.

2. Multiplicative Systems Considered

In the following a distinction will be made between coherent and non-coherent multiplication. In the cases of coherent multiplication the phase difference between the two (equal-frequency) signals is taken into account. With non-coherent multiplication this phase-relationship is not considered and the multiplication is in principle performed between the envelopes of the two signals, which can be of equal or different frequencies.

2.1. *Coherent Multiplication (Cases I and II)*

The block diagram for coherent multiplication is shown in Fig. 1. The two signals multiplied together are at the same intermediate frequency. The following

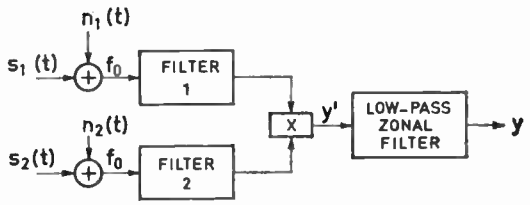

Fig. 1. Coherent multiplication (Case I and when followed by a full-wave rectifier, Case II).

two cases will be considered. In Case I the two signals are in phase, have either identical or different amplitudes, and there is no fading. In Case II the two signals are of random relative phase and have independent Rayleigh-fading amplitudes of the same mean; a full-wave rectifier is assumed after the low-pass zonal filter, since otherwise detection probability could never exceed 50%.

2.2. *Non-coherent Multiplication (Cases III and IV)*

Two schemes of non-coherent multiplication which give identical outputs are shown in Figs. 2 and 3. In Fig. 2 the two signals are of different intermediate frequencies and the result of the multiplication is envelope-detected. In Fig. 3 the two signals (of equal or different i.f.'s) are envelope-detected before (video) multiplication.

† Formerly at the SHAPE Technical Centre, The Hague, Netherlands; now with the Laboratory for Communication Theory, Royal Technical University of Denmark, Lyngby, Denmark.

‡ Since the submission of this paper, a paper by Shaw comparing multiplicative and additive arrays has been published.[14] Through the use of an interesting equivalence with existing results, the detection performance of the multiplicative processing scheme referred to in this paper as Case I is obtained.

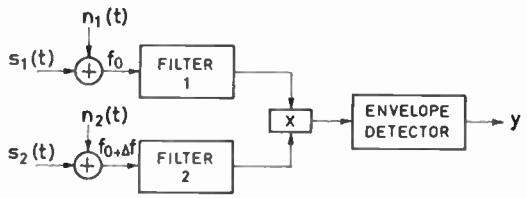

Fig. 2. Non-coherent multiplication (first scheme) (Cases III and IV).

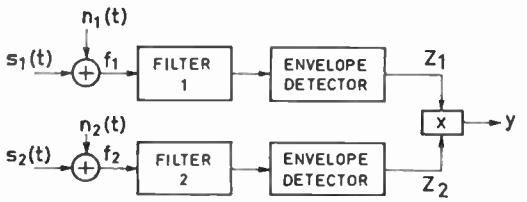

Fig. 3. Non-coherent multiplication (second scheme) (Cases III and IV).

Again two cases will be considered. In Case III there is no fading and the two signals have identical amplitudes. In Case IV the two signals have independent Rayleigh-fading amplitudes of the same mean.

3. Theoretical Results

The theoretical results for the four cases listed in Section 2 are presented below. They will be preceded by the definition of input signal/noise ratio used throughout the paper. The two input signals are assumed to be pulse-shaped and time-coincident.

3.1. *Definition of Input Signal/Noise Ratio*

The average energy of the input signals $s_1(t)$ and $s_2(t)$ (Figs. 1, 2 and 3) is denoted by E_1 and E_2 respectively.

$$E = \int_{-\infty}^{\infty} \overline{s^2(t)}\,dt$$

The noise inputs, $n_1(t)$ and $n_2(t)$, are assumed white and Gaussian, each with the same power spectral density N_0 (single sided). The input signal/noise ratio is then defined as:

$$\frac{E}{N_0} = \frac{E_1+E_2}{N_0} \qquad \text{.....(1)}$$

As will become apparent later, this definition facilitates the comparison between additive and multiplicative processing.

As it will be assumed that matched filtering is used in both channels, the maximum power signal/noise ratios at the filter outputs are E_1/N_0 and E_2/N_0 for the two channels.

3.2. *Coherent Multiplication (Case I)*

The maximum values of the signals alone at the input to the multiplier, in each of the two channels, are written:

$$\begin{matrix} A_1 \cos \omega_0 t \\ A_2 \cos \omega_0 t \end{matrix} \qquad \text{.....(2)}$$

A random (but common) phase angle has been excluded for ease of notation since it is of no consequence in the following.

The noise at the same point in each channel can be split into two components, along and in quadrature to the signal:

$$\begin{matrix} x_{c1} \cos \omega_0 t + x_{s1} \sin \omega_0 t \\ x_{c2} \cos \omega_0 t + x_{s2} \sin \omega_0 t \end{matrix} \qquad \text{.....(3)}$$

The two inputs to the multiplier are therefore:

$$\begin{matrix} (A_1+x_{c1}) \cos \omega_0 t + x_{s1} \sin \omega_0 t \\ (A_2+x_{c2}) \cos \omega_0 t + x_{s2} \sin \omega_0 t \end{matrix} \qquad \text{.....(4)}$$

and the output of the multiplier becomes:

$$y' = \tfrac{1}{2}(A_1+x_{c1})(A_2+x_{c2}) + \tfrac{1}{2}x_{s1}x_{s2} + \text{high-frequency components} \qquad \text{.....(5)}$$

After the low-pass zonal filter there remains:

$$y = \tfrac{1}{2}(A_1+x_{c1})(A_2+x_{c2}) + \tfrac{1}{2}x_{s1}x_{s2} \qquad \text{.....(6)}$$

The signal/noise power ratio in each channel before multiplication is:

$$S_1 = A_1^2/2\sigma^2, \qquad S_2 = A_2^2/2\sigma^2 \qquad \text{.....(7)}$$

where

$$\sigma^2 = E[x_{c1}^2] = E[x_{s1}^2] = E[x_{c2}^2] = E[x_{s2}^2]\dagger \qquad \text{.....(8)}$$

As mentioned earlier, we have with a matched filter:

$$S_1 = E_1/N_0, \qquad S_2 = E_2/N_0 \qquad \text{.....(9)}$$

When no signal is present we have from eqn. (6):

$$y = \tfrac{1}{2}(x_{c1}x_{c2} + x_{s1}x_{s2}) \qquad \text{.....(10)}$$

In this equation x_{c1}, x_{c2}, x_{s1} and x_{s2} are all Gaussian random variables with zero mean and variance σ^2. The p.d.f. (probability density function) for y is available from the literature,‡ and is:

$$p(y) = \frac{1}{2\sigma^2} \exp\{-|y|/\sigma^2\} \quad \text{for all } y \qquad \text{.....(11)}$$

The corresponding c.d.f. (cumulative distribution function) is found by integration to be:

$$P(y) = \begin{cases} 1-\tfrac{1}{2}\exp\{-y/\sigma^2\} & \text{for } y \geq 0 \\ \tfrac{1}{2}\exp\{y/\sigma^2\} & \text{for } y < 0 \end{cases} \qquad \text{.....(12)}$$

From this equation the normalized threshold V/σ^2

† $E[\ ]$ is the notation for statistical expectation. This equation reflects the fact that the noise level is assumed identical in the two channels.

‡ Reference 8, expression (28) for $K = 2$.

corresponding to a certain value of false-alarm probability P_f may be obtained from the equation:

$$P_f = 1 - P(y = V)$$

We find the following values:

V/σ^2	P_f
3·92	10^{-2}
6·24	10^{-3}
8·54	10^{-4}

When a signal is present, the expression for the p.d.f. of y is rather complicated,[8,9] and a Monte Carlo simulation model, which was already available, was used for determining the detectability curves. In this model samples of y are generated according to the definition in eqn. (6). These samples are in turn compared with the analytically determined threshold, V, in order to check for detection, and detection probability is finally estimated as the ratio between the number of actual detections and the total number of trials (repetitions).

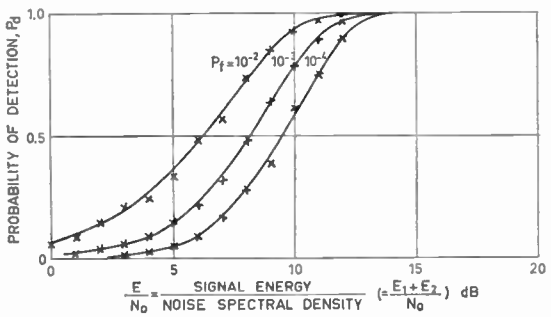

Fig. 4. Coherent multiplication (Case I: $E_1 = E_2$).

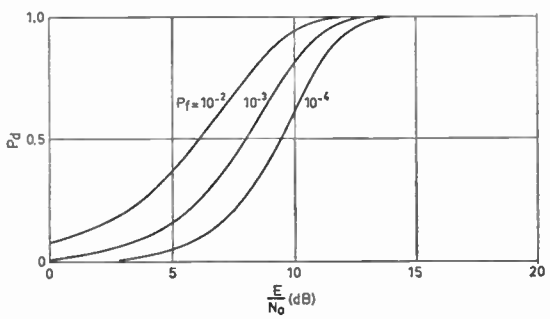

Fig. 5. Detectability curves for matched filter detection (unknown phase).

A set of detectability curves obtained in this manner for $E_1 = E_2$ is shown in Fig. 4. Each point shown is the result of 500 repetitions. The corresponding case, where the signals are added instead of multiplied, results in the curves of Fig. 5. These results are, of course, for matched-filter detection of a signal of unknown phase. A comparison between the results of Figs. 4 and 5 shows that no significant loss is introduced by multiplicative processing for this case.

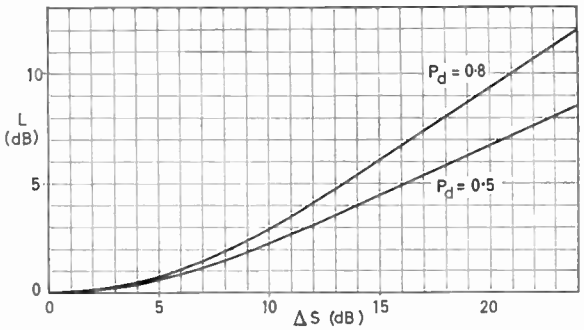

Fig. 6. Coherent multiplication (Case I, $\Delta S = E_1/E_2$). Detectability as a function of the difference in signal level in the two channels.

The effect of having different signal/noise ratios in the two channels before multiplication was next investigated. The difference is defined as $\Delta S = E_1/E_2$. Detectability curves were determined for a number of different values of ΔS by simulation as above. These results are summarized in Fig. 6, where the detectability losses for $P_d = 50\%$ and 80%, relative to the result of Fig. 4, are shown as a function of ΔS. The losses for the three values of P_f† were averaged for each value of ΔS, to obtain the value shown in Fig. 6.

In the case of additive processing the manner in which the total signal energy E is distributed between the two channels is of no consequence provided the channels are weighted in proportion to their signal/noise ratio before addition. If this is done, the curves of Fig. 5 still apply.

These results show that significant losses are introduced by the multiplicative processing when the signal/noise ratio in the two channels differs by more than 5 to 10 dB.

3.3. *Coherent Multiplication (Case II)*

In this case the two signals are of random relative phase and have independent Rayleigh-fading amplitudes. That is, the two signals are noise-like and they may therefore be split into two components in the same way as the noise. The two inputs to the multiplier then become

$$\begin{aligned}&(A_{c1} + x_{c1}) \cos \omega_0 t + (A_{s1} + x_{s1}) \sin \omega_0 t \\ &(A_{c2} + x_{c2}) \cos \omega_0 t + (A_{s2} + x_{s2}) \sin \omega_0 t\end{aligned} \quad \ldots\ldots(13)$$

† These losses only differed by a small amount.

After multiplication and low-pass filtering we find:

$$y = \tfrac{1}{2}\{(A_{c1}+x_{c1})(A_{c2}+x_{c2})+(A_{s1}+x_{s1})(A_{s2}+x_{s2})\} \quad \ldots\ldots(14)$$

In this expression both A and x are zero-mean Gaussian variables. The variance of x is as given by eqn. (8). If the signals in the two channels are of equal level, their variance is

$$\sigma_s^2 = E[A_{c1}^2] = E[A_{s1}^2] = E[A_{c2}^2] = E[A_{s2}^2] \quad \ldots\ldots(15)$$

The power signal/noise ratio in each channel before multiplication is therefore:

$$S_1 = S_2 = \sigma_s^2/\sigma^2 \quad \ldots\ldots(16)$$

With a matched filter we have:

$$S_1 = S_2 = E_1/N_0 = E_2/N_0 \quad \ldots\ldots(17)$$

The p.d.f. of the output, y, of the low-pass filter is of the same form as eqn. (11) but with the variance increased to $(\sigma^2+\sigma_s^2)$:

$$p(y) = \frac{1}{2(\sigma^2+\sigma_s^2)} \exp\{-|y|/(\sigma^2+\sigma_s^2)\} \quad \text{for all } y \quad \ldots\ldots(18)$$

After the full-wave rectifier the output is $u = |y|$, with the p.d.f.:

$$p(u) = \frac{1}{\sigma^2+\sigma_s^2} \exp\{-u/(\sigma^2+\sigma_s^2)\} \quad u \geq 0$$

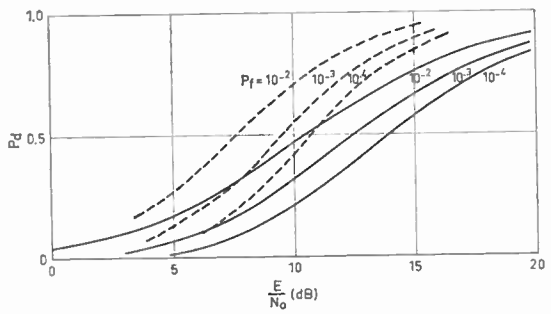

Fig. 7. Coherent multiplication (Case II). Broken line curves are from Fig. 8.

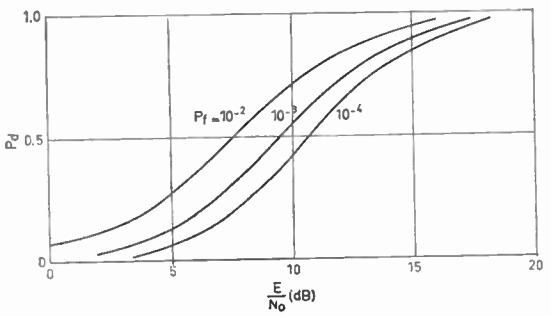

Fig. 8. Analogue integration of envelopes of the two channels for Case II (Rayleigh fading).

The c.d.f. corresponding to the output u is:

$$P(u) = 1-\exp\{-u/(\sigma^2+\sigma_s^2)\} \qquad u \geq 0 \quad \ldots\ldots(19)$$

By substituting $\sigma_s^2/\sigma^2 = E/2N_0$, the detectability curves for Case II may be obtained analytically from this equation. False-alarm probability is

$$P_f = 1-P(u = V)$$

for $\sigma_s = 0$; the corresponding detection probability for any given signal/noise ratio is given by

$$P_d = 1-P(u = V)$$

The set of detectability curves determined in this way is shown in Fig. 7.

Figure 8 gives the theoretical curves for non-coherent addition of two square-law-detected Rayleigh-fading hits, obtained by using the tables by Pearson.[10] These curves are shown for comparison, by broken lines in Fig. 7. As one would expect, coherent multiplication is a rather poor processor for this type of signal.

3.4. *Non-coherent Multiplication (Case III)*

For the multiplication principle shown in Fig. 3, the inputs to the envelope detectors are given by eqn. (4). After envelope detection we obtain the signals:

$$z_1 = \{(A_1+X_{c1})^2+X_{s1}^2\}^{\frac{1}{2}}$$
$$z_2 = \{(A_2+X_{c2})^2+X_{s2}^2\}^{\frac{1}{2}} \quad \ldots\ldots(20)$$

The p.d.f. of z_1 and z_2 are:

$$p(z) = \frac{z}{\sigma^2} \exp\left\{-\frac{z^2+A^2}{2\sigma^2}\right\} I_0\{Az/\sigma^2\} \quad z \geq 0 \quad \ldots\ldots(21)$$

and for noise alone this reduces to:

$$p(z) = \frac{z}{\sigma^2} \exp\{-z^2/2\sigma^2\} \quad z \geq 0 \quad \ldots\ldots(22)$$

The output of the multiplier for noise alone is given by:

$$y = z_1 z_2 \quad \ldots\ldots(23)$$

and has the p.d.f.[11]

$$p(y) = \frac{y}{\sigma^4} K_0\{y/\sigma^2\} \quad y \geq 0 \quad \ldots\ldots(24)$$

($K_0(y)$, $K_1(y)$ are Hankel functions.)

The corresponding c.d.f. is:

$$P(y) = \int_0^{y/\sigma^2} xK_0(x)\,dx = 1 - \frac{y}{\sigma^2} K_1(y/\sigma^2) \quad y \geq 0 \quad \ldots\ldots(25)$$

The Hankel function $K_1(x)$ is tabulated by Watson.[12] The following threshold values were obtained:

V/σ^2	P_f
5·75	10^{-2}
8·23	10^{-3}
10·65	10^{-4}

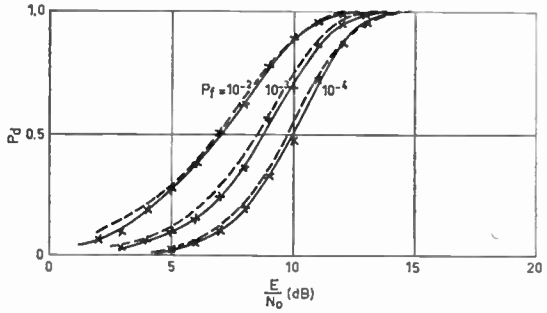

Fig. 9. Non-coherent multiplication (Case III). Broken line curves are from Fig. 10.

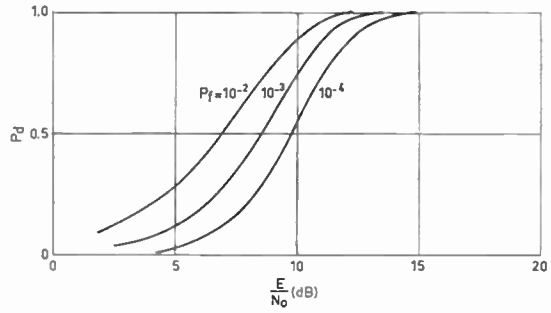

Fig. 10. Analogue integration of the envelopes of the two channels for Case III (no fading).

Simulation was again used for the case where signal is present. Signal-plus-noise samples were generated according to eqns (23) and (20) and the results are shown in Fig. 9. Each point is again the result of 500 repetitions. The corresponding results for addition are shown in Fig. 10 and as broken lines in Fig. 9 for comparison. The loss due to multiplicative processing is quite small, which agrees well with the equivalent case of a logarithmic detector characteristic and linear integration studied by Green.[13]

3.5. *Non-coherent Multiplication (Case IV)*

The inputs to the detectors are in this case given by eqn. (13). After detection is obtained

$$z_1 = \{(A_{c1}+x_{c1})^2+(A_{s1}+x_{s1})^2\}^{\frac{1}{2}}$$
$$z_2 = \{(A_{c2}+x_{c2})^2+(A_{s2}+x_{s2})^2\}^{\frac{1}{2}} \quad \text{.....(26)}$$

each with the p.d.f.

$$p(z) = \frac{z}{\sigma^2+\sigma_s^2} \exp\{-z^2/2(\sigma^2+\sigma_s^2)\} \quad \text{.....(27)}$$

where σ^2 and σ_s^2 are given by eqns. (8) and (15). The p.d.f. of the multiplier output, y, is therefore, similar to eqn. (24):

$$p(y) = \frac{y}{(\sigma^2+\sigma_s^2)^2} K_0\{y/(\sigma^2+\sigma_s^2)\} \quad \text{.....(28)}$$

with the corresponding c.d.f.

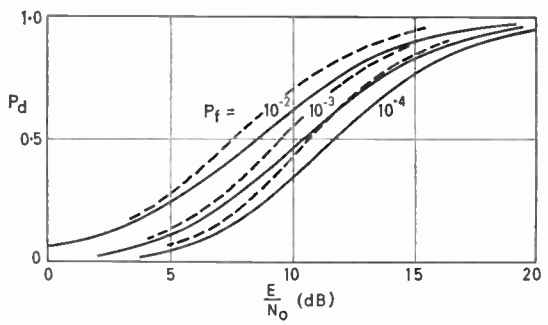

Fig. 11. Non-coherent multiplication (Case IV). Broken line curves are from Fig. 8.

$$P(y) = 1 - \frac{y}{\sigma^2+\sigma_s^2} K_1\{y/(\sigma^2+\sigma_s^2)\} \quad \text{.....(29)}$$

Again substituting

$$\frac{\sigma_s^2}{\sigma^2} = \frac{E}{2N_0} \quad \text{.....(30)}$$

the curves of Fig. 11 have been determined analytically using the thresholds derived under Case III. A comparison with the results of Fig. 8 (shown by broken lines in Fig. 11) shows that multiplicative processing in this case introduces a loss which is about 1 dB.

4. Some Experimental Results

An experimental study was carried out for coherent multiplication, Case I, for comparison with the theoretical results of Figs. 4 and 5.

The block diagram of the experimental set-up is shown in Fig. 12. The outputs of the two channels could be combined by multiplication (Fig. 13(a)) or addition (Fig. 13(b)) followed by low-pass filtering or linear detection respectively. Measurements were also performed on the two channels individually, using linear detection.

The measurements were carried out with signal- and noise-generators and a detection set constructed at the SHAPE Technical Centre. The signal/noise ratio is calibrated by connecting a wattmeter at the output of the filters. With the attenuator at 'SET SNR' on 0 dB and the signal generator in its c.w.-mode the attenuators 'SET NOISE LEVEL' are adjusted until equal amounts of signal and noise are obtained at the filter outputs. The calibration is corrected for the difference from 500 kHz ($= 1/\tau$ for $\tau = 2\,\mu s$) of the filter noise bandwidth. The detection set gates out samples of noise alone and of signal plus noise and compares their amplitudes with a threshold. Whenever the threshold is exceeded a pulse is fed to a counter. For noise alone the threshold is set to give the required false-alarm probability by means of an automatic loop. With signal plus noise present, detection probability is determined.

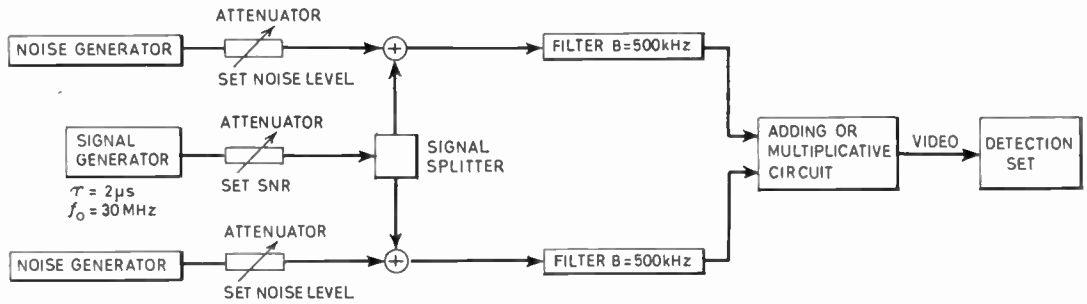

Fig. 12. Block diagram of the experimental set-up.

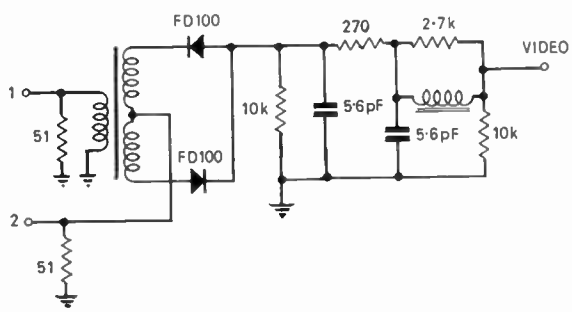

(a) Multiplication circuit.

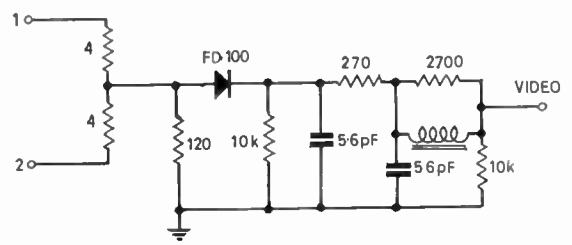

(b) Addition circuit.

Fig. 13.

The measured detectability curves for multiplication are shown in Fig. 14, while the corresponding results for addition are shown in Fig. 15 (and also for comparison as broken lines in Fig. 14). The multiplicative case is seen to be about 0·4 dB inferior to additive processing whereas from the theoretical results for this case no difference would be expected. This, however, is quite a small difference and may probably be attributed to difficulties in implementing ideal multipliers.

Measurements on the individual channels (these were exactly identical) are shown as broken lines in Fig. 15. In this case E/N_0 is the signal/noise ratio of the individual channels. It is seen that addition of the two channels do not quite give the expected result of no loss as compared with the individual channels.† This may have been caused by cross-talk, and consequently noise-correlation, between the two channels, although care was taken to avoid it.

The difference of 1·5 dB between the theoretical detection curves in Fig. 5 and the measured results for the individual channels shown as broken lines in Fig. 15 can largely be explained as the loss due to non-optimum filtering. The absolute calibration of signal/noise ratio is estimated to be accurate to about ±1 dB and the relative accuracy to about ±0·2 dB.

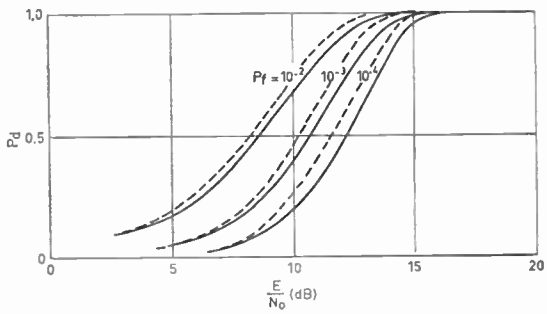

Fig. 14. Experimental results for coherent multiplication (Case I). Broken line curves are from Fig. 15.

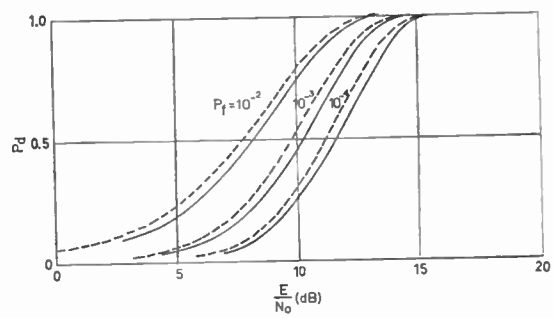

Fig. 15. Experimental results for coherent addition with the results for the individual channels as broken lines.

† The 3-dB gain normally quoted for coherent addition of two samples is accounted for in the signal/noise ratio definition.

5. Conclusions

Multiplicative radar signal processing introduces negligible losses when equal-amplitude, non-fading signals are present in the two channels.

With independently Rayleigh-fading signals (of the same mean) in the two channels, the non-coherent multiplication introduces a loss of about 1 dB. With coherent multiplication followed by full-wave rectification the loss is 3 to 5 dB for detection probabilities, P_d, in the range 50 to 80%.

With coherent multiplication (and undoubtedly also for non-coherent multiplication) and no fading, a significant loss is introduced when the signal/noise ratio in the two channels differs by more than 5 to 10 dB. This would be of importance in certain applications to multiplicative arrays where the outputs of array-elements of different gain would be multiplied together.[4]

It should be noted that these conclusions apply only to the single hit case. If post-detection integration of a large number of hits is carried out the asymptotic losses are: Case I, $L = 1{\cdot}5$ dB; Case II, $L = 1{\cdot}5$ dB; Case III, $L = 0{\cdot}5$ dB; Case IV, $L = 0{\cdot}5$ dB. These results which are quoted without proof are based on the video signal/noise ratio for very weak signals and the central limit theorem.

6. References

1. V. G. Welsby and D. G. Tucker, 'Multiplicative receiving arrays', *J. Brit. Instn. Radio Engrs*, **19**, p. 369, June 1959.
2. V. G. Welsby, 'Multiplicative receiving arrays', 'Electromagnetic Theory and Antennas', Pt. 2, p. 1269, E. C. Jordan (Ed.). (Pergamon Press, Oxford, 1963.)
3. E. Shaw and D. E. N. Davies, 'Theoretical and experimental studies of the resolution performance of multiplicative and additive aerial arrays', *The Radio and Electronic Engineer*, **28**, pp. 279–91, October 1964.
4. A. Ksienski, 'Multiplicative processing antenna systems for radar applications', *The Radio and Electronic Engineer*, **29**, pp. 53–67, January 1965.
5. S. Herscovici and A. Detape, 'Performance of a diversity radar', *Ann. Radioelect.*, **12**, pp. 285–98, October 1957. (In French.)
6. P. Bradsell, 'Moving target indication, a survey of developments since 1948', AGARD Symposium on Radar Techniques for Detection Tracking and Navigation, 21st–25th September 1964.
7. D. G. Tucker, "Signal/noise performance of multiplier (or correlation) and addition (or integrating) types of detector', *Proc. Instn Elect. Engrs*, **102C**, pp. 181–901, February 1955 (I.E.E. Monograph, No. 120R).
8. G. M. Roe and G. M. White, 'Probability density functions for correlators with noise reference signals', *Trans. I.R.E. on Information Theory*, IT-7, No. 1, pp. 13–18, January 1961.
9. J. L. Ekstrom, 'The statistics of the product of two independent modified Rayleigh variates', *Proc. I.E.E.E.*, **52**, No. 11, p. 981, August 1964 (Letter).
10. K. Pearson, 'Tables of the Incomplete Gamma Function'. (Cambridge University Press, 1957.)
11. E. L. R. Webb, 'On the distribution of the product of diode detector waveforms', *Canadian J. Phys.*, **34**, p. 679, July 1956.
12. G. N. Watson, 'Theory of Bessel Functions'. (Cambridge University Press, 1958.)
13. B. A. Green, 'Radar detection probability with logarithmic detectors", *Trans. I.R.E. on Information Theory*, **IT-4**, pp. 50–52, March 1958.
14. E. Shaw, 'A comparison of the detection and resolution performance of multiplicative and additive aerial arrays in the presence of noise", *The Radio and Electronic Engineer*, **30**, pp. 323–35, December 1965.

Manuscript first received by the Institution on 24th August 1965, and in final form on 17th February 1966.

(*Paper No. 1059/RNA50.*)

INSTITUTION NOTICES

Annual General Meeting of the Institution

Members are advised that the Annual General Meeting of the Institution, at which the Annual Report of the Council and the Accounts for 1965–66 will be presented, and officers and Council for 1967 elected, will be held in London on **Thursday, 15th December, 1966.** A formal Notice and Agenda for the Annual General Meeting is published in the July–August issue of the *Proceedings*.

The Annual Report and the Institution's Accounts will be published in the September–October issue of the *Proceedings*. Members not resident in Great Britain who do not at present subscribe to the *Proceedings* may obtain a copy of this issue free of charge on application to the Secretary.

At the conclusion of the formal business of the Annual General Meeting, the President-elect, Professor Emrys Williams, will deliver his Inaugural Address. This Address will subsequently be printed in the January 1967 issue of *The Radio and Electronic Engineer*.

Institution Dinner in Southampton

The Institution's Conference on Electronic Engineering in Oceanography at Southampton University from 12th to 15th September 1966 will be marked by an Institution Dinner. This will be held on the evening of Wednesday, 14th September, at the Polygon Hotel, Southampton, at 7 o'clock for 7.30. The cost of tickets (obtainable from the Institutions Offices) is £2 each, which includes wines at table; the presence of ladies and other guests will be welcomed.

Conference on Computer Technology

A conference on Computer Technology, organized jointly by the I.E.E. Electronics Division and the I.E.R.E. Computer Group Committee, will be held at the University of Manchester, Institute of Science and Technology from 18th to 20th July 1967.

The scope of the meeting will include:

Central processor hardware; hardware problems associated with multi-processing (dynamic addressing, etc.); input and output devices for new applications; data links; graphic input and display units; image handling devices; reliability and maintenance; all aspects of storage; and components and devices.

The Organizing Committee invites the submission of contributions of up to 2,500 words for consideration for inclusion in the conference programme. Those wishing to offer material are invited to submit synopses of about 250 words by 10th October 1966 at the latest.

Further details and registration forms will be available from the I.E.R.E., 8–9 Bedford Square, London, W.C.1.

Members' Distinctions and Appointments

Dr. A. V. J. Martin (Associate Member) has been nominated to the grade of Chevalier du Mérite pour la Recherche et l'Invention "for his international contribution to the progress of electronics". The ceremony took place in Paris on the 15th June 1966, under the presidency of the President of the Academy of Sciences.

Elected an Associate of the Institution in 1946 and transferred to Associate Member in 1950, Dr. Martin took a prominent part in the recent setting-up of an Institution Section in Paris, and serves on its Committee. Now editor and publisher of technical journals in the industrial and medical electronics field, he has held research appointments with the C.N.R.S. and in 1957–58 he occupied a chair as a visiting professor at the University of Pittsburg. His main interests during this period were in ultrasonic methods of testing on which he contributed a paper to the *Journal* in 1956.

The Weizmann Institute of Science has announced that **Mr. Zvi H. Riesel** (Associate Member) has been promoted to an Associate Professorship in the Department of Applied Mathematics. Mr. Riesel was previously a senior scientist at the Institute which he joined in 1954; he was closely concerned with the design of the Institute's digital computer WEIZAC. Registered as a Student of the Institution in 1946, he obtained Graduate Membership in 1950 and was transferred to Associate Member in 1960.

"Guidance for Authors"

Members and others who are contemplating writing papers for *The Radio and Electronic Engineer* are reminded that the Institution has published a leaflet with the above title which may be obtained on application to the Secretary of the Programme and Papers Committee. The leaflet contains information on the requirements of style and presentation of papers, and advice on the preparation of illustrations.

Indications are also given regarding abbreviations; letter symbols and units; in this last connection additional information on future Institution practice was given in the article "The Use of S.I. Units" on pages 61 to 64 of the July issue of the *Journal*.

It is helpful if an intending author first submits a synopsis of his paper to the Committee as this enables the contents of the paper to be discussed in advance of carrying out detailed preparation.

Authors are asked to submit at least two copies of their papers (with prints of the illustrations) in order that the process of consideration by the Papers Committee's referees (normally two in number) can be completed with the least possible delay.

U.D.C.621.372.57

Transfer Function Synthesis with Active Unbalanced Equivalents of the Lattice

By

A. W. KEEN, M.Sc., C.Eng.†

Summary: In communications and control practice increasing use is being made of active-*RC* networks instead of the conventional passive *RLC* types. The network theory literature contains a number of different procedures for the synthesis of such networks but so far there has been very little correlation of these procedures either with each other or with the well-known methods of passive synthesis, which are generally based on the lattice. The object of this paper is to show that such correlation may be achieved. The treatment is comprehensive and is believed to have some tutorial value in the earlier sections but there are also some original features.

As a preliminary step an original development is made of the structure of the lattice in order to bring out the distinction between the restricted (i.e. convertible to bridged-T form) and the general cases of the lattice. The unbalanced equivalents of the latter case generally contain an ideal unity-ratio inverting transformer and, as a transition to active form, it is shown that this may be realized formally by a $(+R, -R)$ network. Hence, the general lattice may be realized as an active bridged-T consisting of two negative impedance converters (NIC's) and the usual inverse pair of passive impedances. Then, when the latter are realized in active $-RC$ form using the standard procedure employed in the literature the same pair of NIC's may be employed. However, there are two special cases of the active transformer replacement, for which one or other of the inverse impedance arms are nullified and the active bridged-T reduces to active T or π form. Then, when the three impedances of the T or π are separated into $+$ and $-RC$ parts, the three negative ones may be brought together and realized by the corresponding network placed in cascade between a pair of NIC's. When the networks so obtained are operated between ideal terminations, for example an ideal voltage source and an open-circuit load, certain simplifications may be made. One of these is identified as the form of realization used (without derivation) by T. Yanagisawa in his well-known paper. The principal conclusion of the paper is that one can develop from the classical lattice a broad class of active-*RC* networks that includes useful forms, not all of which appear yet to have been employed in the literature.

1. Introduction

1.1. *The Passive Lattice Network*

It is well established in classical (passive, reciprocal) network theory[1-3] that an extensive class of physically realizable transfer functions may be produced in the form of a symmetrical lattice network,[4] even under the constant-resistance condition, which allows a single lattice, however complex, to be broken down into a cascade of simpler lattices having, at most, a second-order transfer function. The lattice itself is not a practical form of realization because it requires both the series and cross immittance arms in duplicate. Moreover, one usually needs a network to be of unbalanced ('single-ended') form. In the case of a minimum-phase transfer function (i.e. one having no zeros in the right half-plane) the lattice has an equivalent bridged-T form, which is an acceptable configuration, but in the more general case of a non-minimum-phase function unbalanced equivalents of the lattice generally require an ideal inverting transformer (in particular cases, a pair of coupled coils). The use of a pair of tightly-coupled coils to approximate an ideal transformer, or of a pair of coupled coils to obtain a specified set of self- and mutual-inductances is unsatisfactory because practical coils do not approach sufficiently closely the ideal needed for accurate realization of the desired network. The same remark applies to any coils and coupled-coil pairs needed for the realization of the associated immittance arms.

† Reader in Electronics, Bristol College of Science and Technology (Bath University of Technology).

1.2 *Introduction of Active Elements into the Lattice*

1.2.1. The negative immittance converter (NIC)

The limitations of practical passive unbalanced equivalents of the lattice network are due partly to its connective properties (it consists entirely of reciprocal components) and to its passivity (which precludes loss compensation). With the advent of the transistor, which is both non-reciprocal and active, there has arisen the possibility of overcoming the limitations of reciprocal passive networks. Although the transistor is an acceptable element for design purposes it is not sufficiently close to being an ideal element for theoretical synthesis purposes. However, it has been established, notably by J. G. Linvill,[5] that an active unit called the negative impedance (or immittance) converter (NIC) can be quite closely approximated by a transistor circuit over a useful frequency range. The (ideal) NIC is a two-terminal-pair element which has the property of presenting at either one of its terminal pairs an immittance which is the negative of any immittance connected to the other terminal-pair. The NIC is a significant and acceptable element to network theorists because for a negative impedance to be stable its resistive component must remain non-positive at all real frequencies. The passive impedances of classical network theory are characterized by the property of being positive-real, which includes that of being non-negative at all real frequencies. Therefore, an NIC will convert a positive-real immittance into a short- or open-circuit stable proportional immittance of opposite sign. By the association of the NIC with the conventional set of elements, passive network theory may be extended in a meaningful manner into the active domain.

1.2.2. Active RC-networks

The principal result of this extended theory which has been established so far, chiefly by B. K. Kinariwala,[6] is that a ratio of polynomials in $p = \sigma + j\omega$ having real coefficients and which is positive along at least one section of the $-\sigma$ axis (but not necessarily positive-real), can be expressed as the difference of a pair of functions both of which are realizable as networks of *RC* elements. Such a ratio may therefore be realized with the aid of the NIC and this result allows inductive elements to be dispensed with. An immediate application of this result is to the realization of the arms of the lattice, thereby avoiding the need for inductances, but making avoidance of duplication of the arms by use of the unbalanced equivalent even more desirable since each arm will require an NIC. It has been shown by R. E. Thomas,[7] that, subject to certain restrictions on its pole-zero pattern, a g_{21}-type (i.e. forward voltage gain into an open-circuit load) of transfer function may be realized as an active lattice which can always be reduced to ladder form provided the gain constant is limited. Moreover, for this particular type of function only one (unity-ratio) NIC is required.

1.2.3. Sensitivity to NIC ratio variation

An important matter in active-*RC* synthesis arises from the realization of impedances as differences of *RC* impedances, as a result of which the impedance under realization is rather sensitive to variation of the ratio of the NIC. This problem raises the question of the optimum separation of a given function into the *RC* difference form for minimum sensitivity to the NIC ratio. The problem of optimizing the separation of a polynomial has been solved by I. M. Horowitz[8], and R. E. Thomas[7] has shown that when the lattice form of realization is used, Horowitz's procedure may be applied to minimize the root sensitivity of either the numerator or the denominator to changes in the NIC ratio. Because of the rapid increase of sensitivity with the degree of the transfer function, functions of degree >2 should be broken down into factors of, at most, second degree and these factors realized separately. The lattice cascade method of synthesis is well adapted to this restriction.

1.3. *Lattice-derived Active-RC Networks*

In the present paper attention will be directed to realization forms for active-*RC* synthesis and their inter-relationships, rather than to particular synthesis procedures or to the sensitivity problem, both of which have had considerable treatment in the literature. With each published synthesis procedure there has been given a suitable form for its realization, but usually with no indication of the origin or derivation of the form and also without any attempt at correlation with other configurations that have been proposed.

The class of networks to be given are obtained by substitution of the unity-ratio ideal inverting transformer in unbalanced equivalents of the lattice by an equivalent active network containing a pair of unity-ratio NIC's and by employing the latter separately in active-*RC* synthesis of the associated immittance arms. This class of networks is found to include those of R. E. Thomas[7] and T. Yanagisawa[9] as special cases and, in the realization aspect, the present paper is a generalization of their work.

These lattice-derived networks are particularly appropriate for the realization of two-ports which are specified as a compact set of immittance functions and in this respect the present paper may be regarded as a reciprocal counterpart of a previous publication (A. W. Keen[10]) where non-reciprocal realizations of such networks were given.

An important application is to the design of networks for insertion into uniform transmission systems (e.g. repeaters, equalizers, etc., in telecommunication

channels). From this point of view the present work is an extension of the theory of negative-impedance repeater design to general transfer function synthesis.

2. Active Unbalanced Equivalents of the General Lattice

2.1. *Derivation of the Active Bridged-T Lattice Equivalent*

Consider a uniform transmission system, of characteristic resistance R_0, into which a series impedance $2Z_1$ has been inserted in balanced fashion (see Fig. 1(a)) for the purpose of introducing a required loss. It will usually be desired to preserve a matched system and match may be restored on one side by shunt connection of an 'iterating' impedance

$$\left(R_0 + \frac{R_0^2}{2Z_1}\right).$$

If this impedance is split into two parallel paths (Fig. 1(a)), each of double this value, and both ports are divided symmetrically about the components $R^2{}_0/Z_1$, the upper ends (Y_1', Y_1'') of the latter will have the same potential as the opposite end (X_1) of the upper insertion impedance and the lower ends (Y_2', Y_2'') the same potential as the opposite end (X_2) of the lower insertion impedance. Hence, the pair of connections $(X_1\ Y_1',\ X_2\ Y_2'')$ may be made without disturbing the current-voltage distribution, resulting in the lattice shown at (b). This is called the restricted lattice, because of the presence of the four R_0 elements, which ensure that this lattice is minimum-phase. If this development is done for an unbalanced insertion impedance and the iterating branch is not divided it will be necessary to insert R_0 in series with each of the equipotential connections in order to secure match at both sides and obtain symmetry. In this way the well-known bridged-T equivalent of the restricted lattice will be obtained.

Next, if, having inserted the series impedances Z_1, each is shunted by a negative resistance $-R_0$, as at (d), the development is repeated, the resistors will cancel out in pairs, leaving the simpler lattice form shown at (e). But, despite the simpler form, this is a more general (non-minimum-phase) lattice. Modifying the procedure, as before, to the equivalent unbalanced case results in the active bridged-T (f). These lattice equivalents ((c), (f)) may be checked by applying Bartlett's bisection theorem to the bridged-T or by constructing their immittance matrices which will be found to be the same as for the lattice.

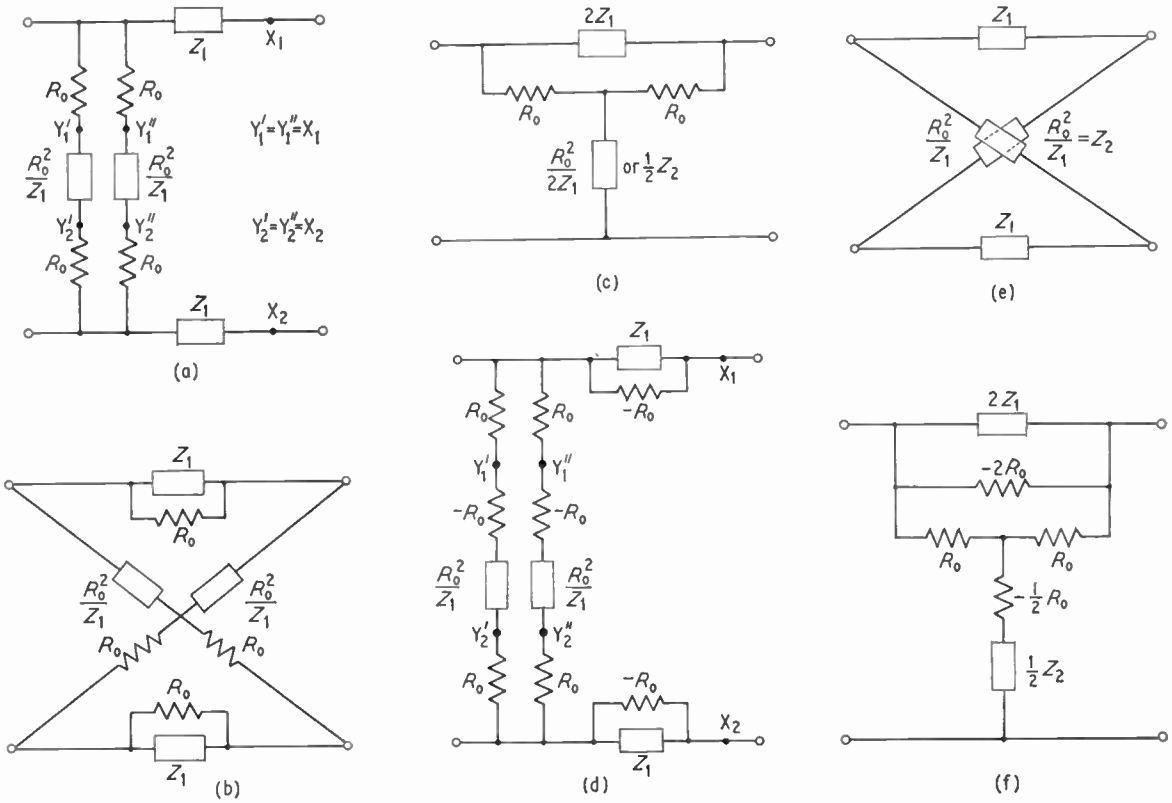

Fig. 1. Development of the restricted (a), (b) and general (d), (e) constant-resistance lattice networks and their bridged-T equivalents (c), (f).

2.2. *Derivation of an Active Equivalent of the Unity-Ratio Inverting Transformer*

2.2.1. The pair of equivalences (b = c), (e = f) in Fig. 1 are not limited to the constant-resistance condition. One may derive the general lattice, in which Z_1 and Z_2 are any pair of positive-real impedances, by putting $Z_1 Z_2 = Z^2_0$ and carrying out the given construction using Z_0 rather than R_0, with the result shown in Fig. 2(a). Generally Z_0 (which disappears in the course of the lattice construction) will be non-positive real (non-p.r.), in which case the active-bridged-T equivalent will not be physically realizable in the ordinary sense. Alternatively, reversing the point of view, one may suppose that Z_1 and Z_2 together are such (i.e. non-p.r.) that Z_0 is a positive-real function, in which case the active parts $(-\frac{1}{2}Z_0, -2Z_0)$ of the bridged-T will be realizable with a pair of NIC's loaded with immittances of opposite sign.

If in the (general) lattice (e), with Z_1 and Z_2 such that $0 < Z_0 < \infty$ and is positive-real, Z_1 is made to tend to infinity and Z_2 to zero, together, then this lattice will degenerate at the limit into a pair of crossed connections, which may be replaced by an ideal unity-ratio inverting transformer, while the active bridged-T reduces to the inner bridged-T portion consisting of the four elements which are multiples of Z_0. The latter portion of Fig. 2(a) is therefore an equivalent of the ideal unity-ratio inverting transformer

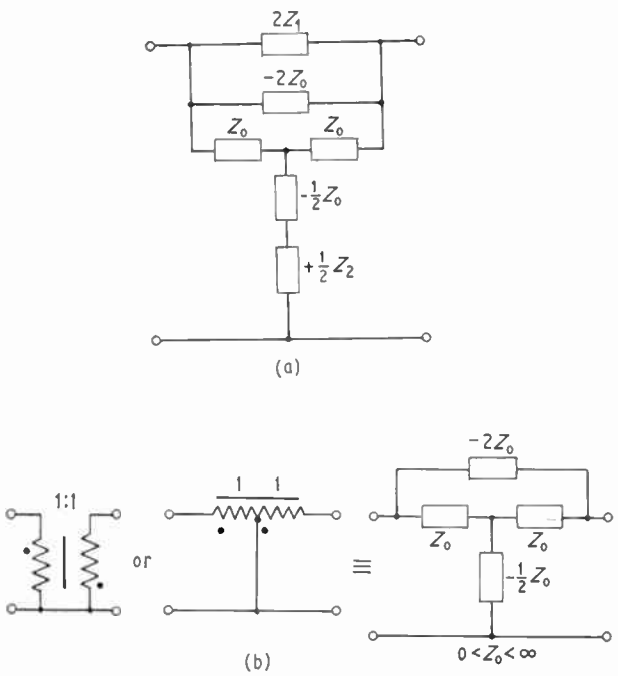

Fig. 2. The general (non-constant-resistance) active bridged-T network (a) and the special case $Y_1 \to 0, Z_2 \to 0$ which is the active equivalent of the unity-ratio ideal inverting transformer (b).

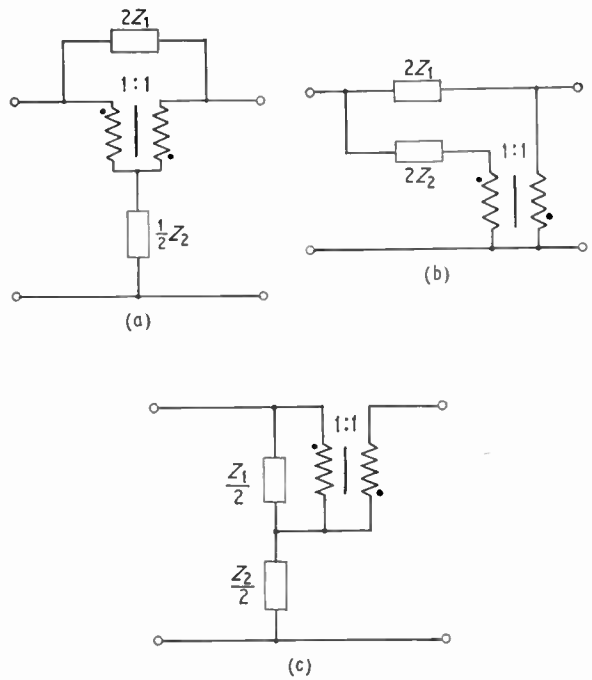

Fig. 3. Some unbalanced equivalents of the general lattice network.

(UNIC) when this is connected as a three-terminal element (Fig. 2(b)) and may replace it in any one of unbalanced equivalents of the general lattice network which employ such a transformer. Three of these equivalents are reproduced for reference in Fig. 3. It will be noted that there is a direct correspondence between the one in Fig. 3(a) (due to Jaumann[11]) and the active bridged-T in Fig. 2(a). Also, the active bridged-T of Fig. 2(b) is of the form generally adopted for the negative impedance repeater in telephony, but with values which give unity gain.

2.2.2 There are basically two kinds (a dual pair) of NIC's and these are most simply characterized by their transmission (or 'chain') matrices, which for the usual unity-ratio case are as follows:—

$$\left[T\right]_{\text{I-NIC}} = \begin{bmatrix} 1 & 0 \\ 0 & -1 \end{bmatrix}, \qquad \left[T\right]_{\text{V-NIC}} = \begin{bmatrix} -1 & 0 \\ 0 & 1 \end{bmatrix}$$

The first kind (I-NIC) inverts an applied current (at either side) without inverting voltage; the other kind (V-NIC) inverts voltage but not current. In either case the result is an input impedance which is the negative of the load impedance. The simplest equivalent circuits for the unbalanced case (as needed here) are shown in Fig. 4. Practical realizations of each type of converter are generally open-circuit stable at one port, short-circuit stable at the other. When a positive-real immittance is connected to either port, its negative will appear at the other port, but for stability at the

latter port, the immittance connected to it will be restricted by the fact that the resistance (conductance) of the mesh into which that port is connected must remain negative when the ideal short circuit (open circuit) is replaced by the Thévenin (Norton) equivalent of any circuit into which the loaded NIC is converted. In general, therefore, the stability of an otherwise passive circuit into which an NIC is connected will be subject to the immittance presented to the NIC being consistent with the stability character of the latter for the particular load immittance. Where two NIC's are employed in the same circuit advantage may be taken of the fact that the two types of NIC have complementary stability characteristics. The pair of UNIC's in the active equivalent of the -1 ideal transformer are operating in a particularly favourable environment, particularly if $Z_0 = R_0$, where R_0 is the terminating resistance (i.e. in the constant resistance case). This is the same configuration as that employed in negative impedance converter type repeaters in line communication.

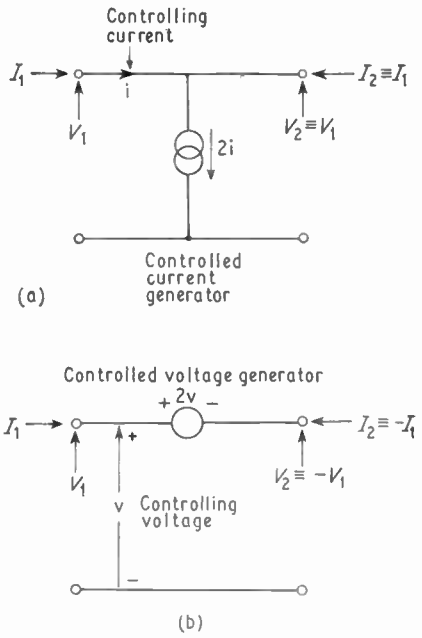

Fig. 4. Controlled-source representations of the two types of three-terminal negative immittance converter.

2.3. *The Z_0 Impedance Variable: Equivalent Circuits: τ, π Reduction*

In the active equivalent of the ideal unity-ratio inverting transformer the value of Z_0 must be non-zero and finite, and should be positive-real but is otherwise quite arbitrary. When this equivalent is associated with the immittance arms $2Z_1$ and $\frac{1}{2}Z_2$ in the general active bridged-T, each UNIC provides a coupling

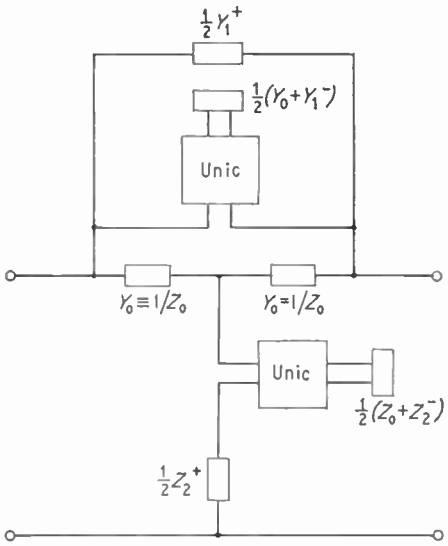

Fig. 5. The general active bridged-T with positive/negative partition of the immittance arms.

$$Y_1 = Y_1^+ - Y_1^-; \quad Y_2 = Y_2^+ - Y_2^-$$
$$Z_1 = Z_1^+ - Z_1^-; \quad Z_2 = Z_2^+ - Z_2^-$$

between its load ($2Z_0$ or $\frac{1}{2}Z_0$) and the adjacent immittance arm ($2Z_1$ or $\frac{1}{2}Z_2$) and there arises the possibility of distributing the arm between the two sides of the associated NIC. There is also the question of the value to be assigned to Z_0, in relation to the associated immittances, and there are two special cases of particular interest. With $2Z_0 = 2Z_1$ these two elements are made to cancel each other out by the upper UNIC and the bridged-T reduces to a T; dually, with $\frac{1}{2}Z_0 = \frac{1}{2}Z_2$ the bridged-T reduces to a π. More generally, thinking of $2Z_1$ (or $\frac{1}{2}Z_2$) in all-parallel (or all-series) form (as in the Foster canonical realizations of *LC*, *RC* and *RL* networks) Z_0 may be chosen to cancel any one or more of the set of parallel (or series) branches, with a corresponding change of the network. In this way numerous active equivalent circuits may generally be obtained, each corresponding to a particular value of Z_0, using the latter as a topological variable. This range of possibilities becomes of particular practical interest when $2Z_1$ or $\frac{1}{2}Z_2$ or both can be realized as the shunt or series combination, respectively, of positive and negative *RC* sub-networks; then the negative *RC* sub-networks may be realized by placing their negatives on the other side of the associated UNIC, as shown in Fig. 5. Having chosen Z_0 to neutralize part of either immittance, leaving an active bridged-T containing only one UNIC, further equivalent networks may be obtainable by applying the T$-\pi$ transformation to part of it and in particular cases this may eliminate the remaining UNIC.

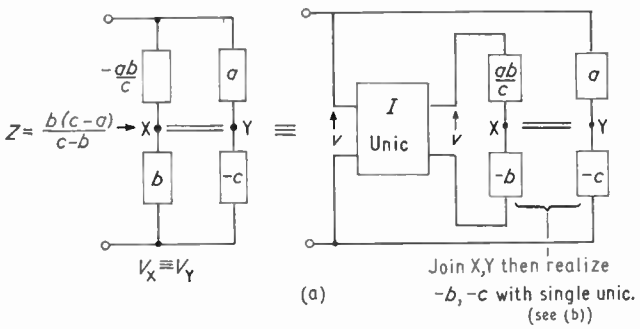

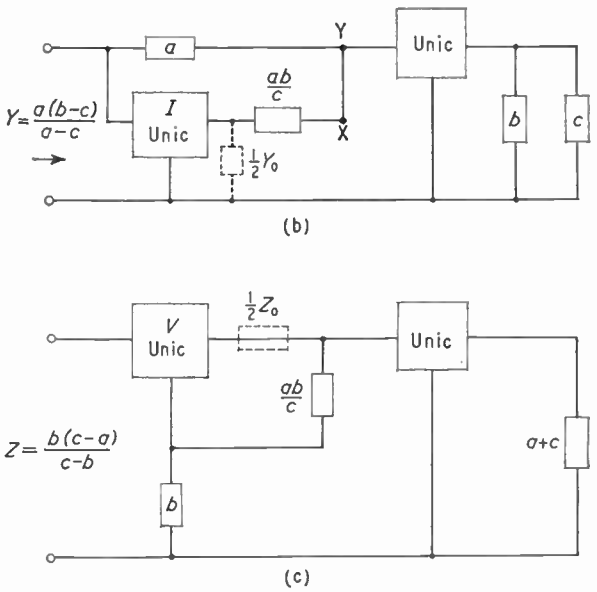

Fig. 6. The balanced bridged-T form (a) used in driving-point *RLC* immittance synthesis and a derived dual pair of forms suitable for active-*RC* realization (b, c). The dashed parts show how $-\frac{1}{2}Y_0$ and $-\frac{1}{2}Z_0$ are obtained at access terminal-pairs.

3. Active-*RC* Synthesis of the General Immittance Function

3.1. In order to assess the possibility of the active branches $-2Z_0$ and $-\frac{1}{2}Z_0$ taking part in the active-*RC* synthesis of the adjacent immittances $-2Z_1$ and $-\frac{1}{2}Z_2$, respectively, consideration has been given to the various synthesis procedures and realization forms that have been proposed for this purpose.

3.2. Using a synthesis procedure analogous to that of S. Darlington for *LC* immittance synthesis B. K. Kinariwala[6] showed that any ratio of polynomials in p having real coefficients and which is positive for at least one section of the $-\sigma$ axis may be realized in the form of an *RC* 2-port loaded by a negative *RC* impedance. (In case this condition on the value along the $-\sigma$ axis is not met this form would be preceded by another UNIC). This method has the disadvantage that it requires the synthesis of the *RC* 2-port from its open-circuit impedance parameters $Z_{11}, Z_{12} = Z_{21}, Z_{22}$. However, the realizability of this network is assured.

3.3. In a previous paper[12] the present writer has manipulated Kinariwala's decomposition into the form of a balanced bridge (see Fig. 6(a)), thereby obtaining an active-*RC* analogue of the J. Bott and R. Duffin method of synthesis for (minimum-real) *LC* immittance functions, and avoiding the synthesis of the 2-port *RC* network that was involved in Kinariwala's method. W. Saraga[13] developed a different decomposition from that of Kinariwala and realized it in the same bridge form.

3.4. The bridge circuit of Fig. 6(a) will be taken as the general form of the active-*RC* realization of the general immittance. For the present purpose it is unsuitable because, although it contains two NIC's, neither occurs with one of its terminal-pairs directly accessible from the access terminal-pair, which is desirable if the adjacent NIC of the active bridged-T replacement of the unity-ratio ideal inverting transformer is to be identified with one that is required for producing the associated immittance. If this form is employed, therefore, then it will be required to realize the parallel (series) combination of $-2R_0$ and $2Z_1$ (or $-\frac{1}{2}R_0$ and $\frac{1}{2}Z_2$). It is possible, however, to obtain from the bridge-circuit a driving-point equivalent of the desired form (see Fig. 6(b)). If either one of the two sides of the bridge are driven from the access-pair through a current-inversion type of UNIC and the signs of the two *RC* impedances comprising that side of the bridge are both reversed then the bridge will remain balanced and if the impedance of the null-branch (X, Y) is made zero by a short-circuit connection the two negative *RC* branches are brought directly in parallel and may therefore be produced by a single UNIC loaded by a pair of *RC* impedances of opposite sign. The result is a different configuration of the same four positive *RC* impedances and two UNIC's, one of the current-inverting type. If this form is used for the realization of $2Z_1$, then the leading UNIC may be identified with that needed for producing $-2Z_0$ and used to produce the latter by placing $2Z_0$ across its interior terminal-pair. There is, of course, a dual circuit which may be constructed by the usual procedure and this may be used to produce $-\frac{1}{2}Z_0$ as well as $\frac{1}{2}Z_2$ (see Fig. 6(c)).

4. The τ and π Reductions of the Active Lattice

4.1. On the basis of the result of 3.4 it will now be supposed that Z_1 and Z_2 of the lattice are realizable as parallel or series (as appropriate) positive-*RC* and negative-*RC* sub-networks, thus

$$Z_1 = Z_1^+ - Z_1^-, \qquad Z_2 = Z_2^+ - Z_2^-$$

in which $Z_1^+, Z_1^-, Z_2^+, Z_2^-$ are all positive-*RC* sub-

networks. Then, with the active bridged-T realization the sub-networks Z_1^- and Z_2^- would be placed on the load side of their respective UNIC networks, with $Z_0 = R_0$. When Z_a^- and Z_b^- are required to be pure reactances the existence of the loads $2R_0$ and $\frac{1}{2}R_0$ on the UNIC's will generally assure that the Kinariwala requirement (that the immittance under inversion be positive over at least one section of the $-\sigma$ axis) is satisfied. If Z_0 is set equal to Z_1 or Z_2, in order to

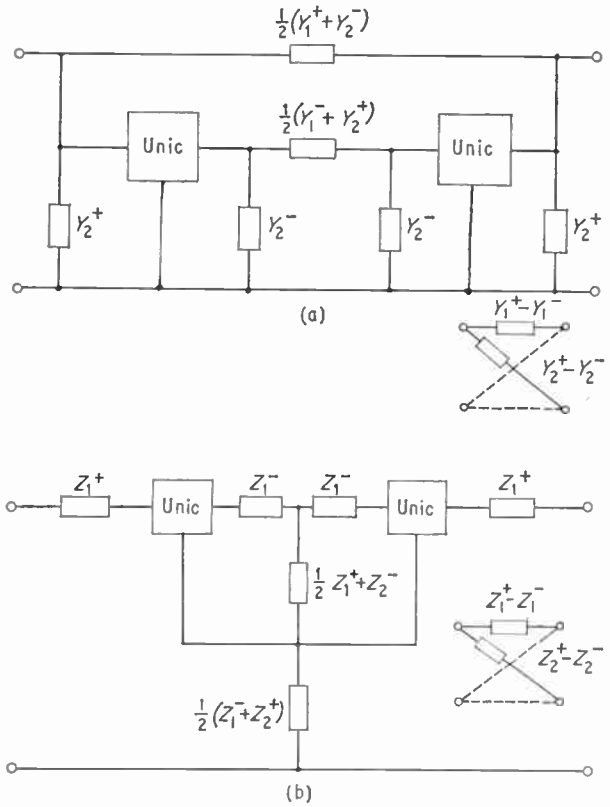

Fig. 7. The π and τ reductions of the general active bridged-T (Fig. 5) with positive/negative division of the immittance arms. The lattice equivalents are shown inset.

obtain the τ or π reduction, then the pair of series elements of value Z_1 in the τ or the shunt elements Z_2 in the π (see Fig. 5) will both have negative-*RC* components. The τ and π networks will then consist of a τ (or π) of positive-*RC* impedances in series (or parallel) with another τ (or π) of negative-*RC* impedances.

4.2. It is not necessary, however, to introduce two additional NIC's (making one per negative sub-network), because a 2-port of negative elements may have the sign of all of its elements reversed by cascading it between a pair of NIC's, both of the same kind, in either order. This assertion may be proved as follows.

For a general 2-port network having the chain matrix $[A, B; C, D]$ and current-inverting UNIC's the overall chain matrix is:—

$$\begin{bmatrix}1 & 0\\ 0 & -1\end{bmatrix}\cdot\begin{bmatrix}A & B\\ C & D\end{bmatrix}\cdot\begin{bmatrix}1 & 0\\ 0 & -1\end{bmatrix}=\begin{bmatrix}A & -B\\ -C & D\end{bmatrix}$$

Now, in terms of the open-circuit impedance parameters:—

$$A=\frac{z_{11}}{z_{21}},\qquad B=\frac{\Delta z}{z_{21}},\qquad C=\frac{1}{z_{21}},\qquad D=\frac{z_{22}}{z_{21}}$$

where

$$\Delta Z = Z_{11}Z_{22} - Z_{12}Z_{21}$$

so, if A, B, C, D correspond to a network of positive elements, the corresponding network of elements of reversed sign will have all of its Z_{ij} reversed in sign, resulting in the chain matrix $[A, -B; -C, D]$. Hence, cascading the positive network between the pair of UNIC's produces the desired result. The same effect may be achieved with two voltage-inverting UNIC's, but not with one of each kind. Thus, from the τ and π reductions one obtains the active-*RC* τ and π equivalents of the lattice given in Fig. 7. These again have two UNIC's, but with six positive-*RC* sub-networks compared with four in the active bridged-T (with $Z_0 = R_0$) and with a less favourable environment for the UNIC's (from the stability point of view), but both UNIC's may have their common terminal grounded.

5. Non-Reciprocal Single-UNIC Forms for Transfer Function Synthesis

The active forms so far derived are exact replacements for the lattice, regardless of terminations. As such they are suitable for the realization of symmetrical 2-ports that are specified by the corresponding immittance matrices. Although they employ NIC's which, considered as 2-ports, are non-reciprocal, they do so in co-reciprocal pairs (or equivalently when the τ or π reduction is made). Under specialized terminations, however, one of the pair of UNIC's in the forms shown in Fig. 7 becomes redundant and, if dispensed with, the network is made non-reciprocal. These single-UNIC forms are appropriate for the realization of a single transfer function (i.e. any one of the 12 or 21 elements of the immittance ([*G*], [*H*], [*Y*], [*Z*]) matrices) and there are four types, corresponding to the four elements of the transmission matrix $[A, B; C, D]$ as follows (see Fig. 8).

5.1. *Voltage-ratio Transfer Function Synthesis*

With an ideal voltage source on (1, 1'), or considering v_1 as an independent input, and with (2, 2') open-circuited, the left-hand side UNIC and its adjacent pair of admittances in Fig. 7(a), or the right-hand side UNIC and its adjacent pair of impedances in (b) become superfluous when they are of the current- or voltage-

inverting type, respectively. The A function that results will depend on whether the remaining UNIC is of current- or voltage-inversion type. Yanagisawa[9] gave these two reductions (but without derivation), both with current-inverting types of UNIC, as a dual pair. Using Yanagisawa's notation for the admittance-based type, namely

$$y_a = \tfrac{1}{2}(Y_1^+ + Y_2^-) \qquad Y_a = \tfrac{1}{2}(Y_2^+ + Y_1^-)$$
$$y_b = Y_2^+ \qquad Y_b = Y_2^-$$

the transfer function is

$$A = \frac{(y_a - Y_a)+(y_b - Y_b)}{y_a - Y_a}$$

as given by Yanagisawa.

(If the UNIC is of voltage inverting type the sign of Y_a in the denominator will be reversed.) For the impedance-derived form, with the corresponding notation,

$$z_a = Z_1^+ \qquad Z_a = Z_1^-$$
$$z_b = \tfrac{1}{2}(Z_2^+ + Z_1^-) \qquad Z_b = \tfrac{1}{2}(Z_1^+ + Z_2^-)$$

the transfer function for a voltage-inverting UNIC is

$$A = \frac{(z_a - Z_a)+(z_b - Z_b)}{z_b - Z_b}$$

which Yanagisawa gives, without proof, for the current-inverting NIC case. For the latter case the sign of Z_b in the denominator should be reversed.

5.2. *Current-ratio Transfer Function Synthesis*

Dually with respect to Section 5.1, with an ideal current source at (1, 1'), or considering i_1 as an independent input, and with (2, 2') short-circuited, the right-hand UNIC and its adjacent pair of admittances, or the left-hand UNIC and its adjacent pair of impedances, will be redundant if the UNIC is of voltage- or current-inverting type, respectively. For a remaining UNIC of the same kind:

$$D = \frac{1}{h_{21}} = \frac{(y_a - Y_a)+(y_b - Y_b)}{y_a - Y_a}$$
$$= \frac{(z_a - Z_a)+(z_b - Z_b)}{z_b - Z_b}$$

which are the same functions as for 5.1, as would be expected.

5.3. *Transfer Admittance Synthesis*

With the same input as for 5.1, but with a short-circuited output as for 5.2, the admittance-based form for 5.1 reduces further because y_b and $-Y_b$ are effectively short-circuited, with the result shown at Fig. 8 (iii), for which the (short-circuit) transfer admittance is

$$-y_{21} = y_a - Y_a$$

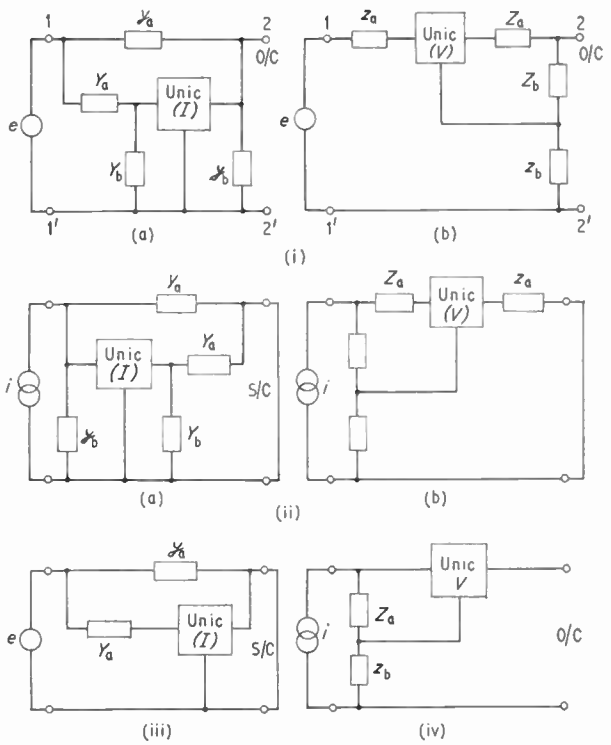

Fig. 8. Reduced forms of those of Fig. 7 for the synthesis of particular transfer functions: (i) g_{21}, (ii) h_{21}, (iii) y_{21}, (iv) z_{21}.

5.4. *Transfer Impedance Synthesis*

Dually with respect to Section 5.3, the impedance-based form for 5.2 reduces further because z_a and $-Z_a$ are effectively open-circuited, with the result shown at Fig. 8(iv), for which the (open-circuit) transfer impedance is:

$$z_{21} = z_b - Z_b$$

The validity of these reductions will be evident if the UNIC's are replaced by their appropriate equivalent circuits from Fig. 4. Once the network of Fig. 5 is made non-reciprocal by reduction, feedback loop stability considerations arise and the usual stability criteria may be applied. A disadvantage of reduction is that it restricts the application of sensitivity minimization procedures, such as that of Horowitz.

6. Synthesis Procedures

6.1. Given any one of the transfer functions one would realize it with the appropriate realization from the preceding section.

In terms of the $[Y]$ parameters:

$$A = \frac{1}{g_{21}} = \frac{y_{22}}{-y_{21}} = \frac{\tfrac{1}{2}(Y_1 + Y_2)}{\tfrac{1}{2}(Y_1 - Y_2)}$$

for the symmetrical lattice. Putting $A = N(p)/D(p)$ and dividing both $N(p)$ and $D(p)$ by

$$K(p) = \prod_{1}^{n-1} (p+\sigma_i)$$

where n is the degree of $N(p)$ or $D(p)$, whichever is the larger, and solving for the lattice arm admittances gives

$$Y_1 = \frac{N(p)+D(p)}{K(p)} \quad \text{and} \quad Y_2 = \frac{N(p)-D(p)}{K(p)}$$

Proceeding in the same way on the dual basis, i.e. with

$$A = \frac{1}{g_{21}} = \frac{z_{22}}{z_{21}} = \frac{\frac{1}{2}(Z_2+Z_1)}{\frac{1}{2}(Z_2-Z_1)}$$

one obtains

$$Z_1 = \frac{N(p)-D(p)}{K(p)}, \qquad Z_2 = \frac{N(p)+D(p)}{K(p)}$$

Exactly the same results are obtained from the $D = -1/h_{21}$ transfer function. Having obtained the lattice arms they are realized in $(+RC, -RC)$ Foster form and used in the appropriate reduced active lattice (Fig. 8).

For example, for

$$A = \frac{p^2+1}{p^2-1}$$

(an 'all-pass' function), with the (arbitrary) choice $K(p) = (p+1)(p+2)$, one obtains

$$Z_1 = \frac{2}{(p+1)(p+2)}, \qquad Z_2 = \frac{2p^2}{(p+1)(p+2)}$$

both of which may be expressed in partial-fraction expansion, as follows:

$$Z_1 = \frac{2}{p+1} - \frac{2}{p+2}, \qquad Z_2 = 2 + \frac{2}{p+1} - \frac{8}{p+2}$$

whence

$$\tfrac{1}{2}(Z_2-Z_1) = 1 - \frac{3}{p+2},$$

Z_1 and $\frac{1}{2}(Z_2-Z_1)$ are realized in Foster form, as shown in Fig. 9(a).

Substituting these in the appropriate reduced lattice form from Fig. 8(i)(b) gives the realization shown in Fig. 9(b).

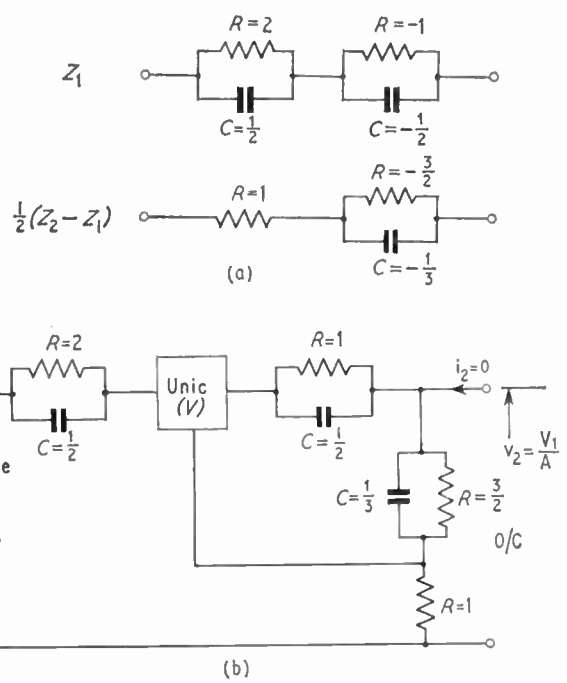

Fig. 9. An example: $A = \dfrac{1}{g_{21}} = \dfrac{p^2+1}{p^2-1}$.

6.2. Transfer admittance and impedance functions $(-y_{21}, z_{21})$ cannot be treated in quite the same way. Thus:

$$B = \frac{1}{-y_{21}} = \frac{N(p)/K(p)}{D(p)/K(p)} = \frac{2Z_1Z_2}{Z_2-Z_1} = \frac{2}{Y_1-Y_2}$$

and

$$C = \frac{1}{z_{21}} = \frac{N(p)/K(p)}{D(p)/K(p)} = \frac{2}{Z_2-Z_1} = \frac{2Y_1Y_2}{Y_1-Y_2}$$

cannot be solved for Z_1 and Z_2 in terms of $N(p)/K(p)$ and $D(p)/K(p)$ as before. If, however, $D(p)$ is already of the form required of $K(p)$, then $N(p)/D(p)$ can be expanded into partial fractions, the positive ones allocated to Z_2 and the negative ones to Z_1. It is the procedure that was employed by J. L. Bower and P. F. Ordung[14] for passive RC lattice synthesis. Otherwise a more general method is necessary and that of J. G. Linvill[15] may be regarded as one solution of the problem. If the denominator Z_2-Z_1 is identified with $D(p)/K(p)$ and expanded into partial fractions as before the positive and negative fractions cannot be assigned to Z_2 and Z_1 of the same network. Hence Linvill's configuration, in which two separate networks (each of which may be a symmetrical lattice) are cascaded about a UNIC. Denoting the two networks a, b:

$$z_{21} = \frac{z_{21a} \cdot z_{21b}}{z_{22a} - z_{11b}}$$

as required, and each network is specified by one driving-point and one transfer impedance and hence can be realized as a lattice.

The method of Bower and Ordung is tantamount to forming a corresponding driving-point immittance function by reversing all negative residues of the required transfer function and is therefore equivalent to specifying the lattice configuration. Provided that z_{21} is minimum-phase, this method of construction of $z_{11}(=z_{22})$ will ensure that the condition of A. Fialkow and I. Gerst[16] is satisfied and hence that the network may be realized in unbalanced form. Then, after separating the network into the sum of two sub-networks by the method of H. Ozaki,[17-19] if necessary, the unbalanced network[3] may be realized by

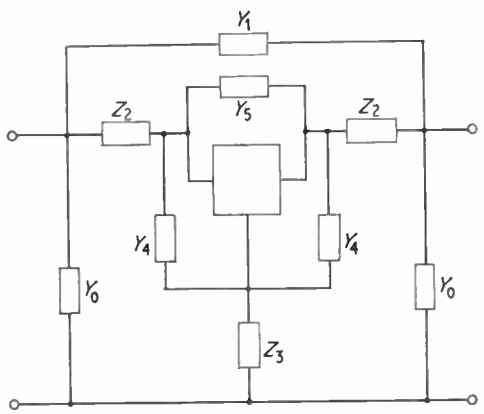

Fig. 10. Alternate π and τ extraction from the general three-terminal network, leaving an active nucleus.

alternate extraction of admittance (π) and impedance (τ) components (Fig. 10). In the general (non-minimum-phase) case, however, this process may terminate, leaving a residual nucleus but this may be realized by an active bridged-T.

7. Conclusion

One may summarize the principal results of this paper as follows:—

(i) A NIC equivalent of the unity-ratio ideal inverting transformer is given that may be used to obtain directly from unbalanced passive equivalents of the lattice their corresponding active counterparts.

(ii) When the associated inverse pair of impedances are replaced by their $-RC$, $-RC$ equivalents the same pair of NIC's as at (i) may be adapted for their realization also. New circuits for this purpose are given in Fig. 6.

(iii) The active bridged-T obtained at (i) may, in two special cases of the arbitrary impedance required in the transformer replacement, be reduced to simpler T or π form, thereby eliminating one of the NIC's needed for the transformer replacement at (i).

(iv) In general, when the arms of the τ or π are realized in active *RC* form a second NIC will be required again, but it is shown that this may be avoided when ideal terminations are employed, i.e. ideal sources with open circuit or short circuit loads.

(v) The procedure followed produces whole classes of forms for realization purposes, rather than particular circuits, and some well-known particular circuits such as those of T. Yanagisawa and R. E. Thomas are produced as special cases.

(vi) The entire procedure represents a logical continuation of the classical lattice procedures and may therefore be helpful for instructional (tutorial) purposes.

8. Acknowledgments

The work reported was carried out in the Department of Electronic and Electrical Engineering of the University of Birmingham during the year 1963–4 and originally published as Departmental Memorandum 186. The author is grateful to Professor D. G. Tucker for providing the facilities for research and to Professor J. T. Allanson for helpful discussion and guidance. Thanks are also due to the referees for constructive suggestions that have been incorporated in the revised text.

9. References

1. W. Cauer, 'Synthesis of Linear Communication Networks' (McGraw-Hill, New York, 1958) (Translation of German edition of 1954).
2. H. W. Bode, 'Network Analysis and Feedback Amplifier Design' (Van Nostrand, New York, 1945).
3. E. A. Guillemin, 'Synthesis of Passive Networks' (Wiley, New York, 1957).
4. A. Fialkow and I. Gerst, '*RLC* lattice transfer functions', *Proc. Inst. Radio Engrs*, **43**, pp. 462–9, April 1955.
5. J. G. Linvill, 'Transistor negative-impedance converters', *Proc. Inst. Radio Engrs*, **41**, pp. 725–9, June 1953.
6. B. K. Kinariwala, 'Synthesis of active *RC* networks', *Bell Syst. Tech. J.*, **38**, pp. 1269–1316, September 1959).
7. R. E. Thomas, 'The Use of the Active Lattice to Optimise Transfer Function Sensitivities', Polytechnic Institute of Brooklyn MRI Symposium Series, Vol. X, pp. 179–188 (Interscience Publishers, New York, 1961).
8. I. M. Horowitz, 'Optimization of negative-impedance conversion methods of active *RC* synthesis', *Trans. I.R.E. on Circuit Techniques*, CT-6, pp. 296–303, 1959.
9. T. Yanagisawa, '*RC* active networks using current-inversion type negative impedance converters', *Trans. I.R.E. on Circuit Techniques*, CT-4, pp. 140–4, 1957.
10. A. W. Keen, 'Active non-reciprocal realization of the compact symmetrical network for transfer function synthesis', *Proc. Instn. Elect. Engrs*, **106**, pp. 1075–9, June 1964.
11. V. Belevitch, 'Theorie des Circuits de Telecommunication', University of Louvain, Belgium (also Gautier-Villars, Paris), 1957.
12. A. W. Keen, 'Network synthesis in the non-reciprocal domain', 'Recent Advances in Network Theory', pp. 159–198 (Pergamon Press, London, 1963).
13. W. Saraga, 'A contribution to active *RC* network synthesis', *ibid.*, pp. 199–205.
14. J. L. Bower and P. F. Ordung, 'The synthesis of resistor-capacitor networks', *Proc. I.R.E.*, **38**, pp. 263–9, March 1950.
15. J. G. Linvill, 'Active *RC* filters', *Proc. I.R.E.*, **42**, pp. 555–64, March 1954.
16. A. Fialkow and I. Gerst, "The transfer function of networks without mutual inductance', *Quart. Appl. Maths*, **12**, pp. 117–31, 1954.
17. N. Balabanian, 'Network Synthesis', Chap. 7 (Prentice-Hall, Englewood Cliffs, N.J., 1958).
18. H. Ozaki, 'Synthesis of *RC* 3-terminal *RC* Networks', Ozaka Univ. Tech. Report, 3(60), pp. 57–77, 1953.

19. H. M. Lucal, 'Synthesis of three-terminal *RC* networks', *Trans. I.R.E. on Circuit Techniques*, CT-2, No. 4, pp. 308–16, 1955.

20. I. W. Sandberg, 'Synthesis of driving-point impedances with active-*RC* networks', *Bell Syst. Tech. J.*, 39, pp. 947–62, July, 1960.

10. Appendix 1

It is assumed that the reader is familiar with the principle of the standard method (believed to be due to J. G. Linvill[15]) of developing immittance functions into differences of *RC* functions and then realizing them with the aid of negative immittance converters, without recourse to inductances or ideal transformers.

Both numerator $N(s)$ and denominator $D(s)$ of the required function are divided by the same polynomial $P(s)$ that has only negative real roots and then expanded into partial fractions. Some of these will be positive, some negative, and so the following development may be made:

$$Z(s) = \frac{N(s)}{D(s)} = \frac{N(s)/P(s)}{D(s)/P(s)} = \frac{N_1/P_1 - N_2/P_2}{D_1/P_1 - D_2/P_2}, \quad P_1 P_2 = P$$

When this is properly done, all four of the functions N_1/P_1, N_2/P_2, D_1/P_1 and D_2/P_2, will be positive *RC* functions. $Z(s)$ may then be realized, following B. K. Kinariwala[6] as a passive *RC* 2-port network loaded with a negative *RC* load that is realized with the corresponding positive load through a negative immittance converter. Alternatively, following I. W. Sandberg[20], $Z(s)$ may be expressed as the sum:

$$Z(s) = \frac{1}{\frac{D_1}{N_1} - \frac{D_2}{N_1} \cdot \frac{P_1}{P_2}} + \frac{1}{\frac{D_2}{N_1} - \frac{D_1}{N_2} \cdot \frac{P_2}{P_1}}$$

and realized in the bridge form shown in Fig. 6(a) with:

$$a = \frac{N_1}{D_1}, \qquad b = \frac{N_2}{D_2}, \qquad c = \frac{N_2}{D_1} \cdot \frac{P_1}{P_2}$$

The refinements of this basic procedure that are generally required to ensure realizability have been dealt with comprehensively by Kinariwala and Sandberg (*loc. cit.*).

An example of the general procedure is given in the text in Section 6.1 and Fig. 9.

Appendix 2

The matrix notation used for the general 2-port network (see accompanying Fig. 11) is conventional, but is summarized here for convenience of reference:

Fig. 11. Current and voltage conventions and notation for the general 2-port network.

$$\begin{bmatrix} i_1 \\ v_2 \end{bmatrix} = \begin{bmatrix} g_{11} & g_{12} \\ g_{21} & g_{22} \end{bmatrix} \cdot \begin{bmatrix} v_1 \\ i_2 \end{bmatrix} \qquad \begin{bmatrix} v_1 \\ i_2 \end{bmatrix} = \begin{bmatrix} h_{11} & h_{12} \\ h_{21} & h_{22} \end{bmatrix} \cdot \begin{bmatrix} i_1 \\ v_2 \end{bmatrix}$$

$$\begin{bmatrix} i_1 \\ i_2 \end{bmatrix} = \begin{bmatrix} y_{11} & y_{12} \\ y_{21} & y_{22} \end{bmatrix} \cdot \begin{bmatrix} v_1 \\ v_2 \end{bmatrix} \qquad \begin{bmatrix} v_1 \\ v_2 \end{bmatrix} = \begin{bmatrix} z_{11} & z_{12} \\ z_{21} & z_{22} \end{bmatrix} \cdot \begin{bmatrix} i_1 \\ i_2 \end{bmatrix}$$

$$\begin{bmatrix} v_1 \\ i_1 \end{bmatrix} = \begin{bmatrix} A & B \\ C & D \end{bmatrix} \cdot \begin{bmatrix} v_2 \\ -i_2 \end{bmatrix}$$

$$A = \frac{1}{g_{21}}, \qquad B = -\frac{1}{y_{21}}, \qquad C = \frac{1}{z_{21}}, \qquad D = -\frac{1}{h_{21}}$$

Note.—The output variable $-i_2$ is employed, rather than i_2, in the transmission, or chain, matrix in order that, for convenience of multiplication, it may be identified with i_1 of the following network when dealing with cascades of networks.

Manuscript first received by the Institution on 12th April 1965 and in final form on 6th September 1965. (Paper No. 1060.)

I.E.R.E. Graduateship Examination, May 1966

PASS LISTS

The following candidates who sat the May 1966 examination at centres outside Great Britain and Ireland succeeded in the sections indicated. The examination, which was conducted at 61 centres throughout the world, attracted entries from 550 candidates. Of these 201 sat the examination at centres in Great Britain and Ireland and 177 sat the examination at centres overseas. The names of successful candidates resident in Great Britain and Ireland will be published in the next issue of the *Proceedings* of the I.E.R.E.

	Candidates appearing	*Pass*	*Fail*	*Refer*
Section A				
Great Britain	111	31	78	2
Overseas	100	23	71	6
Section B				
Great Britain	90	22	58	10
Overseas	77	21	51	5

OVERSEAS

The following candidates have now completed the Graduateship Examination and thus qualify for transfer or election to Graduate or a higher grade of membership.

AHMAD, G. (S), *Karachi, Pakistan*
BALAKRISHNAN, K. (S), *Madras, India*
BALAKRISHNAN, S. *New Delhi, India*
BARNEA, J. *Tel-Aviv, Israel*
BENIRAGAMA, D. K. W. (S), *Colombo, Ceylon*
DEYNEM, H. R. *Bermuda*
EDDO, R. O. (S), *Lagos, Nigeria*
GAVISH, A. *Tel-Aviv, Israel*
GINSBURG, A. (S), *Tel-Aviv, Israel*
GOPALA KRISHNAN, G. *Dehra Dun, India*
GRAVES, G. (S), *Singapore*
KHAN, K. U. *Rawalpindi, Pakistan*
NARAYANA-MURTHI, K. *Delhi, India*
PAUL, R. N. *Agra, India*
PITAWALA, A. B. (S), *Colombo, Ceylon*
RAVINDRA, D. K. (S), *Bombay, India*
RODWELL, W. E. *Bermuda*
SREEDHARA, M. K. (S), *Ernakulam, India*
SRIVASTAVA, H. C. (S), *Lucknow, India*
VENUGOPALAN, K. N. (S) *Delhi, India*
YAP CHO SING *Singapore*

The following candidates have now satisfied the requirements of Section A of the Graduateship Examination.

ACHARYA, B. M. *Mysore, India*
ASH, D. E. (S), *Auckland, New Zealand*
CHAKI, D. R. *Calcutta, India*
CHIU, C. H. (S), *Hong Kong*
DE KLERK, P. A., *Cape Town, South Africa*
DHARIWAL, U. S. J. (S), *Delhi, India*
DRYSDALE, K. W. P. (S), *Sydney, Australia*
DUTTA, N. K. (S), *Calcutta, India*
EDIRISINGHE, E. M. S. (S), *Colombo, Ceylon*
ENWELUZOR, M. P. C. (S), *Lagos, Nigeria*
HALL, S. W. *Fort Victoria, Rhodesia*
JAGGI, T. S. *Delhi, India*
KURUPPU, D. L. U. *Colombo, Ceylon*
LAU HON SHIANG *Singapore*
MANKU, H. S. (S), *Nairobi. Kenya*
MONCKE, L. (S), *Lagos, Nigeria*
NARENDRANATHAN, K. P. *Ernakulam, India*
PARKER, K. S. V. *Hong Kong*
PRASAD, R. C. *Bombay, India*
SHURMER, G. L. *Kano, Nigeria*
SUNDARARAJAH, T. *Colombo, Ceylon*
VAKIL, R. M. *Bombay, India*
ZAVAHIR, M. W. *Colombo, Ceylon*

The question papers set in Section B, Part 5 of the May 1965 Graduateship Examination together with answers to numerical questions and examiners' comments will be published in the July/August issue of the *Proceedings* of the I.E.R.E.

(S) denotes a Registered Student.

U.D.C. 621.373.51

Univibrator Analysis for a Tunnel Diode with a Transmission Line

By

M. N. S. SWAMY, B.Sc.(Hons.), D.I.I.Sc., M.Sc., Ph.D.†

Summary: A univibrator circuit using a tunnel diode and a transmission line is analysed. A graphical method is presented to calculate the width and the magnitude of the univibrator pulse. Conditions for the univibrator action to take place are derived. The effects of variation of the tunnel diode bias and the characteristic impedance of the line on the pulse width are also studied. The modifications to be made in the graphical analysis for the case of a line with small losses are discussed in detail.

1. Introduction

Tunnel diode univibrator circuits have been designed using inductances and their uses as pulse-shaping networks have been studied.[1-5] Mention has also been made in the literature of the tunnel diode univibrator circuits using transmission lines. However, no detailed analysis of such univibrator circuits using transmission lines has been made and a semi-graphical analysis of these circuits is presented in this paper.

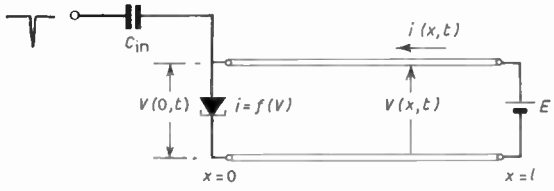

Fig. 1. The circuit of a univibrator using a tunnel diode and a transmission line.

Figure 1 shows a tunnel diode univibrator using a transmission line. The initial operating point A_0 (see Fig. 2) is determined by the supply voltage E and the resistance R_l of the line of length l. The circuit is triggered by a short negative pulse applied to the tunnel diode through the capacitor C_{in}. Let us assume that the amplitude of the trigger pulse is enough to take the operating point to the region satisfying the conditions for the switching action to take place.[6-9] Let us also assume that the trigger pulse is short so that the initial current I_0 in the tunnel diode and the line is not changed during the time the trigger pulse lasts.

Due to the switching of the tunnel diode, the operating point moves from A_0 to A_0'. However, at the same time the boundary conditions, are altered so that voltage and current waves begin to travel from the tunnel diode to the source, resulting in a change of the operating point from A_0' to A_1. It will remain at A_1 for a duration of $2l/a$, where l is the length of the line, $a = 1/\sqrt{(LC)}$ is the velocity of the wave in the line and L, C are the inductance and capacitance per unit length of the line. When the reflected wave returns to the tunnel diode, the operating point shifts from A_1 to A_2 and will stay at A_2 for a duration of $2l/a$. Similar jumps of the operating point will occur along the first positive resistance region of the tunnel diode characteristic until conditions for the switching of the tunnel diode occur and then the operating point moves to a_1. Consequently, transients occur in the line till the operating point finally returns to the equilibrium point A_0 (Fig. 2). We shall now analyse this tunnel diode univibrator circuit.

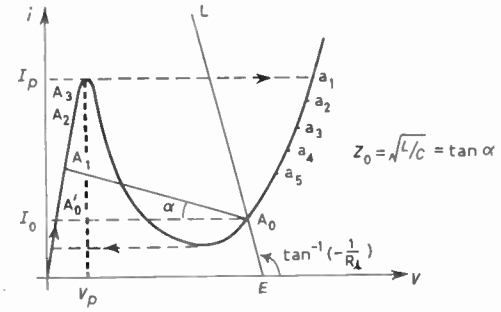

Fig. 2. *V-I* characteristic of the tunnel diode with the d.c. and a.c. load lines.

2. Analysis of the Circuit

We shall make the following assumptions in order to simplify the analysis:

(i) the circuit is triggered without a variation of the bias current I_0;

(ii) the tunnel diode capacitance is negligible;

(iii) the line is lossless.

† Department of Electrical Engineering, Nova Scotia Technical College, Halifax, Canada.

If $v(x, t)$ and $i(x, t)$ denote the voltage and current in the line at a distance x from the tunnel diode at any time t (Fig. 1), then they satisfy the differential equations

$$\frac{\partial v}{\partial x} = L\frac{\partial i}{\partial t} \qquad \text{.....(1)}$$

and

$$\frac{\partial i}{\partial x} = C\frac{\partial v}{\partial t} \qquad \text{.....(2)}$$

with the following initial and boundary conditions:

$$\begin{aligned} v(l, t) &= E; \qquad i(0, t) = f(v) \\ i(0, 0) &= I_0 = f(V_0) = f(E) \end{aligned} \qquad \text{.....(3)}$$

From (1) and (2) we have

$$\frac{\partial^2 v}{\partial x^2} = LC \cdot \frac{\partial^2 v}{\partial t^2} \qquad \text{.....(4)}$$

The solution of eqn. (4) may be represented as

$$v(x, t) - V_0 = F(t - x/a) + G(t + x/a) \qquad \text{.....(5)}$$

Substituting eqn. (5) in eqn. (1) and solving for i we have

$$i(x, t) - I_0 = -\{F(t - x/a) - G(t + x/a)\}/Z_0 \qquad \text{.....(6)}$$

where $Z_0 = \sqrt{L/C}$ is the characteristic impedance of the line. In the above equations, $F(t - x/a)$ represents the incident wave from the tunnel diode towards the source, and $G(t + x/a)$ represents the reflected wave from the source towards the diode. Since F and G are arbitrary, we may choose that

$$F(-x/a) = G(x/a) = 0 \qquad \text{.....(7)}$$

Since $v(l, t) = V_0$, we have

$$G(t + l/a) = -F(t - l/a) \qquad \text{.....(8)}$$

By changing the origin of time we may write eqn. (8) as

$$G(t) = -F(t - 2l/a) = -F(t - T) \qquad \text{.....(9)}$$

where

$$T = 2l/a \qquad \text{.....(10)}$$

If we now represent t as an integral multiple of T plus a time interval t' where $(0 < t' < T)$ we have

$$G_n\{(n-1)T + t'\} = -F_{n-1}\{(n-1)T + t' - T\}$$

or

$$G_n\{(n-1)T + t'\} = -F_{n-1}\{(n-2)T + t'\} \qquad \text{.....(11)}$$

where n denotes the number of the phase of the process.

Hence, for $x = 0$, eqns. (5) and (6) reduce for the nth phase to

$$v_n - V_0 = F_n\{(n-1)T + t'\} - F_{n-1}\{(n-2)T + t'\} \qquad \text{.....(12a)}$$

and

$$i_n - I_0 = -[F_n\{(n-1)T + t'\} + F_{n-1}\{(n-2)T + t'\}]/Z_0 \qquad \text{.....(12b)}$$

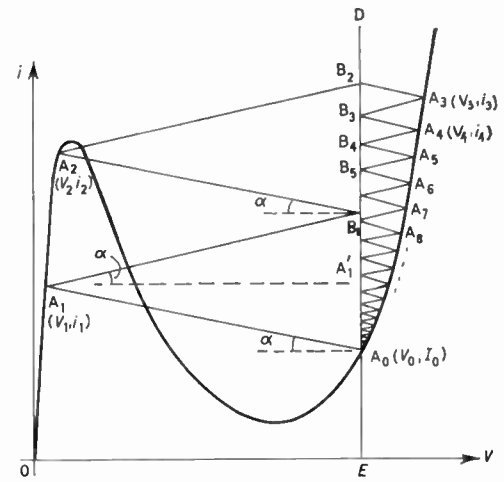

Fig. 3. The characteristic with the different operating points at the end of the different phases.

Hence we get the following equations for v and i for the different values of n:

$$\begin{aligned} v_1 - V_0 &= F_1(t') \\ v_2 - V_0 &= F_2(T + t') - F_1(t') \\ v_3 - V_0 &= F_3(2T + t') - F_2(T + t') \\ &\cdots\cdots \\ &\cdots\cdots \\ v_n - V_0 &= F_n\{(n-1)T + t'\} - F_{n-1}\{(n-2)T + t'\} \end{aligned} \qquad \text{.....(13)}$$

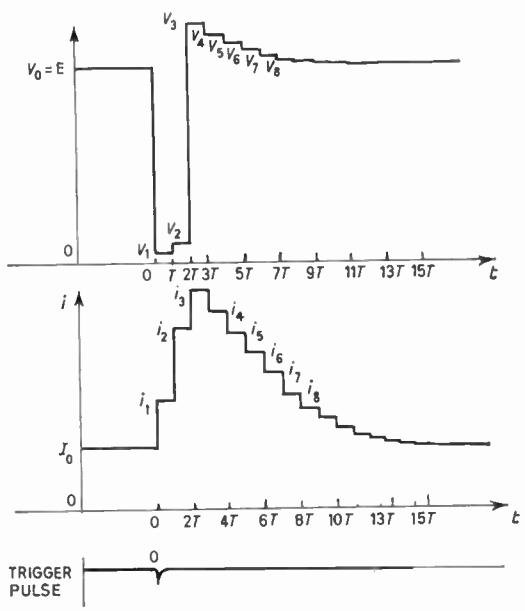

Fig. 4. Voltage and current waveforms at the tunnel diode.

and

$$i_1 - I_0 = -[F_1(t')]/Z_0$$
$$i_2 - I_0 = -[F_2(T+t') + F_1(t')]/Z_0$$
$$i_3 - I_0 = -[F_3(2T+t') + F_2(T+t')]/Z_0$$
$$\cdots\cdots$$
$$\cdots\cdots$$
$$i_n - I_0 = -[F_n\{(n-1)T+t'\} + F_{n-1}\{(n-2)T+t'\}]/Z_0 \quad \ldots\ldots(14)$$

From eqns. (13) and (14), the following relations between v and i can be established.

$$i_1 - I_0 = \{V_0 - v_1\}/Z_0$$
$$i_2 - i_1 = \{2V_0 - (v_1 + v_2)\}/Z_0$$
$$\cdots\cdots$$
$$\cdots\cdots$$
$$i_n - i_{n-1} = \{2V_0 - (v_{n-1} + v_n)\}/Z_0 \quad \ldots\ldots(15)$$

This set of equations may be solved graphically by first rearranging them and writing them as follows:

$$(i_1 - I_0) = (V_0 - v_1)/Z_0$$
$$(i_2 - i_1) - (V_0 - v_1)/Z_0 = (V_0 - v_2)/Z_0$$
$$(i_3 - i_2) - (V_0 - v_2)/Z_0 = (V_0 - v_3)/Z_0$$
$$\cdots\cdots$$
$$\cdots\cdots \quad \ldots\ldots(16)$$

If we now draw a line A_0A_1 at an angle α ($\tan\alpha = 1/Z_0$) with the horizontal to cut the characteristic of the tunnel diode at A_1 (Fig. 3), then the point A_1 is such that the first equation of (16) is satisfied. A_1 gives the position of the operating point after the first phase. We now draw a line A_1B_1 making an angle α with the horizontal to cut the line ED at B_1. Let the line A_2B_1 at an angle α cut the characteristic at A_2. Then the point A_2 is such that the second equation of (16) is satisfied. Thus A_2 gives the position of the operating point at the end of the second phase. This graphical procedure may be repeated to solve the set of eqns. (16), and is shown in Fig. 3. Figure 4 shows the voltage and current waveforms at the tunnel diode which are derived from Fig. 3.

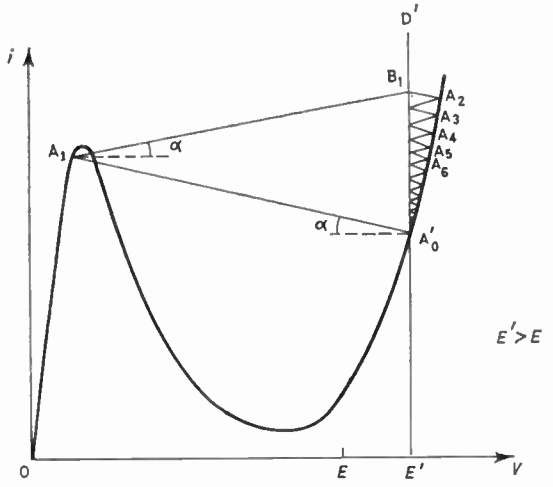

Fig. 5. The effect of bias on the pulse duration.

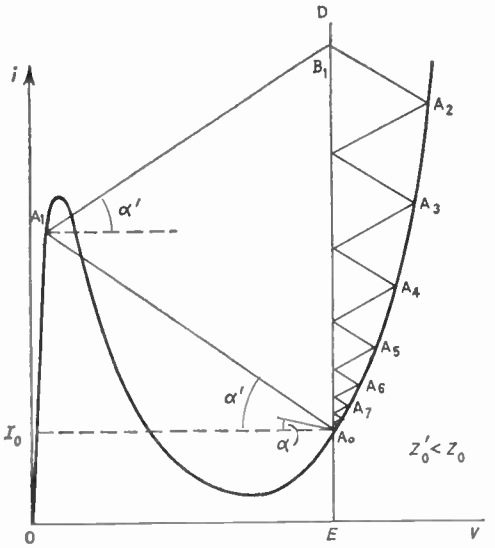

Fig. 6. The effect of Z_0 on the pulse duration.

3. Effects of the Bias and Z_0 on the Pulse Width

If we keep the characteristic impedance of the line constant and vary the bias E, then the equilibrium point A_0 changes. Hence the position of A_1 changes and as a result, those of the points $A_2, A_3, \ldots$. Hence, the total number of points $A_1, A_2, \ldots$, changes as we vary the bias. If the bias is increased, then the total number of points will decrease and as a result the duration of the univibrator pulse decreases (Fig. 5). On the other hand, a decrease of the bias increases the total number of points, thus increasing the pulse duration. We may therefore change the duration of the pulse by varying the bias of the tunnel diode.

If the bias is kept constant and Z_0 varied, then the angle α changes resulting in a change of the total number of points $A_1, A_2, \ldots$, thus changing the pulse width. If we increase Z_0, then α decreases and hence the total number of points increases, thus increasing the pulse duration. Also, a decrease of Z_0 will result in a decrease of the pulse width (Fig. 6). As we will see shortly the characteristic impedance Z_0 of the line cannot be decreased beyond a certain value, as there will be no univibrator action then.

4. Conditions for Univibrator Action

For the circuit of Fig. 1 to act as a univibrator we see from Fig. 3 that there should be at least one point A_1 on the first positive resistance portion of the characteristic of the tunnel diode. Hence we can determine the limiting value of Z_0 for given bias

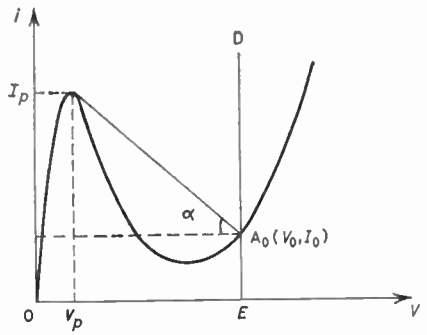

Fig. 7. Minimum value of Z_0 required for univibrator action.

conditions in order that there may be the univibrator action. If I_P and V_P be the peak current and the corresponding voltage of the tunnel diode (Fig. 7), then Z_0 should be such that

$$Z_0 \geqslant (V_0 - V_P)/(I_P - I_0) \qquad \text{.....(17)}$$

Thus $Z_{0(\min)}$, the minimum value of the characteristic impedance of the line is

$$Z_{0(\min)} = (V_0 - V_P)/(I_P - I_0) \qquad \text{.....(18)}$$

It may be observed from eqn. (18) that this minimum value of Z_0 increases as the bias of the tunnel diode is increased.

5. Line with Small Losses

If the line is lossy then the load line will not be vertical but will make an angle of $\tan^{-1}(-1/R_l)$ with the horizontal, where R_l is the ohmic resistance of the line. We may determine the bias point (V_0, I_0) by drawing this load line on the characteristic of the tunnel diode. The differential equations to be solved in this case are

$$\frac{\partial v}{\partial x} = L\frac{\partial i}{\partial t} + Ri$$

and $\qquad \text{.....(19)}$

$$\frac{\partial i}{\partial x} = C\frac{\partial v}{\partial t}$$

(where R = resistance per unit length of the line), with the following initial and boundary conditions:

$$\begin{aligned} &v(l,t) = E; \qquad i(0,t) = f(v) \\ &v(0,0) = V_0 = E - Rl\,I_0 = E - R_l I_0 \\ &i(0,0) = I_0 = f(V_0) \\ &v(x,0) = E - R(l-x)I_0 \end{aligned} \qquad \text{.....(20)}$$

Now the characteristic impedance of the line is

$$\sqrt{\frac{R+Ls}{Cs}} = \sqrt{\frac{L}{C}}\left\{1 + \frac{R}{Ls}\right\}^{\frac{1}{2}} \qquad \text{.....(21)}$$

Assuming the line losses to be very small, the characteristic impedance of the lossy line

$$\simeq \sqrt{L/C} = Z_0 \qquad \text{.....(22)}$$

Also the propagation constant

$$= \sqrt{(R+Ls)Cs} = \sqrt{LCs}\{1 + (R/Ls)\}^{\frac{1}{2}}$$

or propagation constant

$$\simeq (s/a) + \tfrac{1}{2}R\sqrt{(C/L)} = (s/a) + \delta \qquad \text{.....(23)}$$

where

$$\delta = \tfrac{1}{2}R\sqrt{(C/L)} = \tfrac{1}{2}(R/Z_0) \qquad \text{.....(24)}$$

Hence, when the line losses are very small it may be assumed that the characteristic impedance is not changed, but only that v and i are attenuated with an attenuation constant $\delta = (R/2Z_0)$. Hence the solutions for $v(x, t)$ and $i(x, t)$ may be represented as

$$v(x,t) - \{E - R(l-x)I_0\} = [e^{-\delta x}F(t - x/a) + e^{-\delta(2l-x)}G(t + x/a)] \qquad \text{.....(25)}$$

$$i(x,t) - I_0 = -[e^{-\delta x}F(t - x/a) - e^{-\delta(2l-x)}G(t + x/a)]/Z_0 \qquad \text{.....(26)}$$

Since F and G are arbitrary we may choose that

$$F(-x/a) = G(x/a) = 0 \qquad \text{.....(27)}$$

Since

$$v(l,t) = E, \qquad e^{-\delta l}F(t - l/a) + e^{-\delta l}G(t + l/a) = 0$$

Hence,

$$G(t + l/a) = -F(t - l/a) \qquad \text{.....(28)}$$

By changing the origin of time eqn. (28) may be written as

$$G(t) = -F(t - 2l/a) = -F(t - T) \qquad \text{.....(29)}$$

Hence, as in the case of a lossless line, if we represent t as an integral multiple of T plus a time t' $(0 < t' < T)$ we have

$$G_n\{(n-1)T + t'\} = -F_{n-1}\{(n-2)T + t'\} \qquad \text{.....(30)}$$

where n denotes the number of the phase of the process.

Therefore for $x = 0$, eqns. (25) and (26) reduce for the nth phase to

$$v_n - V_0 = F_n\{(n-1)T + t'\} - e^{-2\delta l}F_{n-1}\{(n-2)T + t'\} \qquad \text{.....(31)}$$

$$i_n - I_0 = -[F_n\{(n-1)T + t'\} + e^{-2\delta l}F_{n-1}\{(n-2)T + t'\}]/Z_0 \qquad \text{.....(32)}$$

Now

$$e^{-2\delta l} = (1 - 2\delta l + \ldots) = \left(1 - \frac{R_l}{Z_0} + \ldots\right) \simeq 1 - \frac{R_l}{Z_0} = 1 - 2\delta l \qquad \text{.....(33)}$$

Hence eqns. (31) and (32) reduce to

$$v_n - V_0 = F_n\{(n-1)T + t'\} - (1 - 2\delta l)F_{n-1}\{(n-2)T + t'\} \qquad \text{.....(34)}$$

$$i_n - I_0 = -[F_n\{(n-1)T + t'\} + (1 - 2\delta l)F_{n-1}\{(n-2)T + t'\}]/Z_0 \qquad \text{.....(35)}$$

Therefore we get the following equations for v and i for different values of n:

$$v_1 - V_0 = F_1(t')$$
$$v_2 - V_0 = F_2(T+t') - (1-2\delta l)F_1(t')$$
$$\cdots\cdots$$
$$\cdots\cdots$$
$$v_n - V_0 = F_n\{(n-1)T+t'\} - (1-2\delta l)F_{n-1}\{(n-2)T+t'\} \quad \ldots\ldots(36)$$

and

$$i_1 - I_0 = -[F_1(t')]/Z_0$$
$$i_2 - I_0 = -[F_2(T+t') + (1-2\delta l)F_1(t')]/Z_0$$
$$\cdots\cdots$$
$$\cdots\cdots$$
$$i_n - I_0 = -[F_n\{(n-1)T+t'\} + (1-2\delta l)F_{n-1}\{(n-2)T+t'\}]/Z_0 \quad \ldots\ldots(37)$$

From eqns. (36) and (37) we get

$$i_1 - I_0 = (V_0 - v_1)/Z_0$$
$$i_2 - i_1 = \{-F_2(T+t') + 2\delta l F_1(t')\}/Z_0 \quad \ldots\ldots(38)$$

But

$$F_2(T+t') = (v_2 - V_0) + (1-2\delta l)F_1(t')$$

Hence

$$i_2 - i_1 = (V_0 - v_2)/Z_0 + (4\delta l - 1)F_1(t')/Z_0$$

or

$$i_2 - i_1 = (V_0 - v_2)/Z_0 + \frac{R_l}{Z_0}\cdot\frac{F_1}{Z_0} + \left(\frac{R_l}{Z_0} - 1\right)\frac{F_1}{Z_0}$$

But

$$F_1/Z_0 = I_0 - i_1 = (v_1 - V_0)/Z_0$$

Hence

$$(i_2 - i_1) = \left[(V_0 - v_2) + \left(1 - \frac{R_l}{Z_0}\right)(V_0 - v_1) - R_l(i_1 - I_0)\right]/Z_0$$

Similarly

$$(i_3 - i_2) = \left[(V_0 - v_3) + \left(1 - \frac{R_l}{Z_0}\right)(V_0 - v_2) - R_l(i_2 - I_0)\right]/Z_0$$

$$\cdots\cdots$$
$$\cdots\cdots$$

Thus the following relations between v and i are obtained:

$$(i_1 - I_0) = [V_0 - v_1]/Z_0$$
$$(i_2 - i_1) - \left(1 - \frac{R_l}{Z_0}\right)(V_0 - v_1)/Z_0 = [(V_0 - v_2) - R_l(i_1 - I_0)]/Z_0$$
$$(i_3 - i_2) - \left(1 - \frac{R_l}{Z_0}\right)(V_0 - v_2)/Z_0 = [(V_0 - v_3) - R_l(i_2 - I_0)]/Z_0$$
$$\cdots\cdots$$
$$\cdots\cdots \quad \ldots\ldots(39)$$

The set of eqns. (39) may now be solved by a graphical procedure similar to the one described before for the case of a lossless line. In the present case, we draw lines making angles α with the horizontal so as to intersect the characteristic and the line XY (XY is a line passing through A_0 and having a slope of $-2/R_l$) and not the vertical line as in the case of a lossless line. This is shown in Fig. 8 and the justification for this graphical procedure is given in the Appendix.

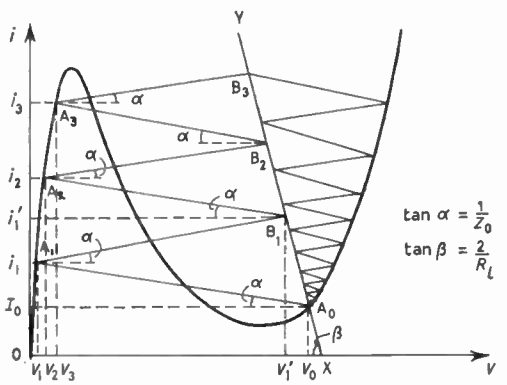

Fig. 8. The characteristic with the different operating points at the end of the different phases, when the line has small losses.

In the case of a lossy line, eqn. (17) is no longer a sufficient condition for the univibrator action to occur. An additional condition, that the load line EL (Fig. 2) must intersect the tunnel diode characteristic at a single point in the positive resistance region, is necessary.

6. Conclusions

This analysis will help in the design of the univibrator circuits. The conditions for the univibrator action to occur can readily be determined and the pulse width found. With a line of large characteristic impedance, the circuit could be used as a variable delay network, or with a line of small Z_0, it could be used as a pulse shaping network. The delay in such circuits may be controlled by varying the bias on the tunnel diode or by varying the parameters of the line.

7. Acknowledgments

The author would like to thank Professor J. C. Callaghan for the discussions in connection with the analysis of the lossy line. Thanks are also due to the referees for their valuable comments. This research work was supported in part by the National Research Council of Canada, under Grant No. A-2875.

8. References

1. C. M. Barrack and M. C. Watkins, 'Tunnel diode relaxation oscillators', *Electronic Design*, pp. 54–57, 22nd June 1960.
2. W. H. Ko, 'Designing tunnel diode oscillators', *Electronics*, **34**, No. 6, pp. 68–72, 10th February 1961.
3. M. N. S. Swamy, 'Application of tunnel diodes in trigger circuits', *J. Instn. Telecomm. Engrs (India)*, **9**, pp. 53–62, January 1963.
4. M. N. S. Swamy, 'A High Speed Tunnel Diode Decade Scaler', Ph.D. Thesis, University of Saskatchewan, 1963.
5. S. P. Gentile, 'Basic Theory and Application of Tunnel Diodes'. (Van Nostrand, Princeton, N.J., 1962.)
6. M. E. Hines, 'High frequency negative resistance circuit principles for Esaki diode applications', *Bell Syst. Tech. J.*, **39**, pp. 477–513, May 1960.
7. M. N. S. Swamy, 'Stability considerations for a tunnel diode circuit', *J. Franklin Inst.*, 274, pp. 444–51, December 1962.
8. R. S. C. Cobbold and H. N. Mahabala, 'A tunnel diode analogue and its applications', *Proc. Instn Elect. Engrs*, **110**, pp. 51–63, January 1963.
9. R. S. C. Cobbold, H. N. Mahabala and M. N. S. Swamy, 'A study of two-terminal current-controlled negative resistance devices with the aid of an analogue', *The Radio and Electronic Engineer*, **30**, No. 1, pp. 55–63, January 1966.

9. Appendix

Explanation of the graphical analysis of the lossy line

If we draw the line A_0A_1 at an angle α with the horizontal to cut the characteristic at A_1 (Fig. 8), then the point A_1 is such that the first equation of (39) is satisfied.

Again referring to Fig. 8, the equations to the lines A_1B_1 and XY are

$$i - i_1 = \tan\alpha.(v - v_1) \qquad \text{.....(40)}$$

and

$$i - I_0 = \tan\beta.(v - V_0) \qquad \text{.....(41)}$$

Solving eqns. (40) and (41), the coordinates (v_1', i_1') of the point B_1 are

$$i_1' = \frac{(V_0 - v_1)\tan\alpha.\tan\beta + i_1\tan\beta + I_0\tan\alpha}{\tan\alpha + \tan\beta} \qquad \text{.....(42)}$$

and

$$v_1' = \frac{(I_0 - i_1) + v_1\tan\alpha + V_0\tan\beta}{\tan\alpha + \tan\beta} \qquad \text{.....(43)}$$

Therefore

$$i_1' - i_1 = \frac{(I_0 - i_1)\tan\alpha + (V_0 - v_1)\tan\alpha.\tan\beta}{\tan\alpha + \tan\beta} \qquad \text{.....(44)}$$

and

$$v_1' - v_2 = \frac{(I_0 - i_1) - (V_0 - v_1)\tan\alpha}{\tan\alpha + \tan\beta} + (V_0 - v_2) \qquad \text{.....(45)}$$

Now from Fig. 8 we have

$$(i_2 - i_1) - (i_1' - i_1) = (v_1' - v_2)\tan\alpha \qquad \text{.....(46)}$$

Substituting eqns. (44) and (45) in eqn. (46) and simplifying we get

$$(i_2 - i_1) + (V_0 - v_1)\frac{\tan\alpha - \tan\beta}{\tan\alpha + \tan\beta}.\tan\alpha = (\tan\alpha)(V_0 - v_2) - \frac{2(i_1 - I_0)\tan\alpha}{(\tan\alpha + \tan\beta)} \qquad \text{.....(47)}$$

Now

$$\tan\alpha = 1/Z_0, \quad \text{and} \quad \tan\beta = 2/R_l$$

Hence

$$\frac{2\tan\alpha}{\tan\alpha + \tan\beta} = \frac{2R_l}{2Z_0 + R_l} \simeq \frac{R_l}{Z_0} \qquad \text{.....(48)}$$

Also

$$\frac{\tan\alpha - \tan\beta}{\tan\alpha + \tan\beta} = \frac{R_l - 2Z_0}{R_l + 2Z_0} = -\left(1 - \frac{R_l}{2Z_0}\right)\left(1 + \frac{R_l}{2Z_0}\right)^{-1} \simeq \left(1 - \frac{R_l}{2Z_0}\right)\left(1 - \frac{R_l}{2Z_0}\right) \simeq -\left(1 - \frac{R_l}{Z_0}\right) \qquad \text{.....(49)}$$

Substituting eqns. (48) and (49) in eqn. (47) we have

$$[(i_2 - i_1) - (1 - R_l/Z_0)(V_0 - v_1)/Z_0] = [(V_0 - v_2) - R_l(i_1 - I_0)]/Z_0$$

Similarly,

$$[(i_3 - i_2) - (1 - R_l/Z_0)(V_0 - v_2)/Z_0] = [(V_0 - v_3) - R_l(i_2 - I_0)]/Z_0$$

. . . . . .

. . . . . . \qquad .....(50)

These eqns. (50) are the same as the set of eqns. (39). Hence the graphical procedure outlined previously may be used for their solution.

Manuscript first received by the Institution on 21st June 1965, and in final form on 24th February 1966. (Paper No. 1061.)

U.D.C. 621-52

Analysis and Synthesis of Feedback Compensated Third-order Control Systems via the Coefficient Plane

By

D. R. TOWILL, M.Sc.,
B.Sc.(Eng.), C.Eng.†

Summary: Third-order unity numerator control systems arise from the use of feedback compensation in order to meet the system specification. The normalization technique described in the paper permits the complete analysis and synthesis of third-order unity numerator linear or quasi-linear control systems by reference to the coefficient plane. Attention is concentrated on systems with a pair of complex roots plus a real root so orientated in the s plane that all three poles significantly affect the system response. Thus compared with certain existing design techniques, no approximations arise from the neglect of the third system pole when such criteria as bandwidth, maximum percentage overshoot, and velocity constant are determined.

Conventional synthesis involves the determination of the system transfer function given the system performance specification. Provided that three independent adjustable parameters are available, three independent performance criteria can be met at one and the same time. It is shown that the coefficient plane yields the appropriate transfer function coefficients directly from a simply constructed coefficient plane contour. For systems with only two adjustable parameters, a performance compromise is necessary. The coefficient plane is ideal for the rapid determination of the best possible compromise between, say, peak amplitude ratio and bandwidth which can be achieved with such a restricted system. An alternative, and even simpler synthesis proposition based on standard forms of transfer function is also illustrated.

List of Symbols

a_n characteristic equation coefficient of s^n
ζ damping ratio of complex pair of roots
ω_n undamped natural angular frequency
θ_i command variable
θ_0 controlled variable
$E = \theta_i - \theta_0$ system error
s true Laplace operator
$S = s/\omega_0$ normalized Laplace operator
ω_0 normalization angular frequency
t true time
$t' = \omega_0 t$ = normalized time
b coefficient of S^2 in normalized transfer function
c coefficient of S in normalized transfer function
$1/T$ modulus of negative real root
T_c servo loop time constant
T_a aerodynamic time constant
K_a aerodynamic gain
K_g roll autopilot feedforward gain adjustment
T_r rate feedback coefficient
T_α acceleration feedback coefficient
μ hydraulic servo desensitizing ratio
C_e slope of valve flow/valve displacement curve for a particular operating point
B fluid bulk modulus
A hydraulic piston cross-sectional area
M moving mass of the hydraulic servo
V volume of oil trapped in one side of a symmetrical hydraulic servo
A_1, A_2 transient response coefficients
ν phase angle
C_v velocity error constant
Ω_1 coefficient of ramp function input
M_p peak amplitude ratio of the steady state harmonic response
ω_B bandwidth angular frequency
p.o. maximum percentage overshoot in the step function response.

† Reader in Engineering Production, Welsh College of Advanced Technology, Cardiff. (Formerly with the Engineering Physics Branch, Royal Military College of Science.)

1. Introduction

The study of the dynamic behaviour of feedback control systems possessing true or approximate third-order transfer functions is a logical extension of the voluminous work based on approximations to second-order systems which has been available to control engineers for the last two decades. Third-order linear systems characterized by system pole zero arrays which cannot be approximated in the s plane to second-order systems can have transient responses which are completely different in nature to any which may be obtained from second-order systems. This is due to all three system poles contributing significantly to the system response. Such systems first became apparent in the work of Graham and Lathrop[1, 2] in their study of third-order systems to determine the best values of system transfer function coefficients based on the step function response alone. Chu and Yeh[3] then categorized the third-order root locus and correlated the transient response with system pole geometry for third-order unity numerator systems only, whilst sample transient responses for (0, 3), (1, 3) and (2, 3) systems in terms of system pole zero geometry have been recorded by Elgred and Stephens.[4] The first number in the bracket refers to the number of system zeros, whilst the second refers to the number of system poles. A design technique was then developed by Hausenbauer and Lago[5] which enabled transient and steady state performance criteria to be met by (1, 3) systems emanating from type 1 systems compensated by conventional R-C networks. However, the design charts developed in this paper were restricted to system pole-zero arrays for which the damping ratio of the complex pole pair is 0·50 or 0·707.

Two somewhat different approaches to system design are represented by the concept of optimum transfer functions on the one hand, and the derivation of particular transfer function coefficients meeting performance criteria based on deterministic inputs on the other. For third-order unity numerator systems ((0, 3) systems), the coefficient plane provides a rapid technique which can be used to greatly simplify either approach. Towill[6] has developed the coefficient plane concept to the stage where all the main performance criteria can be shown directly in terms of the transfer function coefficients. Coefficient plane techniques can be applied equally well to analysis and synthesis. There is no approximation involved at any stage of the synthesis procedure, which has been developed specifically to determine the transfer function coefficients required to meet a given performance specification. Provided the designer can determine the transfer function coefficients in terms of the component characteristics the available answers are absolute. Use of the coefficient plane results in a simple, rapid, algebraic method of system synthesis which always retains the dynamic significance of the situation. For any point in the coefficient plane the performance criteria relating to step function, ramp function, and harmonic response is available by inspection. Realistic transfer function coefficients for particular applications are quickly recognized and easily remembered. The techniques are applicable to such widely varying examples as a missile autopilot and a mechanical hydraulic servomechanism. Realistic (0, 3) systems result from inherent or deliberate introduction of some form of feedback compensation. Mechanical hydraulic servos can possess inherent feedback compensation, whilst in the missile autopilot the feedback compensation terms must be measured using such instruments as rate gyroscopes. Use of the coefficient plane generally renders redundant the root locus technique in the design of type (0, 3) systems wherein all three poles are significant. Coefficient plane techniques can also be used equally well for those non-linear systems which can be suitably modelled using small perturbation theory.

2. Origins of the Coefficient Plane

Historically there are two distinctly separate lines of development of the use of the coefficient plane for the analysis and synthesis of feedback control systems. The general method, due to Mitrovic,[7] involves plotting the effect of changes in two coefficients of the characteristic equation,

$$a_0 + a_1 s + a_2 s^2 + a_3 s^3 + \ldots a_n s^n = 0 \quad \ldots\ldots(1)$$

on a pair of roots of this characteristic equation, $(n-2)$ coefficients of the equation being kept constant during this procedure. If these roots form a complex pair with damping ratio ζ and undamped natural frequency ω_n, the original Mitrovic theory allows a_0 and a_1 to be easily computed as a function of ζ and ω_n. Using a_0 and a_1 as the co-ordinates of the coefficient plane, a grid for various discrete values of ζ and ω_n may be drawn, and hence the best values of a_0 and a_1 may be chosen. The method is therefore extremely useful for dominant mode design techniques since the coefficients required to achieve a given complex pole pair can be determined. Certain rules developed by Mitrovic can be used to ascertain whether these particular poles are in fact the dominant poles. Absolute stability can be investigated by considering the $\zeta = 0$ case. For systems with feed-forward gain adjustment and pure rate feedback compensation, a_0 and a_1 can be adjusted independently, and thus using Mitrovic's method plus the dominant mode philosophy, the compensation terms are completely defined. In practice, feed-forward gain is often fixed by static stiffness requirements, and rate and acceleration feedback are then used to force the dominant poles into the desired geometry. Under these circumstances it is the a_1 and a_2 coefficients which are treated as the co-ordinates in the coefficient

plane. Siljak,[8] and Elliott, Thaler and Heseltine,[9] have extended the basic Mitrovic method to allow any two coefficients of the characteristic equation to be used as co-ordinates of the coefficient plane. The Mitrovic concept of the coefficient plane is therefore an alternative to the root locus method as a design technique for nth order systems where the dominant mode philosophy is applicable and the designer can interpret the performance specification in terms of a second order pole-zero array.

A second development of the use of the coefficient plane for analysis and synthesis of feedback control systems was originated *en passant* by Graham and Lathrop[1] in order to display the transient responses of third-order linear systems in two dimensional form. This development is restricted to third-order systems only, and is the very antithesis of the dominant mode philosophy. In order to use this particular form of the coefficient plane a dimensionless normalization frequency ω_0 is used to rewrite the lowest and highest coefficients of the system characteristic equation simultaneously equal to unity. It is then possible to use the two normalized coefficients, b and c, of the system transfer function as the co-ordinates of the coefficient plane. Performance criteria such as peak amplitude ratio, maximum percentage overshoot, normalized bandwidth, and normalized velocity constant can then be shown as a function of these coefficients with startling clarity.

This paper is devoted to the second method of using the coefficient plane, which, in the limit can be looked upon as a very considerable extension of Mitrovic's method for the particular system where $a_0 = a_3 = 1$ and a_1 and a_2 are the variable coefficients of the coefficient plane. The essential difference between the two uses of the coefficient plane is that Mitrovic obtains roots of the characteristic equation, whereas in the second method the performance criteria of interest are given directly. Only third-order unity numerator systems are considered here.

3. Normalization Technique Applied to Third-Order Unity Nnmerator Systems

In order to reduce the third-order unity numerator system to a form which is convenient to handle, the normalization technique will be applied to the third-order system defined by

$$\frac{\theta_0}{\theta_i}(s) = \frac{1}{1+a_1 s+a_2 s^2+a_3 s^3} \qquad \text{.....(2)}$$

where s is the true Laplace operator. The relationship between the true Laplace operator s and the normalized Laplace operator S is as follows

$$S = s/\omega_0 \qquad \text{.....(3)}$$

For the third-order system of eqn. (2) we may write

$$\omega_0 = (1/a_3)^{\frac{1}{3}}$$

and therefore the normalized system transfer function is

$$\frac{\theta_0}{\theta_i}(S) = \frac{1}{1+cS+bS^2+S^3} \qquad \text{.....(4)}$$

where

$$c = \omega_0 . a_1$$

$$b = \omega_0^2 . a_2$$

In the time domain, the relationship between true time t for the system of eqn. (2) and the normalized time t' for the system of eqn. (4) can be rewritten

$$t' = \omega_0 . t \qquad \text{.....(5)}$$

It is the normalized transfer function coefficients b and c which are used as the co-ordinates of the coefficient plane. These coefficients exactly determine the *form* of the transient or frequency response, and hence such performance criteria as maximum percentage overshoot (p.o.) and peak amplitude ratio (M_p). Time and frequency scales for a given form of response are determined basically by the normalization frequency ω_0. Thus given b, c and ω_0, performance criteria such as response time, bandwidth, and velocity error constant may be determined absolutely.

As will be shown later, the root locus technique is not required in the analysis or synthesis of third-order unity numerator systems with three significant roots. However, it is useful to include the normalized root locus for the evaluation of sensitivity functions as defined by Truxal,[10] or as a general cubic solver for systems possessing system zeros.

Most third-order unity numerator servomechanisms possess characteristic equations which may be factorized into a first-order term and a second-order term with complex poles. We may therefore write the normalized system transfer function of eqn. (4) as

$$\frac{\theta_0}{\theta_i}(S) = \frac{1}{1+cS+bS^2+S^3}$$

$$= \frac{1}{(S+1/T)(S^2+2\zeta\omega_n S+\omega_n^2)} \qquad \text{.....(5)}$$

and the root locus in the coefficient plane will thus be the variation of T, ζ and ω_n in terms of b and c. Variation of ζ and ω_n with b and c would be a Mitrovic plot. Since we are interested not only in the complex poles but the real pole as well because all three affect system performance, it is convenient to plot the root locus in two separate parts. Figure 1(a) shows the complex poles, and for any value of b and c the normalized roots can be measured in polar or cartesian co-ordinates as desired. The corresponding negative real root, $(1/T)$ can be obtained from Fig. 1(b).

The relationship between the true root plane in s,

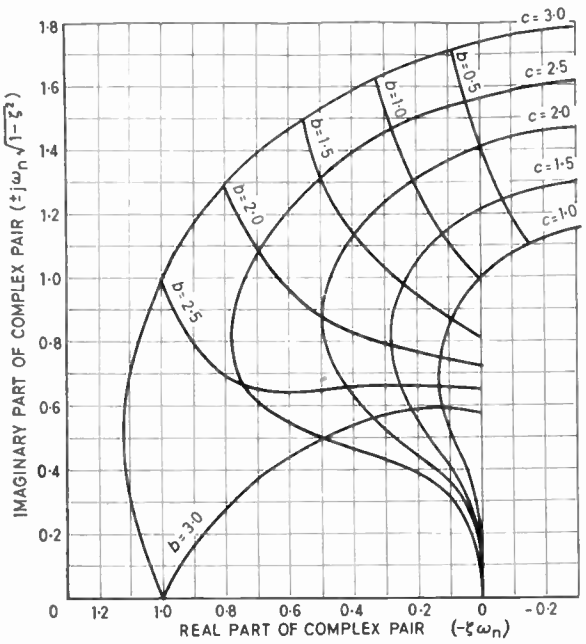

(a) Complex roots.

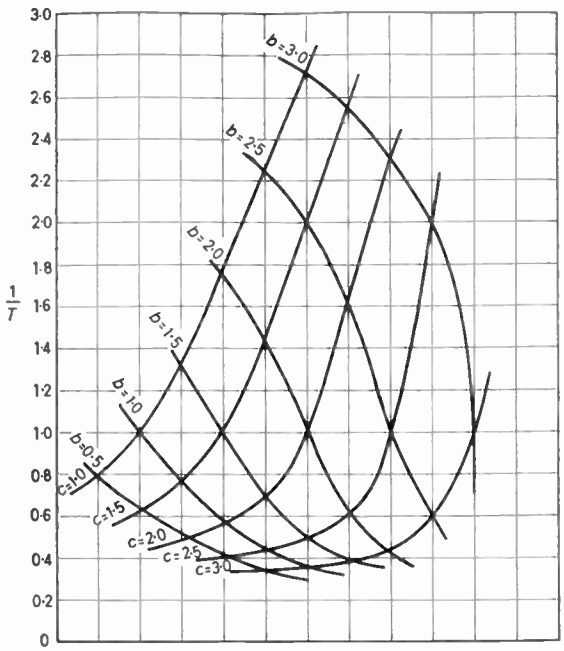

(b) Negative real root.

Fig. 1. Roots of the cubic $S^3 + bS^2 + cS + 1 = 0$.

and the normalized root plane in S is shown in Fig. 1(c). True roots are therefore given by

$$\frac{\theta_0}{\theta_i}(s) = \frac{\omega_0^3}{\left(s + \frac{\omega_0}{T}\right)(s^2 + 2\zeta\omega_n\omega_0 s + \omega_n^2\omega_0^2)} \quad \text{.....(6)}$$

Limits of b and c shown have been chosen somewhat arbitrarily, but are based on the following arguments. Firstly $b = c = 3{\cdot}0$ corresponds to a system with three equal normalized negative real roots at -1, which point may therefore be looked upon as the limit encountered in *servo* design. Secondly, all the optimum transfer function coefficients defined by various performance indices lie within the region bounded by the ordinates $b = 3{\cdot}0$, $c = 3{\cdot}0$, and thirdly, this same region contains very nearly all the third-order unity numerator systems wherein all three poles affect the system performance. There will, of course, be perfectly acceptable systems with coefficients not lying in the region bounded by $b = 3{\cdot}0$, $c = 3{\cdot}0$. These cases are not covered in this paper since one of the following conditions is fulfilled by such systems and therefore other design techniques are readily applicable:

(a) there are three negative real roots; or

(b) negative real root dominates the important features of the system response. System can therefore be treated, in the s plane or otherwise, as a first-order system; or

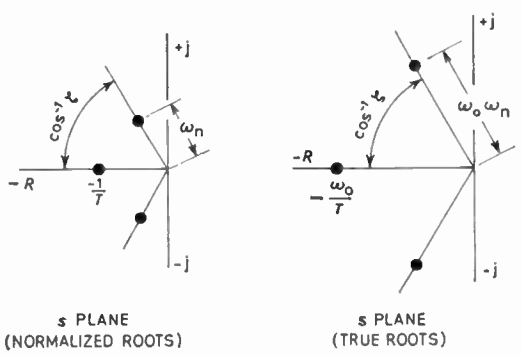

(c) Relationship between normalized roots and true roots.

(c) complex pole pair dominate the important features of the system response. System can therefore be treated in the s plane or otherwise, as a second-order system.

If the Routh-Hurwitz stability criterion is applied to the normalized system transfer function of eqn. (4), the simple absolute stability requirement is found to be

$$bc > 1{\cdot}0 \quad \text{.....(7)}$$

Equation (7) may be interpreted in the coefficient plane as the limiting stability hyperbola defined by $bc = 1{\cdot}0$. It is shown[6] that for systems with unity feedback path, or for systems redrawn into the unity feedback path form, contours of constant gain margin are hyperbolae defined by bc = constant. In particular, gain margin of 0·33, which is about the absolute minimum allowable in practice corresponds to the hyperbola $bc = 1{\cdot}5$.

Therefore in the coefficient plane we shall not only show the absolute stability line $bc = 1{\cdot}0$, but also a suitable relative stability line $bc = 1{\cdot}5$, the region between the two contours representing an unacceptable design area.

4. Feedback Compensation Control Systems

All feedback control systems are compensated by the negative feedback of the controlled variable. Additional compensation can then be achieved, if desired by the negative feedback of the first and higher order derivatives of the controlled variable. Pure feedback compensation (no instrumentation lags) is used to vary the coefficients of the system characteristic equation and hence can be used to position system poles. Principles of feedback compensation have been previously studied using Mitrovic's method,[9] s plane techniques,[11] and Routh's criterion,[12] to develop design methods suitable for any order of system. Since pure feedback compensation will result in a unity numerator system, it follows that third-order feedback compensated systems are ideal for synthesis in the coefficient plane, with all the attendant advantages over conventional techniques outlined in the introduction.

The third-order missile roll autopilot shown in Fig. 2 consists of a first-order lag

$$\left(\frac{1}{1+T_c.s}\right)$$

representing the electro-hydraulic servomechanism controlling the control surface deflection, and the missile roll rate is related to the control surface deflection by a scalar gain K_a, and an aerodynamic lag

$$\left(\frac{1}{1+T_a.s}\right)$$

where K_a and T_a are functions of altitude.[13] A position control autopilot will measure actual roll position, ϕ_0, using a gyroscope, and this will be the fundamental feedback signal. K_g is the feed-forward gain adjustment representing signal amplifiers, etc. Feedback compensation is shown to include a pure rate feedback term $T_r\dot{\phi}_0$ measured with a perfect rate gyroscope, and a pure acceleration feedback term $T_\alpha\ddot{\phi}_0$ measured with a perfect angular accelerometer. The signal leaving the comparator is

$$\phi_D - \phi_0(1 + T_r.s + T_\alpha.s^2)$$

and the autopilot transfer function is thus

$$\frac{\phi_0}{\phi_D}(s) = \frac{1}{1+\left(T_r+\frac{1}{K_gK_a}\right)s+ +\left(T_\alpha+\frac{T_a+T_c}{K_gK_a}\right)s^2+\left(\frac{T_aT_c}{K_gK_a}\right)s^3} \quad \ldots\ldots(8)$$

Using the normalization technique, we may define the normalized coefficients in terms of component values by

$$\omega_0 = \left(\frac{K_gK_a}{T_aT_c}\right)^{\frac{1}{2}} \qquad c = \omega_0\left(T_r + \frac{1}{K_gK_a}\right)$$

$$b = \omega_0^2\left(T_\alpha + \frac{T_a+T_c}{K_gK_a}\right)$$

It can be seen by inspection that if K_g, T_r and T_α are infinitely adjustable, any desired combination of b, c and ω_0 may be achieved, and it therefore follows that any three independent performance specifications can be met by this system at one and the same time. More important still is that if the desired values of b, c and ω_0 are known, the desired compensation terms K_g, T_r and T_α are available as the result of just three simple calculations.

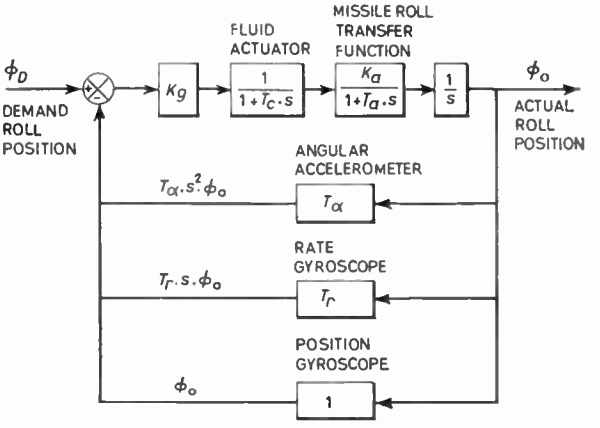

Fig. 2. Feedback compensated missile roll autopilot.

Figure 3 shows a mechanical hydraulic servo and the corresponding small perturbation theory block diagram which can be constructed by considering the individual flow equations. As shown the servo is primarily stabilized by a leakage flow across the piston since the inherent stabilization effect of pressure drop flow may be neglected for such a servo.[14] Note that the leakage flow feedback term does not appear at the comparator. Feed-forward gain is adjusted by altering the valve desensitizing ratio μ and the valve flow/valve opening characteristic C_c. C_c is itself non-linear and therefore the transfer function coefficients will be a function of the steady state operating point chosen. Synthesis of such a non-linear system requires that a number of steady state operating points be considered, which in turn necessitates the evaluation of the corresponding set of transfer function coefficients. For a given steady state operating point, the system transfer function for the hydraulic servo is

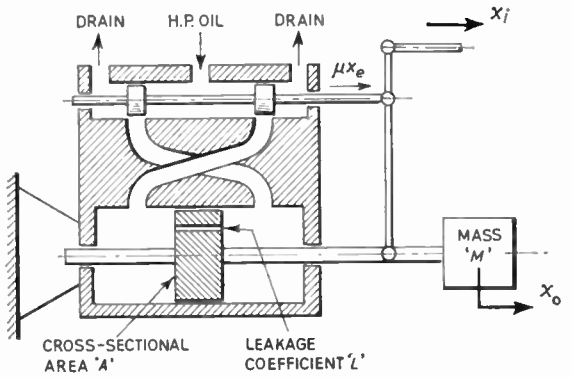

(a) Typical mechanical hydraulic servomechanism.

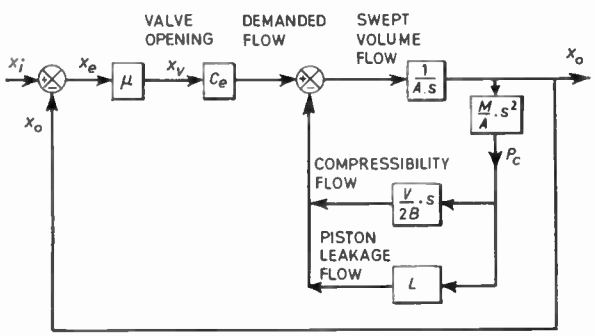

(b) Block diagram for small perturbation mode.

Fig. 3. Hydraulic quasi-linear servomechanism.

$$\frac{x_0}{x_i}(s) = \frac{1}{1+\left(\frac{A}{\mu C_e}\right)s+\left(\frac{LM}{A\mu C_e}\right)s^2+\left(\frac{VM}{2\mu C_e BA}\right)s^3} \qquad \text{.....(9)}$$

and using the normalization technique, the normalized coefficients of eqn. (9) become

$$\omega_0 = \left(\frac{2\mu C_e BA}{VM}\right)^{\frac{1}{2}} \qquad c = \omega_0\left(\frac{A}{\mu C_e}\right)$$

$$b = \omega_0^2\left(\frac{LM}{A\mu C_e}\right)$$

Although not immediately apparent from the normalized coefficients, if (μC_e), A and L are treated as infinitely adjustable design variables, it is possible to obtain these three quantities independently of each other in terms of the fixed servo quantities such as M, and the desired values of ω_0, b and c. Manipulation yields

$$\left.\begin{aligned} A &= \omega_0\sqrt{\frac{VMc}{2B}} && \text{.....(a)} \\ L &= \frac{\omega_0 bV}{2B} && \text{.....(b)} \\ (\mu C_e) &= \omega_0^2\sqrt{\frac{VM}{2Bc}} && \text{.....(c)} \end{aligned}\right\} \quad (10)$$

and the hydraulic servo can therefore be designed using simple arithmetic if the performance specification can be interpreted as requirements in b, c and ω_0. The hydraulic servo is therefore a feedback compensated system in exactly the same way as the missile roll autopilot previously discussed. Since the performance specification would normally be quite different for the hydraulic servo compared to the missile autopilot, it is to be expected that desired values of b and c might differ considerably for the two applications. In practice the hydraulic servo piston area A might not be a variable, but might be determined by loading or stiffness considerations, in which case only two design variables, L and (μC_e) can be adjusted. Hence unless further compensation is introduced, the designer can fix only two of the characteristics ω_0, b and c. Having fixed two of the three characteristics, the third is automatically defined. Under such circumstances the coefficient plane can greatly assist the designer since it is then easy to evaluate the criteria of interest as functions of L and (μC_e) and thereby choose the best compromise values of these two design variables.

5. Performance Index Optimum Transfer Functions

Performance indices have been used extensively in control engineering literature in an attempt to crystallize mathematically the designer's intuition in selecting an acceptable form of system response. If the economic use of components results in a genuine third-order system, performance indices can be of great help in indicating suitable design regions in the coefficient plane, and hence in indicating preferred transfer function coefficients. In this paper interest in the optimum normalized coefficients is restricted to the case where the system under consideration is a complete autonomous system, not, say, a third-order minor loop system enclosed in a sixth-order major loop, since the requirements of the third-order system transfer function coefficients are not the same in both cases.[6]

Performance indices are normally based on the system response when following a step function input. Three such indices are

$$\left.\begin{aligned} &\int_0^\infty |E|\,dt = \text{integral of absolute error (i.a.e.)} && \text{(a)} \\ &\int_0^\infty E^2\,dt = \text{integral of absolute error squared (i.a.e.s.)} && \text{(b)} \\ &\int_0^\infty t|E|\,dt = \text{integral of time} \times \text{absolute error (i.t.a.e.)} && \text{(c)} \end{aligned}\right\} \quad \text{.....(11)}$$

where $E = \theta_i - \theta_0$, is the instantaneous system error. The transfer function coefficients of eqn. (4) which

minimize these integrals have been determined and are tabulated in Table 1.[6]

Table 1

Optimum coefficient defined by common performances indices

Quantity	Performance index		
	i.a.e.	i.a.e.s.	i.t.a.e.
Optimum b	1·40	1·00	1·75
Optimum c	2·075	2·00	2·15
Normalized bandwidth	1·28	1·53	1·04
63% Response time	2·25	2·10	2·42

Normalized bandwidths and normalized 63% response times are also tabulated. Figure 4 shows the system pole arrays, transient responses, and frequency responses of these three optimum systems, and using the normalized 63% response times or the normalized bandwidths as markers the true frequency or transient

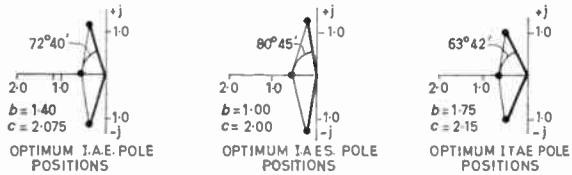

(a) Pole configurations.

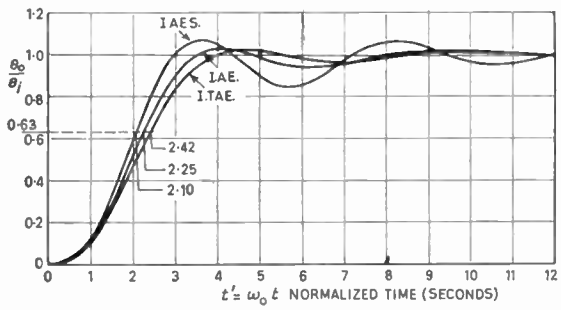

(b) Transient responses.

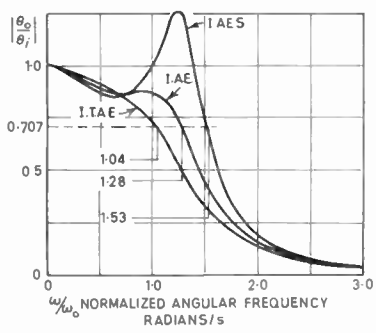

(c) Frequency responses.

Fig. 4. Performance index optimum systems.

responses may be readily obtained. Graham and Lathrop[1] found that the i.t.a.e. performance index has exceptional merit in the selection of useful system transfer functions and pole zero arrays, and this is to some extent confirmed by a comparison of either the transient or frequency responses shown in Fig. 4 since it may be argued that the i.t.a.e. responses are to be preferred to the other two.

If three infinitely adjustable independent design variables are available, then the design problem is solved by simply equating coefficients to the i.t.a.e. optimum values provided the form of response is acceptable. Such a design approach has been advocated by Vaughan[15] in the design of hot gas actuators. As an example of the ease of design under these circumstances, consider the autopilot of Fig. 2 for the flight condition where $T_c = 0{\cdot}035$ seconds, $K_a = 335$ rad/s/rad, and $T_a = 0{\cdot}179$ seconds. Suppose that the i.t.a.e. optimum form is acceptable, and that a bandwidth of 30 rad/s is required, then the design problem is to determine K_g, T_r and T_α. From Table 1 $(\omega_B/\omega_0) = 1{\cdot}04$, and hence $\omega_0 = 28{\cdot}8$ rad/s.

Using the a_3 coefficient

$$K_g = \frac{\omega_0^3 . T_a . T_c}{K_a} = \frac{28{\cdot}8^3 \times 0{\cdot}035 \times 0{\cdot}179}{335} = \frac{1}{2{\cdot}23}$$

Now

$$a_2 = \frac{b}{\omega_0^2} = \frac{1{\cdot}75}{28{\cdot}8^2} = 0{\cdot}00211$$

and

$$T_\alpha = a_2 - \left(\frac{T_a + T_c}{K_g K_a}\right)$$

$$= 0{\cdot}00211 - \left(\frac{0{\cdot}035 + 0{\cdot}179}{335/2{\cdot}23}\right) = 0{\cdot}00068 \text{ seconds}^2$$

Furthermore,

$$a_1 = \frac{c}{\omega_0} = \frac{2{\cdot}15}{28{\cdot}8} = 0{\cdot}0746$$

Hence,

$$T_r = \left(a_1 - \frac{1}{K_g K_a}\right) = \left(0{\cdot}0746 - \frac{2{\cdot}23}{335}\right) = 0{\cdot}0679 \text{ seconds}$$

However, if three independent design variables are available they may not be infinitely adjustable due to physical limitations, or alternatively only two design variables may be available. Under these circumstances the normalized optimum i.t.a.e. coefficients do not necessarily indicate the best design, since in any compromise design the effect of ω_0 must be considered. Nevertheless, in many practical cases the true optimum values of b and c will not be significantly different from the normalized optimum values of $b = 1{\cdot}75$, $c = 2{\cdot}15$.[16] In any case we would expect that a particular region, not a particular point, in the coefficient plane would result in acceptable dynamic behaviour and that this would be confirmed by the

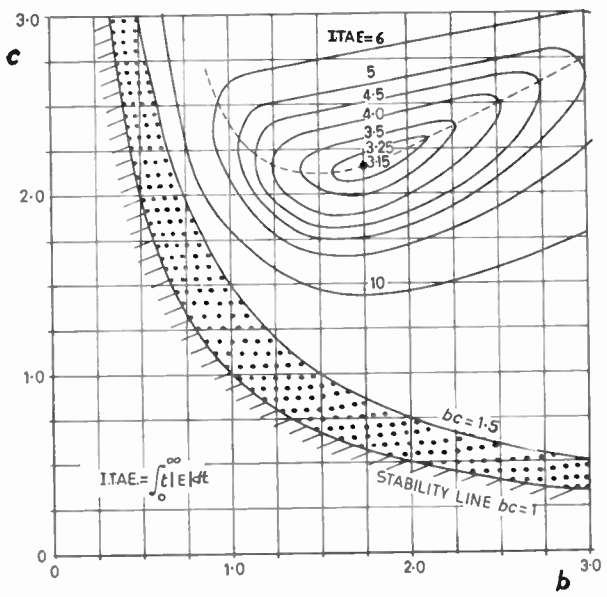

Fig. 5. Integral of time × absolute error (i.t.a.e.) performance index contours in the coefficient plane.

value of the integral itself. Figure 5 shows contours of i.t.a.e. plotted in the coefficient plane, and we might well arbitrarily define the region enclosed by the i.t.a.e. = 4 contour as a suitable design region. We could then adjust the two variables available until the design point is in this region coupled with an acceptable value of ω_0. This aspect will be investigated further in a later section.

6. Performance Specification in Terms of Response to Deterministic Inputs

At the present time it is relatively rare to specify system performance by means of the i.t.a.e. optimum transfer function coefficients allied to specification of the frequency scale or the bandwidth as advocated by Vaughan. The recent appearance of the i.t.a.e. performance index at text book level will probably lead to a considerable increase in this type of approach.[17, 18]

It is, however, common practice to specify system performance by considering the system response to deterministic inputs and this practice is likely to continue; this approach gives satisfactory results, and is well understood. Where necessary, compromises in the coefficient plane can then be made on the basis of these performance criteria. Before developing synthesis techniques suitable for determination of system transfer function coefficients meeting particular specifications it is necessary to portray the various criteria directly in the coefficient plane.

Truxal[19] has stated that the three most commonly used independent performance criteria are:

(a) maximum percentage overshoot (p.o.) following a step function input;

(b) velocity error constant (C_v) which measures the steady state position lag when following a ramp function input. $C_v = \infty$ corresponds to zero steady state lag;

(c) bandwidth (ω_B) which is the highest frequency at which the system amplitude ratio is $1/\sqrt{2}$.

When applied to third-order unity numerator systems these three criteria can be met simultaneously provided three independent infinitely adjustable variables are available. To these three criteria can be added a fourth, M_p, which is the peak amplitude ratio of the steady state harmonic response and which is often used as an alternative to p.o.

7. Transient Response

The step function response of the system defined by eqn. (5) for $\zeta < 1{\cdot}0$ is of the form

$$\theta_0(t') = 1 - A_1 e^{-t'/T} + A_2 e^{-\zeta\omega_n t'} \cos(\omega_n\sqrt{1-\zeta^2}\,t' + v) \quad \ldots\ldots(12)$$

where A_1, A_2 and v are dependent on b and c. Relative significance of the two response modes of eqn. (12) also depend on b and c, as can be seen in Fig. 6, which shows sample responses plotted in the coefficient plane. Accurate plots of these same responses as obtained from digital computer are

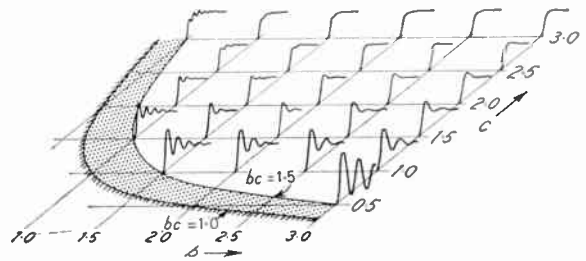

Fig. 6. Sample transient responses plotted in the coefficient plane.

available.[20, 21] Maximum percentage overshoot contours of Fig. 7 have been obtained by determination of the transient response for many sample points in the coefficient plane and then using suitable interpolation techniques. Results have not been included for that region of the coefficient plane where the maximum percentage overshoot does not occur at the first overshoot since for these systems it is more usual to specify M_p and not p.o. Sixty-three per cent response times, i.e. the time taken to reduce the error to 37% of the initial value are shown in Fig. 8, and have been included because this time is a unique

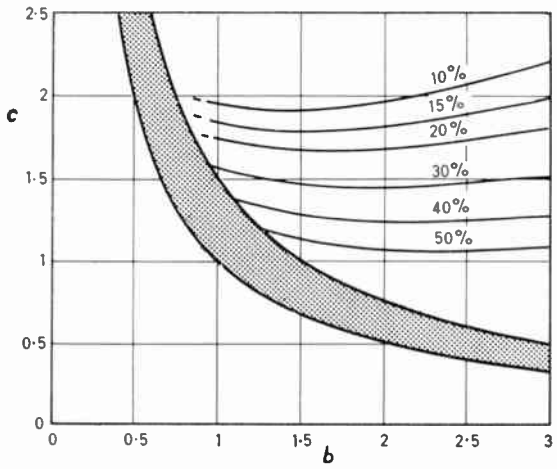

Fig. 7. Maximum percentage overshoot.

measure in the normalized time domain. It should be noted in passing that the transient response obtained towards the top left-hand corner of the coefficient plane is nothing like the transient response which may be obtained from a second-order system. In particular, the oscillatory response obtained for $b = 0{\cdot}5$, $c = 3{\cdot}0$, is very similar to the experimental response which may be obtained from a practical hydraulic servo.[22] There are two reasons why this type of response (far removed from the i.t.a.e. optimum type of response) is acceptable. Firstly, the servo is part of a major loop, for example when used as an aircraft power control, and the aircraft itself will act as a very-low-pass filter. The oscillations will therefore be considerably attenuated and will not be observable in the aircraft motion. Secondly, the compromise required in the design of a genuine third-order system with only two variables available has already been mentioned. It is found with realistic hydraulic servos that small perturbation mode design in the region ($b = 0{\cdot}5$, $c = 3{\cdot}0$) gives a high stiffness and a high normalization frequency together with an acceptable form of response when only two variables, say, gain and piston leakage are available for adjustment.

8. Ramp Function Response

The true error transfer function may be written

$$\frac{\theta}{\theta_i}(s) = \frac{\theta_i - \theta_0}{\theta_i} = 1 - \frac{\theta_0}{\theta_i}(s) = \frac{a_1 s + a_2 s^2 + a_3 s^3}{1 + a_1 s + a_2 s^2 + a_3 s^3} \qquad \text{.....(13)}$$

Applying a ramp function input $\theta_i = \Omega t$ and using the Final Value Theorem we have

$$\theta_{ss} = \Omega a_1 \qquad \text{.....(14)}$$

By definition of velocity error constant we have

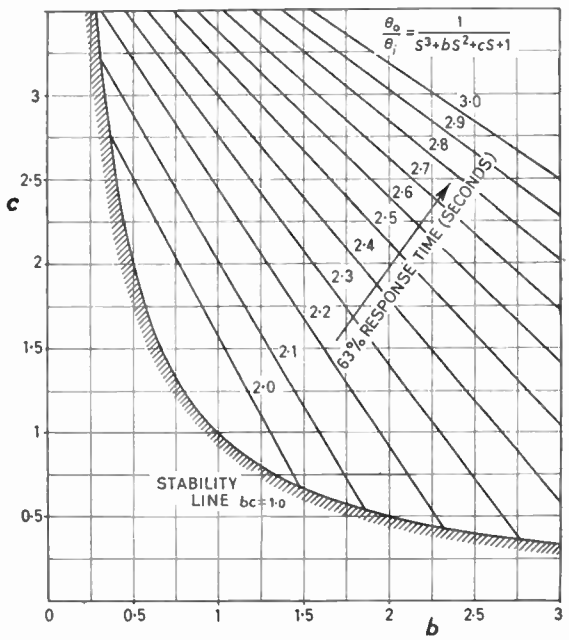

Fig. 8. 63% transient response times.

$$\theta_{ss} = \frac{\Omega}{C_v} \qquad \text{.....(15)}$$

and therefore

$$C_v = \frac{1}{a_1} = \frac{\omega_0}{c} \qquad \text{.....(16)}$$

Constant C_v contours in the coefficient plane are therefore horizontal straight lines as shown in Fig. 9. A high value of C_v is obtained by keeping c low, and it can be seen either from the roots shown in Fig. 1 or from the transients of Fig. 6 that the negative real

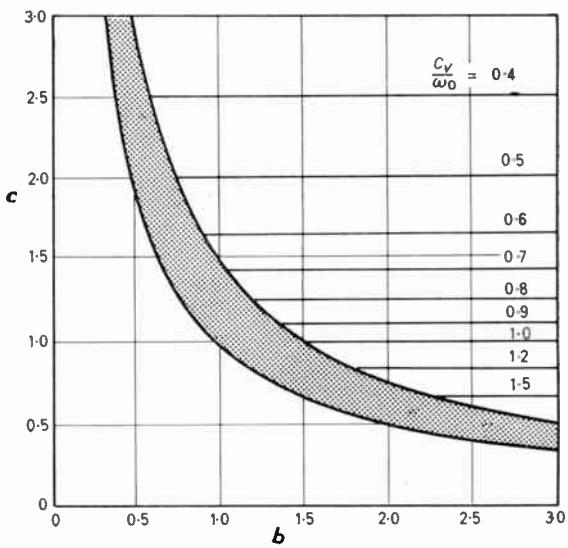

Fig. 9. C_v contours in the coefficient plane.

pole has relatively little effect on the system response, and therefore specifications which require that C_v is relatively high will be found to have a second-order dominant mode unless an integrating dipole is used to boost C_v without significantly affecting transient and frequency responses.

9. Frequency Response

The amplitude ratio of the system defined by eqn. (4) at any frequency is given by

$$\left|\frac{\theta_0}{\theta_i}(j\omega)\right| = \frac{1}{\sqrt{(1-b\omega^2)^2+(c\omega-\omega^3)^2}} \quad \ldots\ldots(17)$$

Towill[6] and Meadows[23] have independently shown that four different types of frequency response can exist for the system with amplitude ratio defined by eqn. (17), as shown in Fig. 10. The categories may be described as follows:

(a) no resonance peak exists (no maxima or minima);

(b) resonance peak exists (one maximum);

(c) resonance peak greater than unity exists, but there is a dip in the amplitude ratio characteristic below unity for some frequencies between zero and the resonant peak frequency (one maximum and one minimum);

(d) resonance peak less than unity exists, and there is a dip in the amplitude ratio characteristic below the M_p value for some frequencies between zero and the resonant peak frequency (one maximum and one minimum).

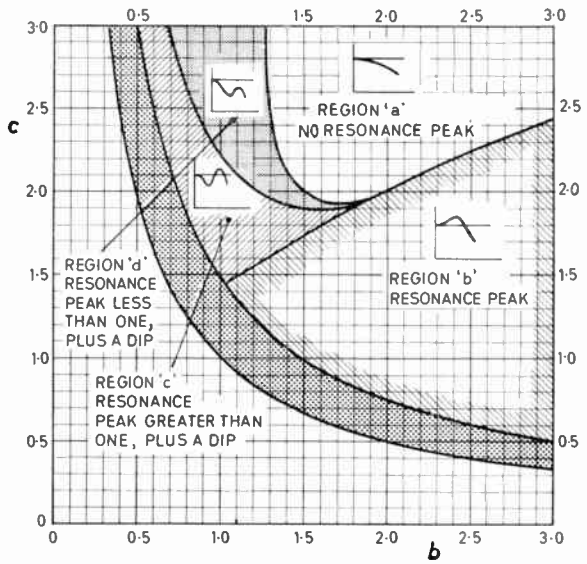

Fig. 10. Division of the coefficient plane into regions of various forms of frequency response.

The boundaries in the coefficient plane can be determined by examining eqn. (17) for the existence of maxima and minima. For the area where a maximum and a minimum exists, the boundary between categories (c) and (d) can be found by determination of the $M_p = 1{\cdot}0$ contour.

Generally speaking, region (b) is highly desirable for many applications, but region (a) is also often suitable provided the rate of fall-off in amplitude ratio

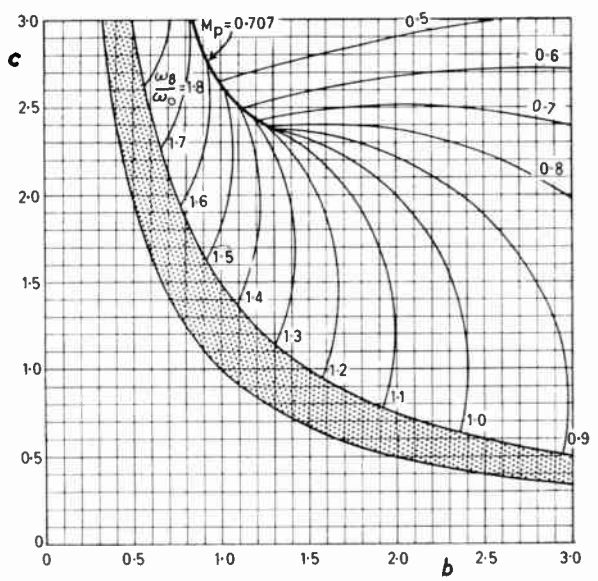

Fig. 11. Bandwidth contours in the coefficient plane.

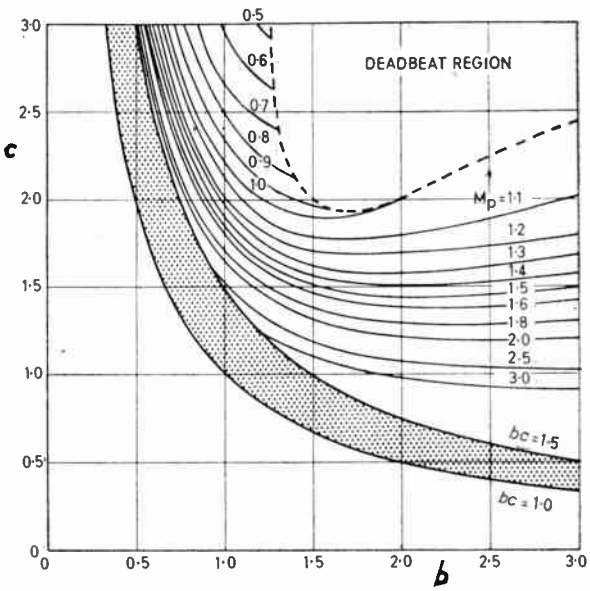

Fig. 12. M_p contours in the coefficient plane.

is not excessive at low frequencies, i.e. the harmonic response is fairly flat. For minor loop applications, where other considerations are important, type (c) response may be acceptable due to the subsequent filtering action of the major loop which will filter out an otherwise excessive value of M_p. Bandwidth contours are obtained by equating the steady state amplitude ratio to $1/\sqrt{2}$, and are shown in Fig. 11. The discontinuity in bandwidth occurs when $M_p = 0{\cdot}707$ since an infinitesimal decrease in M_p immediately reduces the bandwidth from what was formerly the highest of the three roots of the subsidiary equation for bandwidth to the lowest and now only root of this equation.

M_p contours are shown in Fig. 12, and have been obtained by digital computation of M_p for many sample points in the coefficient plane and then using suitable interpolation techniques to determine the required contours.

10. Analysis of Feedback Compensated Systems

The great simplicity of presentation of performance criteria in the coefficient plane should not be allowed to hide the fact that the third-order unity numerator system has now been solved for all time for the accepted criteria used with deterministic inputs. The solution is in absolute terms and no approximation whatsoever has been made. Many thousands of computations have been undertaken to ensure that designers are presented with the data which is really needed in their work.

Given the system transfer function in the form of eqn. (8), the analysis problem is trivial. ω_0, b and c are computed, and the form of frequency response, bandwidth, C_v, M_p and p.o. are available by simply indicating the co-ordinates (b, c) on the relevant charts. The charts can also be used to determine the performance criteria in terms of pole positions which may be obtained during the design of high-order systems. Figure 13 shows a typical high-order pole zero array with three dominant poles, all of which make a significant contribution to system performance. The pole positions can be measured off and a_1, a_2 and a_3 of eqn. (2) determined. Normalization then yields ω_0, b and c and hence the performance criteria of interest. If the poles correspond to, say, a particular value of feed-forward gain on the root locus, then the process can be repeated for several values of gain, and subsidiary graphs drawn showing the effect of feed-forward gain on performance criteria so that a best choice of feed-forward gain can be made.

The charts are also relevant for systems with integrating dipoles provided the effect on C_v is allowed for.

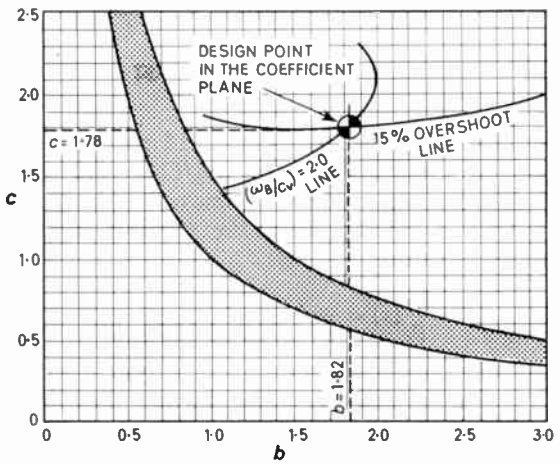

Fig. 14. Use of the coefficient plane to determine the normalized transfer function coefficients of the system with 15% overshoot and $(\omega_B/C_v) = 2{\cdot}0$.

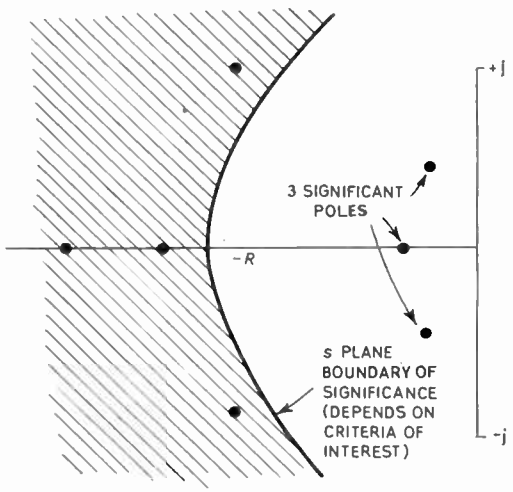

Fig. 13. Reduction of high-order system to three significant poles.

11. Synthesis of Feedback Compensated Systems

Using the coefficient plane it is possible to develop simple, exact, and elegant design techniques to determine system transfer functions and hence compensation terms directly. Suppose that p.o., ω_B and C_v are specified in a system with three independent design variables available so that the specification can be exactly achieved. Now since C_v and ω_B are both linear in ω_0, if (ω_B/C_v) is derived from the specification, ω_0 is eliminated whilst b and c are being determined. For example, suppose the specification states that p.o. = 15%, and $(\omega_B/C_v) = 2{\cdot}0$. The 15% overshoot contour is available from Fig. 7, and (ω_B/C_v) contour can be determined from Fig. 11, by taking a particular bandwidth contour and computing from eqn. (16) the value of c on this contour which fulfils the (ω_B/C_v) requirement. This is repeated for as many bandwidth

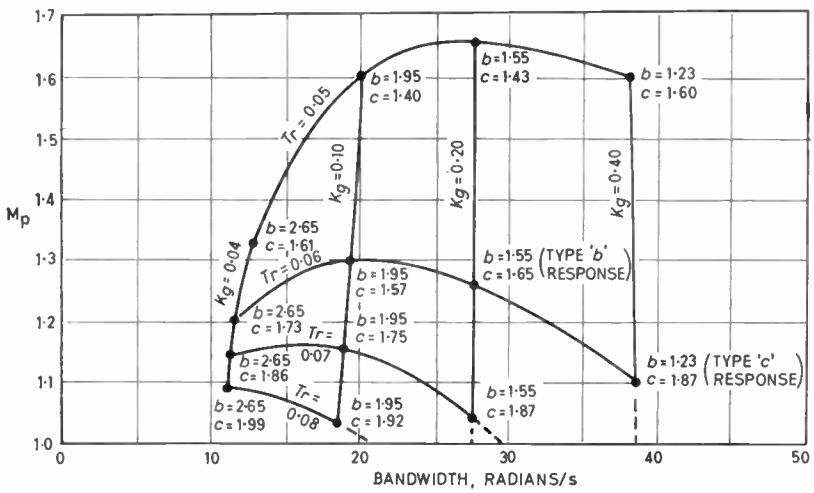

Fig. 15. Subsidiary graph showing M_p and bandwidth as a function of T_r and K_g for the autopilot with only two design variables.

contours as necessary. Figure 14 shows the 15% overshoot contours and the $(\omega_B/C_v) = 2{\cdot}0$ contour, the intersection uniquely defines the design point $b = 1{\cdot}82$, $c = 1{\cdot}78$, giving the required normalized transfer function

$$\frac{\theta_0}{\theta_i}(s) = \frac{1}{1+1{\cdot}78S+1{\cdot}82S^2+S^3} \qquad \ldots\ldots(18)$$

As an example of synthesis for a system with only two design variables, consider the autopilot shown in Fig. 2 where an angular accelerometer is not provided and therefore K_g and T_r are the only adjustments available. It is required to obtain values of K_g and T_r which give reasonable compromise between peak amplitude ratio and bandwidth for the flight case already considered. The procedure is to sample K_g and T_r, and for each combination to evaluate ω_0, b and c. (ω_B/ω_0) and M_p are then obtained from Figs. 11 and 12 respectively. Figure 15 shows the subsidiary graph relating true bandwidth to M_p. The trade-off shows that if the type of frequency response associated with region (c) of Fig. 10 is acceptable, then a bandwidth of about 38 rad/s can be obtained with an M_p of 1·1. If it is desired to avoid the 'dip' in this type of response, then a better compromise may be the type (b) response with a bandwidth of about 27·5 rad/s and an M_p of 1·26. A further factor affecting the designer's decision is whether the bandwidth of 27·5 rad/s is too low for acceptable following of the command signal, or whether the bandwidth of 38 rad/s is high enough to pass a significant proportion of any noise signals present. By using the coefficient plane the designer has all the relevant criteria available before passing judgment on a suitable compromise.

12. Conclusions

The coefficient plane enables genuine third-order unity numerator systems to be designed with great rapidity, and the method can also be extended to cover the design of non-linear systems. Unity numerator systems are the family of feedback control systems deliberately or inherently stabilized by feedback compensation.

Since all common performance criteria can be exhibited in the coefficient plane it is thus possible to completely design many systems by solving three simple arithmetical equations, and establishing exact performance by reference to standard curves.

Optimum and near optimum coefficients are easily remembered. For example, $b = c = 2{\cdot}0$ is a useful system for general application, whilst for some minor loop applications, such as a hydraulic servo, suitable coefficients are $b = 0{\cdot}5$, $c = 3{\cdot}0$.

13. Acknowledgments

The author wishes to thank Sir Donald Bailey, Dean, Royal Military College of Science, Shrivenham, for permission to include in this paper certain extracts from Reference 6.

14. References

1. D. Graham and R. C. Lathrop, 'The synthesis of "optimum" transient response: criteria and standard forms', *Trans. Amer. I.E.E.*, 72, Pt. II, *Applications and Industry*, No. 9, pp. 273–88, November 1953.
2. R. C. Lathrop and D. Graham, 'The transient performance of servomechanisms with derivative and integral control', *Trans. Amer. I.E.E.*, 73, Pt. II, *Applications and Industry*, No. 11, pp. 10–17, March 1954.

3. Y. Chu and V. C. M. Yeh, 'Study of cubic characteristic equation by the root locus method', *Trans. Amer. Soc. Mech. Engrs*, **76**, April 1954.
4. O. I. Elgred and W. Stephens, 'Effect of closed-loop transfer function pole and zero locations on the transient response of linear control systems', *Trans. Amer. I.E.E.*, **78**, Pt. II, *Applications and Industry*, No. 42, pp. 121–7, May 1959.
5. C. R. Hausenbauer and G. V. Lago, 'Synthesis of control systems based on approximation to a third-order system', *Trans. Amer. I.E.E.*, 77, Pt. II, *Applications and Industry*, No. 39, pp. 415–21, November 1958.
6. D. R. Towill, 'The design of a class of third-order control systems using the coefficient plane', Royal Military College of Science, Engineering Physics Branch, Tech. Note No. 19. May 1965.
7. D. Mitrović, 'Graphical analysis and synthesis of feedback control systems', *Trans. Amer. I.E.E.*, **78**, Pt. II, *Applications and Industry*, No. 40, pp. 476–503, January 1959.
8. D. D. Siljak, 'Generalization of Mitrovic's method', *Trans. Inst. Elect. Electronic Engrs on Applications and Industry*, **83**, No. 74, pp. 314–20, September 1964.
9. D. W. Elliott, G. J. Thaler and J. C. W. Heseltine, 'Feedback compensation using derivative signals—Mitrovic's method', *Trans. Amer. I.E.E.*, **82**, Pt. II, *Applications and Industry*, No. 68, pp. 269–74, September 1963.
10. J. G. Truxal, 'Control System Synthesis', p. 272. (McGraw-Hill, New York, 1955.)
11. G. J. Thaler, J. D. Bronzino and D. E. Kirk, 'Feedback compensation: a design technique', *Trans. Amer. I.E.E.*, **80**, Pt. II, *Applications and Industry*, No. 57, pp. 300–5, November 1961.
12. D. W. Elliott, G. J. Thaler and J. Heseltine, 'Feedback compensation using derivative signals—Routh's criterion and root loci', *Trans. Amer. I.E.E.*, **82**, Pt. II, *Applications and Industry*, No. 68, pp. 262–8, September 1963.
13. D. R. Towill and P. J. Davies, 'Philosophy, design and development of MIARTES', *Trans. I.E.E.E. on Education*, **E-8**, No. 4, pp. 140–9, December 1965.
14. T. H. Lambert and R. M. Davies, 'Investigation of the response of an hydraulic servomechanism with an inertial load', *J. Mech. Eng. Sci.*, **5**, No. 3, March 1963.
15. D. R. Vaughan, 'Hot gas actuators: some limits on the response speed', *A.S.M.E. J. of Basic Engineering*, March 1965.
16. D. Graham and R. C. Lathrop, 'The influence of time scale and gain on criteria for servomechanism performance', *Trans. Amer. I.E.E.*, **73**, Pt. II, *Applications and Industry*, No. 13, pp. 153–8, July 1954.
17. Stanley M. Shinners, 'Control System Design', p. 93. (John Wiley, New York, 1964.)
18. A. Susini, 'Filters, Amplifiers and Servomechanisms', p. 232. (Heywood and Co. Ltd., London, 1963.)
19. J. G. Truxal, *ibid.*, page 281.
20. D. R. Towill, 'Step function response of a linear, zero displacement error, third-order control system', Royal Military College of Science, Engineering Physics Branch Tech. Note No. 13, October 1964.
21. D. R. Towill, 'Third-order control system analysis simplified', *Design Electronics*, 2, No. 10, pp. 18–23, July 1965.
22. S. G. Glaze, 'Analogue technique and the non-linear jack servomechanism', Proceedings of the Symposium on Recent Mechanical Engineering Developments in Automatic Control, Institution of Mechanical Engineers, London, 1960.
23. N. C. Meadows, 'Resonance peaks in third-order type 1 control systems', *Proc. Instn Elect. Engrs*, **112**, No. 5, pp. 1035–8, May 1965. (I.E.E. Paper No. 4771S.)

Manuscript first received by the Institution on 3rd December 1965, and in final form on 11th May 1966 (Paper No. 1062/C85.)

STANDARD FREQUENCY TRANSMISSIONS

(Communication from the National Physical Laboratory)

Deviations, in parts in 10^{10}, from nominal frequency for July 1966

July 1966	24-hour mean centred on 0300 U.T.			July 1966	24-hour mean centred on 0300 U.T.		
	GBZ 19·6 kHz	MSF 60 kHz	Droitwich 200 kHz		GBZ 19·6 kHz	MSF 60 kHz	Droitwich 200 kHz
1	− 299·8	− 300·9	+ 0·2	16	− 300·2	− 299·6	+ 2·2
2	− 299·9	− 300·3	+ 0·2	17	− 300·4	− 299·7	+ 2·2
3	− 299·9	− 300·7	0	18	− 301·3	− 299·4	+ 2·4
4	− 300·2	− 300·8	+ 0·5	19	− 301·5	− 299·3	+ 2·8
5	− 300·0	—	+ 0·4	20	− 301·0	− 300·0	+ 2·8
6	− 301·4	—	+ 0·6	21	− 300·2	− 300·5	+ 2·5
7	− 300·3	− 301·2	+ 0·9	22	− 300·5	− 300·6	+ 2·9
8	− 299·6	− 300·4	+ 1·5	23	− 301·3	− 300·6	+ 2·9
9	− 300·2	− 300·9	+ 1·4	24	− 300·6	− 301·3	+ 2·8
10	− 300·3	− 301·0	+ 1·5	25	− 301·1	− 300·5	+ 3·1
11	− 300·4	− 300·7	+ 1·6	26	− 301·6	− 299·8	+ 3·7
12	− 300·3	− 300·4	+ 1·3	27	− 301·7	− 300·1	+ 3·7
13	− 299·4	− 300·4	+ 1·0	28	− 300·0	− 300·0	+ 3·7
14	− 300·1	− 300·3	+ 2·4	29	− 299·4	− 300·2	+ 4·1
15	− 300·6	− 300·0	+ 2·1	30	− 300·3	− 300·8	+ 4·1
				31	− 301·7	− 300·7	+ 3·8

Nominal frequency corresponds to a value of 9 192 631 770·0 Hz for the caesium F,m (4,0)–F,m (3,0) transition at zero field.

# of current interest . . .

Committee of European Associations of Manufacturers of Passive Electronic Components (CEPEC)

As a result of preliminary discussions during the year 1964, an organization of national manufacturers' associations of passive electronic components was formed in January 1965 under the name of the Committee of European Associations of Manufacturers of Passive Electronic Components (CEPEC).

Members of the Committee are representatives nominated by the national associations of Belgium, France, Germany (the Federal Republic), Italy, the Netherlands and the United Kingdom; these associations being:

BELGIUM	Fédération des Entreprises de l'Industrie des Fabrications Metalliques (FABRIMETAL). R. Lorent
FRANCE	Syndicat des Industries de Pièces détachés et Accessoires Radio-électriques et Électroniques (SIPARE) and Syndicat des Constructeurs Français de Condensateurs Électriques Fixes (SCFCEF). Y. Simmler
GERMANY	Zentralverband d. Elektrotechnischen Industrie E.V.—Fachverband Schwachstromtechnische Bauelemente 23 (ZVEI). K. Plumke
ITALY	Associazione Nazionale Industrie Elettrotechniche ed Elettroniche Gruppo 14 e 15 (ANIE). C. San Pietro
NETHERLANDS	Groep Fabrieken voor Passieve Elektronische Bouwelementen in Nederland (FAPEL). P. de Vos
UNITED KINGDOM	Radio and Electronic Component Manufacturers Federation (RECMF). A. C. Bentley

The Committee was formed with the object of carefully observing any technical difficulties liable to impede the development of the interchange of products in Europe and to co-operate in overcoming such impediments.

CEPEC has dealt so far with problems of technical standards (norms and specifications). It is not intended to replace national specifications but to arrive at a harmonization through recommendations to appropriate standardization bodies such as I.E.C., N.A.T.O., etc. A technical committee and working groups have been formed and this approach has proved to be both efficient and successful.

At present, at the request of the U.K., CEPEC is considering the 'Burghard Report' which contains British proposals for common standards for electronic components, which could well form a basis for a European system.

In accordance with the Committee's rules of procedure, Mr. Plumke was elected President for the first two-year period. Mr. Simmler, now Vice-President, has been elected President for the next period beginning in January 1967; the Vice-President will be Mr. Bentley.

Satellite Communications

The Australian Postmaster-General, Mr. A. S. Hulme, said recently that it might not be long before Australia was using space satellites for internal as well as external communications.

Mr. Hulme was opening the first meeting of the Pacific area regional working group of the Interim Communications Satellite Committee which met in Sydney from 26th June to 1st July. This committee is managing the satellite programme for a 51-nation partnership. The meeting was attended by 30 delegates from 13 countries interested in commercial satellite communications in the Pacific area.

The Postmaster-General said that the present thinking was concentrated mainly on satellites for external communications, but Australia might use satellites internally much quicker than many people thought.

The board chairman of the U.S. Satellite Corporation, Mr. James McCormick, told the delegates that technical advances in satellite communications would be limited only by the amount of money made available for development. He said that while he agreed that technical advances in communications has remained ahead of the world's economy and social progress, demands for the commercial use of satellites would catch up with the available facilities within about 10 years.

Mr. McCormick forecasts that in the near future computers would be linked internationally by satellite, world communications need never again be handicapped by large volumes of traffic, and direct international television would be limited only by the varying time factors in different countries.

Mr. Hulme has already stated that Australia would be using the world-wide satellite communication system for telephony by 1968. It is understood that there is a possibility that test television material will be transmitted across the Pacific Ocean between Australia and the U.S.A. next year through a satellite stationed over Fiji.